Technische Universität München
Lehrstuhl für Kommunikationsnetze

Design and Optimization of Wavelength-Switched Optical Core Networks

Dipl.-Ing. Univ. Matthias Scheffel

Vollständiger Abdruck der von der Fakultät für Elektrotechnik und Informationstechnik der Technischen Universität München zur Erlangung des akademischen Grades eines

Doktor-Ingenieurs (Dr.-Ing.)

genehmigten Dissertation.

Vorsitzender:		Univ.-Prof. Dr. sc. techn. Gerhard Kramer
Prüfer der Dissertation:	1.	Univ.-Prof. Dr.-Ing. Jörg Eberspächer
	2.	Univ.-Prof. Dr.-Ing. Phuoc Tran-Gia, Julius-Maximilians-Universität Würzburg

Die Dissertation wurde am 29. Juni 2011 bei der Technischen Universität München eingereicht und durch die Fakultät für Elektrotechnik und Informationstechnik am 24. November 2011 angenommen.

Abstract

This work deals with the design of optical core networks based on wavelength division multiplexing. After giving an overview of fiber-optic communication technology and presenting the network architecture, we sketch the planning process. In order to solve the design problems, mathematical optimization is employed using realistic node and link models. Three specific network planning problems are investigated. First of all, redundant network topologies are calculated which are able to compensate single and dual network element failures. Our second analysis explores the total capital expenditure for an opaque and a translucent lightpath design according to a detailed cost model. The third investigation focuses on an availability-oriented routing approach which systematically adds redundant capacity to achieve a desired end-to-end availability. All approaches are demonstrated by means of typical communication networks.

Kurzfassung

Diese Arbeit befasst sich mit dem Design von optischen Kernnetzen basierend auf Wellenlängenmultiplex. Nach einem Überblick über die Glasfaserkommunikation und einer Beschreibung der Netzarchitektur wird der Planungsprozess skizziert. Zur Lösung der Planungsaufgaben werden Verfahren der mathematischen Optimierung eingesetzt unter Verwendung realitätsnaher Knoten- und Linkmodelle. Drei spezifische Netzplanungsaufgaben werden untersucht. Als erstes werden zur Kompensation von Einzel- oder Doppelfehlern bei Netzelementen redundante Netztopologien bestimmt. Die zweite Studie ermittelt die gesamten Investitionskosten für ein opakes und transluzentes Lichtpfaddesign gemäß einem detaillierten Kostenmodell. Die dritte Untersuchung widmet sich einem verfügbarkeitsorientierten Ansatz zur Verkehrslenkung. Dabei wird systematisch redundante Kapazität bereitgestellt, um die gewünschte Ende-zu-Ende-Verfügbarkeit zu erreichen. Die Verfahren werden an typischen Kommunikationsnetzen demonstriert.

Acknowledgements

It would not have been possible to write this doctoral thesis without the support of several people who have contributed to my work in a technical and personal manner.

First of all, I want to thank my principal supervisor Prof. Eberspächer for giving me the opportunity to work at his institute of communication networks and conduct research in the transport network area. It was a pleasure to experience your enthusiasm, expertise, and advice. Another major contribution was to provide a productive and friendly atmosphere that stimulated me to do my best. Moreover, I am deeply grateful to Prof. Phuoc Tran-Gia and Prof. Gerhard Kramer for being the second examiner and presiding my thesis committee.

Many colleagues at the institute have supported me via fruitful technical discussions. Special thanks go to Dr. Dominic Schupke for arousing my interest in scientific research and inspiring me. Another big credit goes to Dr. Robert Prinz for discussing about numerous ideas and software implementation challenges to optimize my work. Moreover, I am indebted to all members of the photonic networks and network resilience group: Dr. Claus Gruber, Dr. Thomas Fischer, Dr. Thomas Schwabe, Dr. Moritz Kiese, Dr. Christian Merkle and Dr. Carmen Mas.

Last but not least, my family has always been an important pillar for me. I am so grateful to my parents Maria and Hagen who allowed me to grow up in a caring home and supported my education. Above all, I want to express deep thanks to my beloved wife Martina and my lovely son Jonas for giving me so much strength and making me complete.

Contents

1 Introduction

Optical networks based on wavelength division multiplexing form the fundament of the Internet offering all the services we appreciate so much. Despite bandwidth-hungry applications such as file hosting, multimedia, and video conferencing, fiber-optic transmission technology has evolved to satisfy the continuous demand for higher bitrates in wide area transport networks.

1.1 Motivation

Fiber optics offer much smaller signal attenuation compared to copper wire, thereby allowing for long transmission distances without the need for amplification. At the same time, the utilizable frequency range is very broad so that data can be transmitted simultaneously at multiple carrier frequencies within the same medium. The dense multiplexing of signals in the wavelength domain has paved the way for the success of optical networks. Instead of having to provide new transmission lines, existing fibers can be lit with more wavelengths to increase the network capacity. Additionally, optical network equipment plays a crucial role for cost-efficient network deployment. If the signal power along the fiber becomes too small, all wavelengths within a broad frequency window can be refreshed by a single optical amplifier. As a consequence, expensive transceiver equipment that electrically terminates the wavelengths becomes obsolete to a certain extent.

Especially in the view of economically challenging times it becomes evident that communication networks must be carefully designed in order to yield revenues in turn for investments. Too optimistic traffic forecasts leave the network resources underutilized and can destroy the business model. Instead, strategies must be developed to allow for cost-efficient network configurations. This is where network planning comes into play. It is a challenging task to consider all relevant aspects and get reliable information about the expected services and their requirements. Furthermore, technological progress brings new possibilities that can reduce the capital expenditures. Optical switching is such an innovation. It allows to relay wavelength signals between fiber links in the optical domain without having to do electrical signal conversion and electrical switching. Typically, the expenses for such electrical signal processing dominate the overall network investments. However, there are also a number of challenges that must be solved. Firstly, optical signals must be regenerated electronically before the accumulated signal-to-noise ratio causes significant bit errors at the receiver side. Secondly, optical switching does not provide the ability to change the wavelength at the network nodes

by default. As a consequence, data must be sent on the same wavelength from origin to destination. Identifying a wavelength that is available along the entire route for all the lightpaths that should be established is a difficult task. All these aspects demand for an efficient network design.

1.2 Organization of Thesis

This work deals with the design of optical core networks based on wavelength division multiplexing. We evaluate the overall planning process and develop an integrated design methodology starting from a green field. Investigations in the context of this thesis have been published by the author in [SSG03a, SSG03b, Sch04, MSSW05, Sch05a, Sch05b, Sch05c, Sch06a, Sch06b, Sch06c, Sch06d, SGSP06, SPG+06, GS07, KS07, SKS07]. The document is organized as follows.

The next chapter presents an overview of network design aspects. We explain the fundamentals of optical core networks including fiber-optic communication technology, network architecture and protocols, and network resilience. After this, the network planning problem is analyzed by considering typical planning tasks and sketching the planning process. We motivate the application of mathematical optimization techniques to be able to compute optimal results. The chapter is concluded by the specification of a detailed network and cost model to derive an appropriate representation of the real world. Based on these foundations, three specific network design problems are investigated in the following chapters. Numerous case studies are carried out for all approaches by means of typical communication networks.

In Chapter 3, we calculate redundant network topologies for given geographical node locations which are able to compensate single and dual network failures. Due to computational complexity, a heuristic approach is developed to preselect a set of best candidate network edges from a fully meshed topology. Out of those edges, a subsequent mathematical optimization model computes the topology with minimum routing costs while offering path protection. Routing costs are measured in terms of total length of all lightpaths. The number of network edges that can be allocated for the topology is restricted to various values in order to analyze the impact of topologies with different mesh degree on the network resources. The computed topologies are used as input for the following studies.

Next, Chapter 4 explores the overall capital expenditures of two conceptually different optical transmission paradigms, namely an opaque and a translucent network design. The former approach performs signal regeneration at each transit node whereas the latter concept permits optical switching with selective signal regeneration. For each scenario, we formulate an optimization model that minimizes the total investment costs for the overall routing, resilience, and dimensioning problem by means of the detailed cost model. In order to handle the complexity of the design, preliminary steps are performed before solving the mathematical program: translucent paths are designed

by allocating transponders and intermediate regenerators and a set of shortest disjoint routes is computed to restrict the routing options. The wavelength assignment task for translucent lightpaths including a potential allocation of extra wavelength converters to resolve wavelength conflicts is performed in a subsequent step.

Our third analysis in Chapter 5 focuses on an availability-aware routing approach. In contrast to standard resilience schemes which address failure survivability, the novel virtual link design deliberately adds redundant capacity to achieve a desired end-to-end availability. Virtual links consist of node-disjoint path segments that can be flexibly combined with normal links to establish a connection between two nodes. We develop an optimization model that minimizes the routing costs measured in terms of total link kilometers of normal and virtual links while guaranteeing specific availability requirements.

Finally, Chapter 6 summarizes the main findings and gives an outlook on open issues which can be addressed by future research.

2 WDM Network Design

This chapter gives an overview of optical core networks and their design. The next section presents the key aspects of WDM networks highlighting fiber-optic communication, typical network architectures, and the importance of network resilience. Section 2.2 illustrates the network planning process and motivates the application of mathematical optimization. In Section 2.3, we present a detailed network and cost model. Finally, Section 2.4 summarizes this chapter.

2.1 Optical Core Networks

Optical wavelength division multiplexing (WDM) networks constitute the core of the Internet. In the following subsections, we take a look at the transmission characteristics of fiber-optic communication and the network architecture along with related protocols.

2.1.1 Fiber-Optic Communication

The success story of optical core networks is based on the attractive transmission characteristics of fiber optics and technological advance in the design of key network components for cost-efficient networking solutions. This subsection introduces fundamental aspects of optical long-haul networks. A detailed explanation is beyond the scope of this work. The interested reader is referred to [RSS09], for example. The basic functional principle of digital data transfer via a point-to-point fiber-optic communication system between two remote locations is as follows.

At the transmitter side, the information (bits and bytes) is converted from electrical to optical form by modulating a laser. Lasers are semiconductor devices that emit light by stimulated emission of radiation. A voltage applied at doped layers induces the transition of atoms from higher to lower energy state creating photons which in turn produce new photons. The laser emits coherent light at a narrow frequency range which is also denoted as wavelength. Bits can be encoded into the signal via modulation by changing the characteristics of the carrier signal. Typical modulation schemes are simple on-off keying, amplitude-shift keying, or phase-shift keying, for example. For high-speed transmissions over long distances, indirect modulation is applied by adding an external modulator. Multi-level modulation schemes can map multiple bits onto a single symbol. When inserting the optical signal into the optical single-mode fiber, a portion

of the light will be reflected at the surface and the rest will penetrate the medium. The angle under which the latter light component is refracted can be calculated by the law of refraction subject to the optical material density (refractive index) of the fiber and the ingress angle. The outcome plays an important role for guiding the optical signal by total reflection. This phenomenon causes light to be reflected entirely if the ingress angle is below a certain value. However, total reflection at a material transition is only possible from a medium with higher refractive index to a medium with lower optical density. For this reason, optical fiber consists of an inner core and a surrounding cladding with different refractive index to keep the signal in the core. Besides, a surrounding plastic coating protects the fiber.

At the receiver side, a photodetector, typically a photodiode, translates the optical signal back into electrical form. The photoelectric effect causes the emission of electrons when absorbing the energy of the incoming light. Moreover, a receiver performs signal amplification, retiming, reshaping, and regeneration to recover clock and data.

Bidirectional transmission can be realized in various ways. Firstly, each fiber is used for one transmission direction only, which requires at least two fibers for mutual communication. Secondly, the counter-directed signals are transmitted at different wavelengths within the same fiber. Thirdly, the same wavelength may be used for both signals if precautions are taken to prevent reflections at the end points.

One crucial advantage of optical networks is the small signal attenuation of optical fiber over a large frequency range. Compared to other guided transmission media like copper, a signal can travel over a long distance without the need for amplification. This circumstance significantly reduces network costs due to fewer amplifier stages. Moreover, optical networks allow for high transmission rates using wavelength division multiplexing (WDM) technology by transmitting data simultaneously at different carrier frequencies within a single optical fiber. Optical amplifiers are inserted into fiber optics in order to restrengthen the signal power after fiber segment lengths of typically 80 to 100 kilometers. They enable cost-efficient solutions by amplifying all wavelengths within a broad frequency band at the same time.

In today's networks, wavelength connections are typically provided in a point-to-point manner, i.e. the optical signal is converted to electrical form at each transit node via combined receiver/transmitter units, the so-called transponders. Optical switches are now available which permit transparent wavelength channel forwarding in the optical domain across node boundaries. However, physical effects deteriorate the signal quality and impose limitations when setting up end-to-end lightpaths throughout the network. Consequently, electrical regeneration is still required to a certain extent.

2.1.2 Network Architecture and Protocols

Communication systems are based on the Open Systems Interconnection (OSI) model defined by the International Organization for Standardization (ISO). It serves as refer-

ence architecture for describing internetworking. Seven vertical layers are defined to group functions into logical clusters. Each layer offers services to its upper layer and can request services from its lower layer via an appropriate interface.

Another clustering of network functionality is defined by so-called planes that deal with different tasks. A data plane is defined which is responsible for transporting data between the nodes. The control plane handles signaling, routing, and resource discovery. These functions facilitate an automated provisioning of services in the data plane. Finally, a management plane provides an interface for network configuration and management functions.

Moreover, different network architectures are applied subject to the geographical dimensions of a communication network. Core networks form the backbone structure for ultra-long transmission distances whereas metro networks transport traffic within a smaller region. Business and residential customers are connected to access networks which perform traffic aggregation.

Optical core network technologies and protocols have dramatically changed in the last twenty years [BSBS08, GBB+06]. In the past, voice services were the dominating traffic in long-haul telecommunication networks. Synchronous Optical Network (SONET) and Synchronous Digital Hierarchy (SDH) technology were designed to meet these needs by providing circuit-switched connections and an appropriate multiplexing/demultiplexing time division multiplexing (TDM) scheme to support various bitrates. Over the years, the popularity of the Internet rapidly increased the data traffic, eventually outpacing classical voice traffic. The Internet Protocol (IP) became the common convergence layer for all web-based services. However, SONET/SDH technology was not ideally suited to transport bursty IP traffic. As result, other technologies like Generic Framing Procedure (GFP) and Optical Transport Network (OTN) have been developed to transport IP over WDM. The future Internet architecture is expected to further change due to new overlay services and network virtualization that may yield a simplified layering model [TTGA08].

The concepts presented in this thesis are not limited to a specific technology or protocol. We abstract from individual frame/packet formats at Open Systems Interconnection (OSI) Layers 2/3 and focus on wavelength-switched networks. In order to apply the routing according to our planning results in a real network, one requires appropriate management software which may be offered by generalized multiprotocol label switching (GMPLS)/Automatically Switched Optical Network (ASON) control plane. Moreover, the control plane offers the intelligence to detect and localize failures and react according to the pre-planned compensation actions.

2.1.3 Network Resilience

Network resilience refers to the ability of a communication network to recover from failures. A typical failure scenario is a backhoe which cuts fiber cables while digging in

the ground. Moreover, hardware or software failures in the network components can happen. Another option is optical signal degradation due to aging effects of the network components which may cause an increased bit error rate at the receiver side. In order to rapidly recover from failures, network resilience schemes utilize redundant network resources to redirect affected traffic along alternative routes that are still available. Thus, backup capacity is required in addition to the working resources used for normal routing in the failure-free case. A fault can be detected via loss of light or an increased bit error rate, for example. After this, the defect must be localized and the nodes responsible for activating the resilience mechanism are to be notified via signaling in case they are not aware of the failure. One can classify resilience concepts into a number of categories. In the following, we present the most important aspects. A detailed survey of survivable networks and their design can be found in [Gro03].

Protection schemes pre-calculate alternative routes and configure the backup resources in advance of any failure, i.e. before any traffic is transported. When a failure happens, affected traffic can be immediately switched to the alternative path after it has been detected. This is opposed to restoration strategies where more actions are to be taken "on the fly", i.e. the computation of alternative paths and/or the reservation of backup resources is performed after failure detection. Thus, restoration concepts typically react slower. Moreover, resilience schemes may either provide an individual alternative path for every working link of a routed connection or offer a redundant end-to-end path between origin and destination node. The corresponding concepts are denoted link and path protection/restoration, respectively.

In case of protection one can distinguish dedicated and shared protection mechanisms. The former strategy exclusively allocates backup resources to specific protection paths. Shared protection on the other hand makes backup resources available for multiple protection paths. This is only valid if the corresponding failure events happen statistically independent from each other. Dedicated path protection can be configured in terms of a 1+1 or 1:1 transmission mode. In the former case, data is sent simultaneously along the working and the protection path and the receiver selects the best signal whereas 1:1 protection switches the signal to the protection path only in case of a failure on the primary path.

Protection schemes can be adapted to protect against multiple simultaneous failures. A 2:1 path protection configuration offers two protection paths for each primary path to compensate dual failures, for example. We note that all paths must fail independently from each other to provide the desired degree of resilience.

The article [CMH+07] illustrates various resilience schemes and classifies them in a common framework. The need for resilience depends on the type of services that are provisioned by the network. Due to the wide range of applications present in today's networks, operators and providers must have differentiated resilience mechanisms in order to fulfill the specific requirements in a cost-effective manner [GC05].

One important issue when providing network resilience is the interaction of recovery functions at multiple layers. We assume an IP-over-WDM architecture where the

physical layer can provide transparent optical paths that look like a direct links from an IP point of view despite traversing a number of nodes. Due to the high bitrates, an enormous number of IP traffic flows is routed over the links. In case of a fiber cut, multiple optical paths are interrupted simultaneously provoking a great number of traffic flow interruptions in the electrical layer. Resilience strategies in the physical layer operate more rapidly because they allow to restore optical links at wavelength granularity rather than rerouting individual IP flows. However, setting up a transparent optical protection path over multiple hops requires careful engineering which can limit the realtime reconfiguration actions at the time of an outage [GG06]. Ideally, the WDM layer can compensate a failure before there are any impacts visible in the IP layer. On the other hand, the finer traffic granularity in the electrical layer enables a more efficient implementation of recovery schemes according to the desired degree of resilience. Furthermore, available resources can be utilized more efficiently. Thus, a combination of resilience mechanisms at the optical and electrical layer is beneficial but necessitates a careful coordination of activities [DGA+99].

2.2 Network Planning

Network planning is a complex process because it deals with various aspects. This section gives an introduction to the design of optical core networks and describes its challenges.

2.2.1 Planning Process

Optical communication networks have paved the way for the information age. Due to growing demands, new services, and improved networking technologies, network operators continuously have to invest in their infrastructure. However, the prices for classical network services like telephony or Internet access are continuously decreasing due to strong competition. Thus, it is essential to improve the return on investment in order to stay profitable. Suitable network planning techniques support network operators to efficiently spend their money.

A fundamental issue of network planning is to develop suitable network models. On the one hand, the models must include all relevant characteristics in order to allow for a realistic network design. On the other hand, the huge amount of parameters and variables cannot be incorporated down to the last detail because of computational complexity. Thus, it is important to find a suitable balance between details and abstractions in the modeling process. An appropriate network model facilitates systematic target-oriented planning strategies in contrast to unpromising designs by hand using rules of thumb. Depending on the focus of the network design, planning approaches may deal with numerous aspects. As an example we would like to mention the uncertainty about underlying assumptions like estimated future traffic requests [LG04, LG05]. Moreover,

one may examine planning strategies with respect to different future time frames or perform a combined analysis considering multiperiod planning [MSE08].

Figure 2.1 gives an overview of the network planning process and the most important subproblems. For a general introduction to the planning of telecommunication networks, the interested reader is referred to [Rob98]. Detailed insights into latest optimization trends can be found in [EKW09].

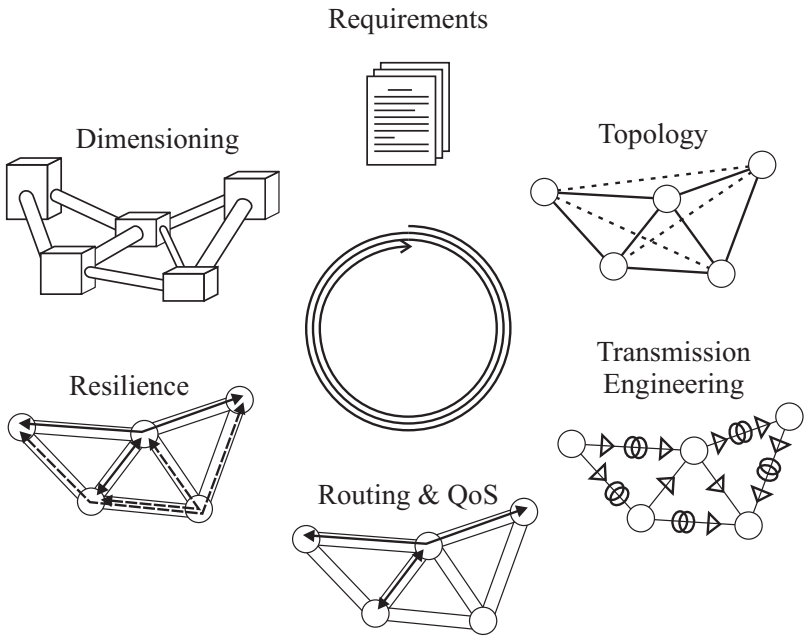

Figure 2.1: Overview of the network planning process and subproblems.

- The starting point of the planning process is defined by a specification that clearly describes the requirements that must be fulfilled. This includes details about the types of services, the traffic volumes, and the required quality of service (QoS).
- In case of green field planning where no infrastructure is given, one might design a network topology as first logical step. The main related tasks include the selection of node locations and the allocation of network edges. At this point the topology is a purely logical structure of the network without any capacities. However, a review of the topology can also be beneficial when upgrading a network to remove traffic bottlenecks by providing a shortcut edge between two non-adjacent nodes.
- Transmission engineering is another crucial topic. Particularly in optical wide area networks (WANs), the signals travel long distances and encounter a number of undesirable physical effects. In order to be able to detect the transported information correctly at the receiver, one must design the transmission system accordingly. Examples falling into this category are the selection of transmitters supporting an adequate transmission distance, the placement of optical amplifiers to boost the signal power, and dispersion compensation techniques to prevent pulse broadening.

- The Routing problem is responsible for identifying a path along which the traffic is to be sent. It must satisfy all traffic demands. In optical WDM networks, traffic is transported via lightpaths inside optical fibers. Depending on the node architecture, the wavelength cannot be translated at each node. Thus, routing may involve the task of determining valid wavelength configurations. For a number of services, routing must fulfill certain QoS parameters like latency, jitter, or packet loss. In the end, what matters is the Quality of Experience (QoE) performance perceived by the user [FHTG10].

- Network resilience refers to all measures for compensating failure scenarios. Due to the enormous transmission rates per wavelength and dense WDM, a fiber cable cut caused by a backhoe interrupts a great number of connections. In order to rapidly recover from such outages, one can allow for alternative transmission paths.

- The network dimensioning problem allocates equipment at the nodes and edges to support the routing. Additionally, it must consider the extra resources required for network resilience.

At first glance, the overall network planning problem seems to be solvable by a logical sequence of separate tasks. However, when analyzing the tasks in detail, one can see the mutual reactions between them. As an example, the network topology has strong impacts on routing and resilience. If a network is only sparsely meshed, the demands must be routed on long paths. Furthermore, it may not be possible to establish disjoint paths that do not have a common transit node or edge to enable single failure survivability. Implementing network resilience schemes in a separate step after the routing often significantly deteriorates the performance in terms of totally required network resources. When applying a simple shortest path routing according to a link metric, an alternative path can become very long. This is due to the fact that any node/edge of the primary path must not be used by a backup path to guarantee route disjointness. In contrast, the shortest pair of disjoint routes typically has a significantly shorter total length.

It is important to note that an ideal network planning approach performs all the above steps at the same time. However, this is usually not feasible due to computational complexity. The overall network design is therefore subdivided into several tasks that are solved independently of each other. Each module adds another piece of information about the overall network configuration and the results serve as input for subsequent planning steps. Due to the interaction of many planning tasks, it is an important challenge of network planning to group the various design aspects according to the relevance of their impact on each other and develop appropriate planning methods. The results can be evaluated after each stage and previous design steps may be repeated if modifications are desired. In this case, additional conditions may be added to adapt the network configuration so that the desired overall performance can be accomplished.

2.2.2 Mathematical Programming

The goal of network planning is to model a problem and find the best solution. Due to the problem complexity, there is great amount of individual decisions to be made which influence each other. Complete enumeration is not practicable because the number of potential solutions is very high for realistic scenarios and grows exponentially with the number of variables. Global optimization techniques can help to solve such problems. Mathematical programming represents a deterministic optimization approach. It can find the true optimum without getting stuck in a local maximum or minimum. This is in contrast to stochastic optimization or heuristic approaches which usually do not allow to assess the quality of the found solution. A thorough theoretical insight into mathematical programming is presented in [BT97].

Most network planning problems cannot be solved to optimality by a simple algorithm consisting of a finite set of instructions. As an example we would like to mention the shortest path algorithm by Dijkstra [Dij59]. It determines the least cost paths from one node to all other nodes in a graph consisting of a set of nodes and edges with assigned costs. The cost of a path is given by the sum of all edge costs along the path. This problem can be solved in polynomial time and the algorithm can be applied separately for finding the shortest paths for a given set of demands. However, when considering capacity restrictions on nodes and/or edges and integer demand flows, the problem becomes much more difficult (NP-complete). It is no longer possible to apply the shortest path algorithm because the routing of one path may prohibit the utilization of another route due to lack of capacity. Instead, identifying the optimal solution for such a multi-commodity flow problem relies on integer linear programming.

Mathematical optimization is a technique to determine the globally optimal solution of planning problems. An optimization problem is characterized by a number of decision variables that should be selected such that an objective function of these variables is minimized or maximized. Furthermore, constraints on the variables are specified in terms of equations to define valid solutions that fulfill all requirements. The set of all valid solutions is denoted solution space. The general form of a linear programming (LP) model consisting of three variables x_1, x_2, x_3 can be stated as follows.

$$\text{Minimize/maximize} \quad c_1 \cdot x_1 + c_2 \cdot x_2 + c_3 \cdot x_3 \tag{2.1}$$

$$\text{subject to} \quad a_{11} \cdot x_1 + a_{12} \cdot x_2 + a_{13} \cdot x_3 \geq b_1, \tag{2.2}$$

$$a_{21} \cdot x_1 + a_{22} \cdot x_2 + a_{23} \cdot x_3 \leq b_2, \tag{2.3}$$

$$a_{31} \cdot x_1 + a_{32} \cdot x_2 + a_{33} \cdot x_3 = b_3, \tag{2.4}$$

$$x_1, x_2, x_3 \geq 0. \tag{2.5}$$

All equations involve linear terms, only. The objective function in Equation (2.1) minimizes the total cost or maximizes the profit. The following three constraints may specify inequalities or equalities. The Variables are defined as positive real values

according to Equation (2.5). An LP model can be solved by the simplex algorithm, for example. More details are explained in [BT97].

For many network planning problems, the variables cannot take arbitrary real values but need to be modeled as discrete integer numbers. Capacities at nodes and edges are typically allocated in certain granularities, for example. Simply rounding the solution for real variables to integer values does not yield the best solution and often not even represents a valid solution. In the following we want to show conceptually how an integer linear programming (ILP) model is solved compared to the respective linear programming (LP) problem. An example ILP formulation is declared by Equations (2.6) to (2.11).

$$\text{Minimize} \quad 1.2 \cdot x_1 + x_2 \tag{2.6}$$

$$\text{subject to} \quad 2 \cdot x_1 + x_2 \geq 6, \tag{2.7}$$

$$0.8 \cdot x_1 + x_2 \geq 4, \tag{2.8}$$

$$x_1 \leq 6, \tag{2.9}$$

$$x_2 \leq 6, \tag{2.10}$$

$$x_1, x_2 \in \mathcal{Z}_+^0. \tag{2.11}$$

The graphical representation of this problem is depicted in Figure 2.2. The grey area shows the feasible region of the corresponding linear problem based on the given constraints. Valid solutions of the integer linear problem are indicated by small circles. Dashed straight lines represent points with identical objective value. One can observe that the objective function decreases for lines that are shifted in parallel toward the origin. The best solution for the linear problem is the intersection point of the straight lines representing Constraints (2.7) and (2.8), respectively. When examining the integer linear problem, we notice that solution $x_1 = 1$, $x_2 = 4$ is traversed by the line with minimum possible objective value.

In general, ILP problems are solved by the branch and bound algorithm. The concept comprises a branching procedure that recursively segments the total feasible region of all candidate solutions into smaller regions. In doing so, the entirety of all subregions corresponds to the parent region. Starting from the root node, a tree is created whose nodes correspond to the partitioned regions. Bounding is performed at each node by calculating an upper and a lower limit for the objective. This is done via linear relaxation by omitting the constraint that all variables must only take discrete values. Thus, the corresponding linear problem is solved at each node along the tree. If the solution turns out to be integer, the node does not need to be processed further. Otherwise, the node is split into two or more subregions.

Figure 2.3 illustrates a branch and bound structure of our example ILP. The linear relaxation at the root node yields a fractional solution. After that, we split the feasible range for x_1. The regions $x_1 \leq 1$ and $x_1 \geq 2$ are selected for the left and right node,

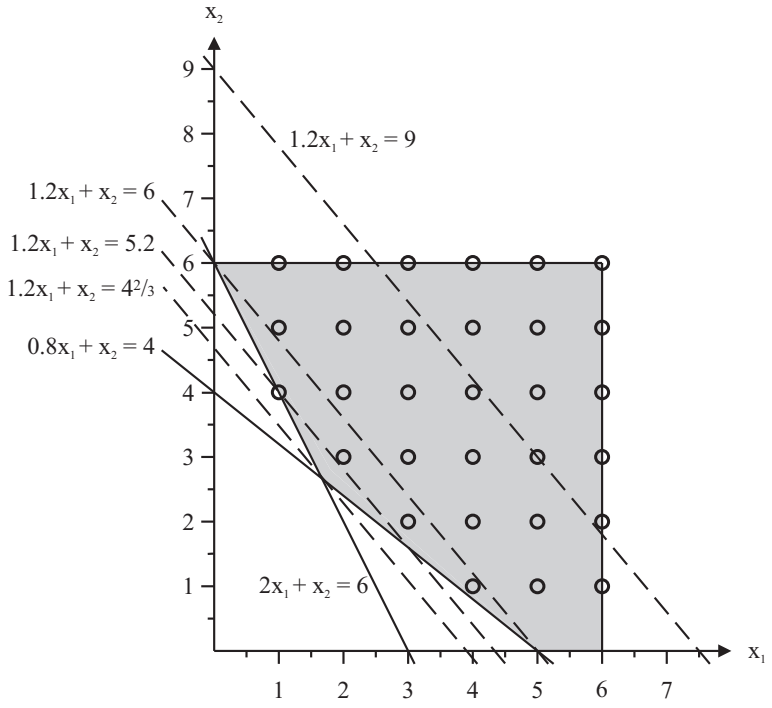

Figure 2.2: Graphical solution of an example ILP model.

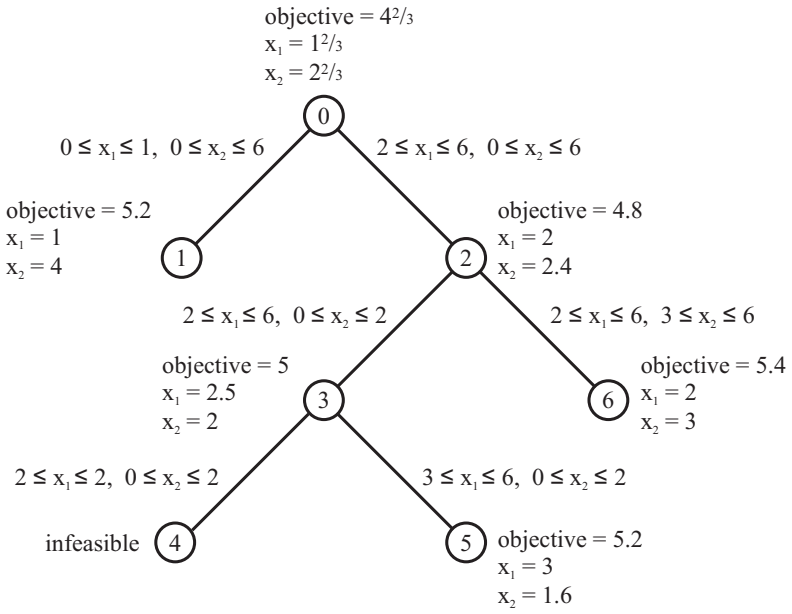

Figure 2.3: Branch and bound sequence for solving the example ILP model numerically.

respectively. This strategy prevents that the same solution as for the root node is obtained again because the previous fractional value is excluded. At the left node, the linear relaxation calculates an integer solution with objective 5.2. At the right node, we get an objective of 4.8 and a fractional solution. If the right objective was larger

than the left objective, one could prune the node. The linear relaxation solution always represents a lower bound for the best integer solution in case of a minimizing objective. Since an integer solution with better objective is already found, a further processing would not be necessary. The pruning concept can significantly speed up the branch and bound process. In our case, it turns out that the best integer solution is $x_1 = 1$, $x_2 = 4$ with objective 5.2 when evaluating the entire tree.

2.3 Network and Cost Modeling

In this section we present the network and cost model that form the basic framework of our investigations. Since different terms are used in the literature, clear definitions are introduced in the following to provide a consistent terminology throughout the thesis.

2.3.1 Network Terminology

Graphs are widely used in the context of information and telecommunication technology to model and analyze networks. We represent the equipment infrastructure of the network by a physical graph. The graph consists of nodes and edges that can interconnect them. A *physical node* is a network facility where traffic originates, terminates, or is relayed to other nodes. It summarizes all components responsible for adding, dropping, and switching optical connections. Besides, other functionalities such as signal amplification or wavelength multiplexing/demultiplexing are usually available to support the processing of transmission signals. A *physical edge* comprises all fiber optics between its end nodes. Supplementary components that prevent from signal degradation are also included. Two nodes are *adjacent* if there exists an edge that interconnects them. Equivalently, two edges are called adjacent if they share a common node. An edge is said to be *incident* on a node (and vice versa) in case the node is an end point of the edge. The *degree* of a node refers to the number of incident edges on the node. In our investigations we restrict to *simple graphs*, i.e. networks that do not have any parallel edges or loops. *Parallel edges* are characterized by identical end nodes and a *loop* starts and ends at the same node. We assume that all fibers between two adjacent nodes follow the same trace and consequently can be modeled by a single physical edge. When laying fibers they are allocated in terms of one or more *fiber cables* where dozens of fibers are bundled together. In many countries, the installation of fibers is subterrestrial due to legislation. A common option for the underground engineering works is to construct a trench and insert a *cable conduit* that protects the optical fibers against external influences.

Figure 2.4 depicts a small example network graph consisting of three physical nodes and one physical edge between each pair of nodes. Arrows at the end of the physical edges indicate that they support *bidirectional* transmission, i.e. data can be sent in

both directions. The total transmission capacity of a physical edge is determined by the number of bidirectional fiber links. We define a *link* as single transmission capacity unit on a physical edge of arbitrary granularity. Thus, a link may refer to an OC-n signal when dealing with SDH/SONET, a wavelength, or even an entire fiber. Alternatively, the synonym *channel* is used. We assume that a bidirectional fiber link actually consists of a pair of counter-directed *unidirectional* fibers. Every fiber enables the transmission in one direction, solely. Instead of treating each pair of unidirectional fiber links individually, their characteristics are respectively summarized by a single bidirectional link. Every fiber link consists of a sequence of *fiber spans* denoting a fiber segment which is terminated by optical amplifiers at both ends.

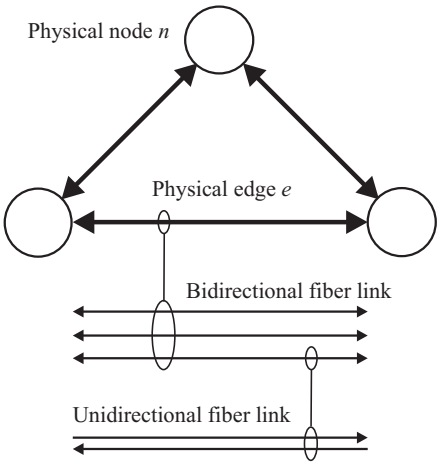

Figure 2.4: Bidirectional physical network model illustrated by example network.

We clearly distinguish between routes and paths. A *route* denotes an ordered list of edges that form a closed way from an origin node to a destination node. In contrast to that, a *path* represents a sequence of cross-connected links to establish an end-to-end data connection between the end nodes. In order to set up a path, real network capacity must be allocated on all traversed nodes and edges along its route. Multiple paths may follow the same route, but each path requires dedicated link resources unless the capacity is shared between them.

A graph must be *connected* so that there exists at least one route between every node pair. We restrict our analysis to simple paths by excluding routing configurations where a node is traversed more than once. Every traffic request between two nodes is assumed to be symmetric, i.e. the demands from one node to the other node and vice versa are identical. Furthermore, we expect that transmission capacity at physical nodes and edges is allocated equally for both directions. *Routing* is the process of calculating a route between two nodes. For network planning, it is also essential to consider the required resources to provision the actual path. A single wavelength link represents the fundamental transmission capacity granularity of optical networks. Data is routed from origin to destination node by exclusively reserving a wavelength link or sharing its capacity with other traffic at each traversed edge. In order to multiplex/demultiplex smaller bitrates, the capacity of a wavelength link is typically subdivided into several

time slots via TDM. In our investigations, we consider traffic requests in the order of gigabit per second (Gbit/s) at wavelength granularity. Thus, a path can be interpreted as a wavelength connection between the end nodes.

2.3.2 Edge Model

This subsection presents the fiber link model that characterizes the optical transmission system on the network edges. Figure 2.5 depicts a pair of unidirectional fiber links. Each link transports signals in only one direction as indicated by the arrows. The minimal fiber link configuration consists of a single fiber span (FS) and dispersion compensating fiber (DCF). We note that the actual dispersion management may be implemented by pre-, post-, or mix-compensation. If the fiber link is too long, the wavelength signal must be boosted by an inline amplifier (IA) to compensate the attenuation and other loss effects. Typically, inline amplifiers are inserted after an equidistant length l^{IA}. Furthermore, a dynamic gain equalizer (DGE) is required if the link exceeds the critical length l^{DGE}. All components of a fiber link are visualized in Figure 2.5. Link parts enclosed in curly brackets may occur zero or multiple times depending on the fiber link length. The square brackets around the DGE symbolize that this element either exists or not.

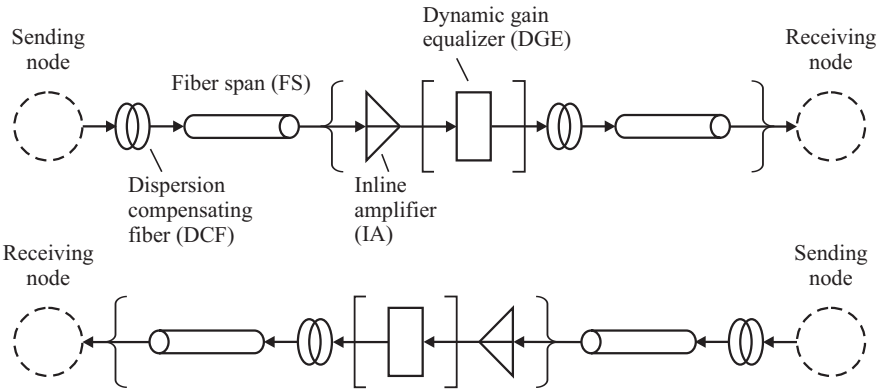

Figure 2.5: Pair of unidirectional fiber links consisting of fiber spans, inline amplifiers, dispersion compensating fibers, and dynamic gain equalizers.

Figure 2.6 shows how the two unidirectional fiber links can be modeled as a single bidirectional link. We assume that bidirectional transmission is always implemented by a pair of fibers applying unidirectional transmission per fiber. The bidirectional counterpart is used to simplify the network model.

From a mathematical point of view, the equipment quantity can be calculated according to Table 2.1. The number of inline amplifiers and dynamic gain equalizers are determined by dividing the fiber link length by the critical distances l^{IA} and l^{DGE} and rounding down, respectively. For the dispersion compensating fiber, we omit the rounding because it is not limited to integer granularity. Table 2.2 shows the distances between the components used in our subsequent case studies.

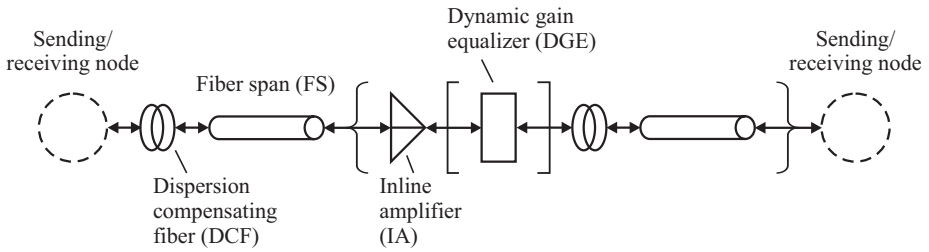

Figure 2.6: Bidirectional fiber link model.

Table 2.1: Calculation of fiber equipment quantity per fiber link on edge e with length l_e.

Equipment quantity		
Inline amplifier	Dispersion compensating fiber	Dynamic gain equalizer
$\lfloor l_e / l^{\mathrm{IA}} \rfloor$	l_e / l^{DCF}	$\lfloor l_e / l^{\mathrm{DGE}} \rfloor$

Table 2.2: Normal component spacing of fiber equipment for span length l^{SP}.

Component spacing		
Inline amplifier	Dispersion compensating fiber	Dynamic gain equalizer
$l^{\mathrm{IA}} \equiv l^{\mathrm{FS}}$	$l^{\mathrm{DCF}} = l^{\mathrm{FS}}$	$l^{\mathrm{DGE}} = 4 \cdot l^{\mathrm{FS}}$

Our cost model is based on the capital expenditure overview of various WDM network elements presented in [GLW+06]. Commonly, it is very difficult to obtain detailed cost values because they are kept confidential. Furthermore, actual prices depend on the functionality of the equipment, the maturity of the manufacturing process, and discounts that may be granted to attract customers. The proposed cost model was developed by network operators in conjunction with equipment vendors. It offers a consistent framework to compare capital expenditures (CAPEX) in opaque and transparent network designs. The term CAPEX refers to all investment costs of a company that contribute to the physical assets such as property, plant, or equipment. All cost values are normalized to the price of a 10 Gbit/s transponder with a transmission range of 750 km, i.e. they represent the cost ratio of the respective network element and the transponder.

The counterpart of CAPEX are operational expenditures (OPEX) which summarize the ongoing costs for running the network like salaries, leasing, and so on. These costs depend on the internal operational processes of a network provider and are beyond the scope of this work. However, in order to provide future cost-efficient network solutions, new modeling concepts to facilitate a joint optimization of both terms are expected to play an important role [VCP+06, Gru09].

The total physical edge costs can be subdivided into expenses for the raw edges and the fiber links. Table 2.3 contains the raw edge costs for cable conduits and fiber cables per

kilometer. Fiber link costs are depending on the transmission technology t. We distinguish long haul (LH), extended long haul (ELH), and ultra long haul (ULH) systems and assume that the maximum transmission distance l_t^{MTD} doubles when upgrading to the next level according to Table 2.4. The respective costs for IA and DCF per span are given in Table 2.5.

Table 2.3: Cable conduit and fiber cable costs per kilometer.

Cable conduit cost c^{CC}	Fiber cable cost c^{FC}
5.0	0.5

Table 2.4: Maximum transmission distance of the transmission technologies.

Transmission technology t	Maximum transmission distance l_t^{MTD} [km]
Long-haul (LH)	$l_{\text{LH}}^{\text{MTD}}$
Extended long-haul (ELH)	$2 \cdot l_{\text{LH}}^{\text{MTD}}$
Ultra long-haul (ULH)	$4 \cdot l_{\text{LH}}^{\text{MTD}}$

Table 2.5: Costs of inline amplifier and dispersion compensating fiber depending on the transmission range.

Transmission range t	Inline amplifier cost c_t^{IA}	Dispersion compensating fiber cost per span c_t^{DCF}
LH	3.0	0.9
ELH	3.8	1.0
ULH	4.7	1.2

2.3.3 Node Model

Network nodes consist of transmitter and receiver hardware to handle local egress and ingress signals, respectively. Furthermore, switching functionality is necessary to cross-connect transit wavelength channels.

Opaque Node Architecture

Opaque nodes terminate each incoming optical signal in the electrical domain. They still represent the most prevalent node architecture in today's optical transport networks. As a consequence, each multi-hop connection consists of a chain of point-to-point

optical links between adjacent nodes. Transponders are necessary to provide the optical-to-electrical (OE) and electrical-to-optical (EO) signal conversion.

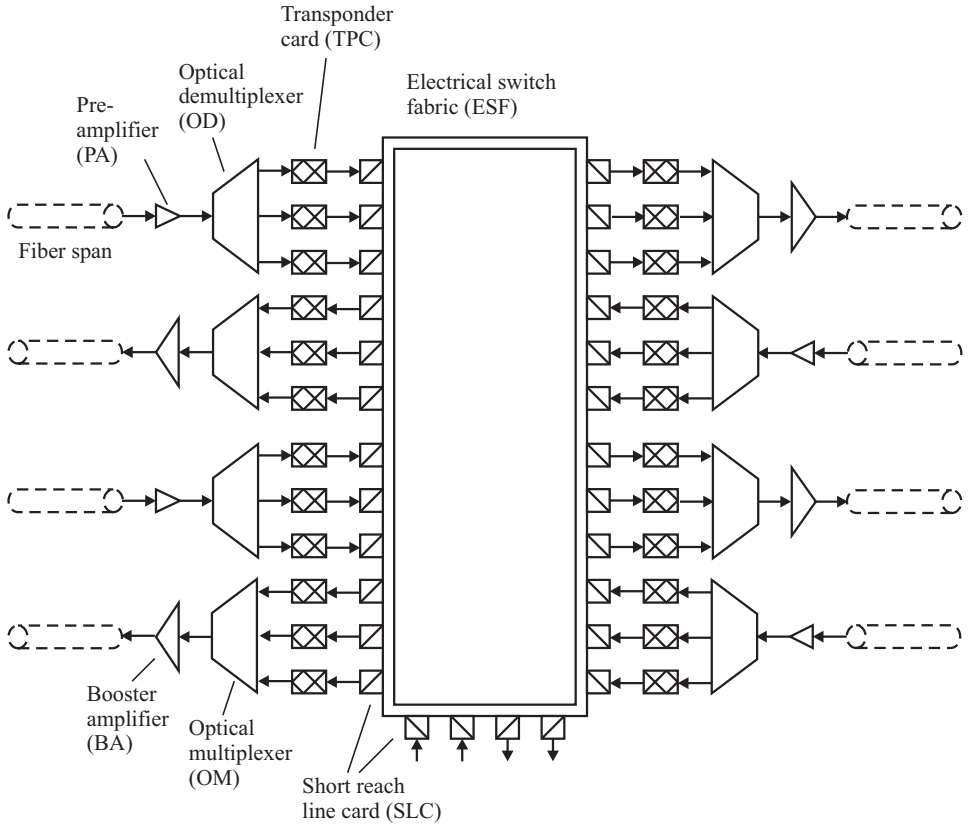

Figure 2.7: Unidirectional opaque node model.

Figure 2.7 depicts the architecture of a unidirectional opaque node. Incoming wavelength signals on a fiber link are amplified by a pre-amplifier (PA) and demultiplexed on separate output lines via an optical demultiplexer (OD) to process the channels individually. A transponder (TP) converts between a colored narrow band signal at International Telecommunication Union (ITU) wavelength grid and a non-colored client signal. Usually, transponders only support a certain bitrate and protocol. Afterwards, the signal is translated into the electrical domain by a short reach line card (SLC) before entering the electrical switch fabric (ESF) where it is cross-connected to the appropriate outgoing port. An egress short reach line card converts the data back to optical form and passes it to a transponder that emits a long-range signal. Subsequently, all wavelength signals destined for the same fiber are combined via an optical multiplexer (OM). Finally, a booster amplifier (BA) increases the power level of all channels to compensate for losses. At the local ingress and egress side, non-colored SLCs provide a defined interface for client signals.

An equivalent bidirectional opaque node model is presented in Figure 2.8. It merges related pairs of unidirectional components into a single bidirectional element. We note that the bidirectional architecture is used to make the network model more compact.

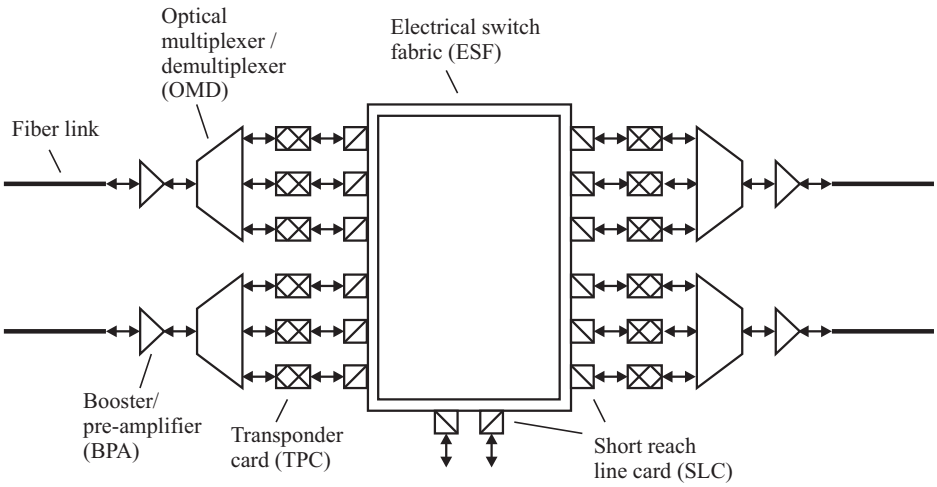

Figure 2.8: Bidirectional opaque node model.

The transformation still maintains the desired level of detail because we focus on bidirectional wavelength connections. However, one must keep in mind that the network components offer their functionality in one direction only. Thus, the elements must be allocated pair-wise to support the bidirectional architecture.

The advantage of opaque nodes is that all optical signals are completely refreshed at each node due to the optical-to-electrical-to-optical (OEO) conversion including regeneration with retiming and reshaping (3R regeneration). Besides, the outgoing wavelength can be chosen arbitrarily since the electrical signal simply needs to be switched to the corresponding transponder. This circumstance prevents channel blocking situations where two or more connections try to utilize the same wavelength because the carrier frequency can be altered at any intermediate node. The resulting paths are thus called virtual wavelength paths (VWPs).

However, electrical signal regeneration results in significant costs because of a high number of transponders. In contrast to optical amplifiers, electrical transponders cannot process multiple wavelength channels but must be allocated per wavelength and for each incident fiber. Another challenge is the scalability of electrical switch fabrics with respect to higher bitrates.

Table 2.6: Costs of booster and pre-amplifier for an opaque node.

Booster amplifier cost c^{BA}	Pre-amplifier cost c^{PA}	Booster/pre-amplifier cost $c^{\mathrm{BPA}} = 0.5 \cdot \left(c^{\mathrm{BA}} + c^{\mathrm{PA}}\right)$
3.0	2.0	2.5

The costs of the network components are presented in table format. Table 2.6 shows the normalized values for BA, PA, and a virtual booster/pre-amplifier (BPA). The price of an optical multiplexer/demultiplexer (OMD) depends on the number of wavelength

channels in fiber optics as shown in Table 2.7. Transponder costs vary subject to transmission range and bitrate according to Table 2.8. We introduce a quantifier $q < 1$ for the 2.5 Gbit/s transponder to be able to express its price based on the 10 Gbit/s transponder cost. The same factor q is applied for the electrical switch fabric in Table 2.9.

Table 2.7: Optical line terminal cost depending on the wavelength channel capacity per fiber.

Wavelength channels $\lvert\mathcal{W}\rvert$	Optical line terminal cost $c^{\text{OLT}}_{\lvert\mathcal{W}\rvert}$
40	4.5
80	6.7

Table 2.8: Transponder cost depending on the transmission range and bitrate.

Transmission range t	Bitrate b [Gbit/s]	Transponder cost $c^{\text{TP}}_{b,t}$
LH	2.5	$1.0 \cdot$ q
	10.0	1.0
ELH	2.5	$1.4 \cdot$ q
	10.0	1.4
ULH	2.5	$1.9 \cdot$ q
	10.0	1.9

Table 2.9: Electrical switch fabric cost per port depending on the bitrate.

Bitrate b [Gbit/s]	Electrical switch cost per port c^{ES}_{b}
2.5	$0.28 \cdot$ q
10.0	0.28

Transparent Node Architecture

The optical-to-electrical-to-optical (OEO) signal conversion of opaque nodes was necessary in the past because an alternative signal processing in the optical domain did not exist. Technological advance in the last few years has made it possible to do the switching optically. Figure 2.9 presents an alternative transparent node architecture. It is motivated by potential cost savings when optically bypassing transit traffic instead of performing electrical signal processing.

At each incoming fiber optics, the signal power of all wavelength links is enhanced by a transparent node pre-amplifier (TPA). After separating the WDM signals via optical

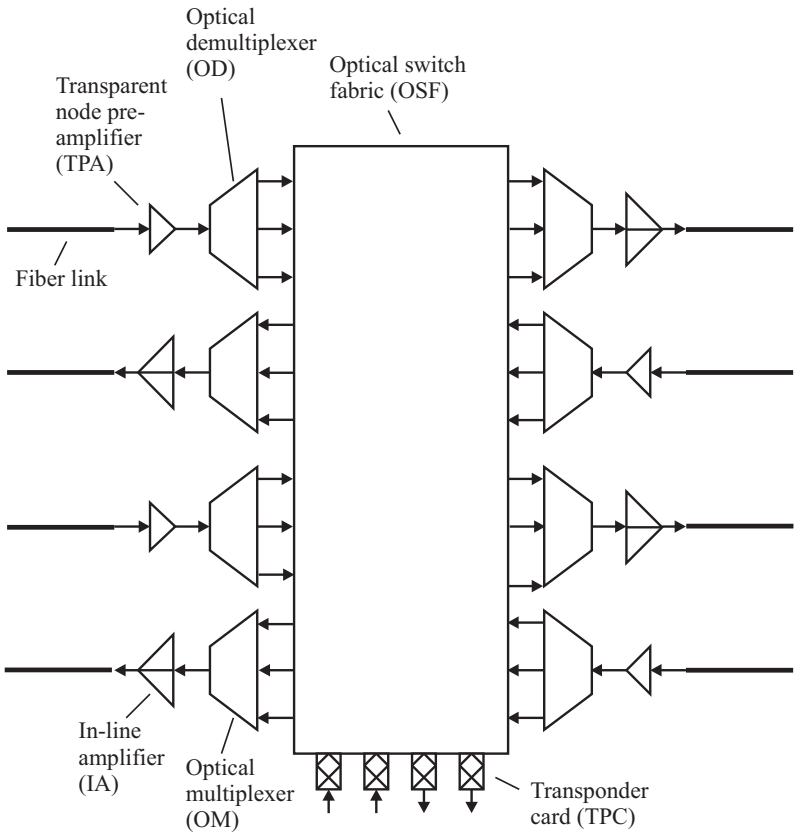

Figure 2.9: Unidirectional transparent node model.

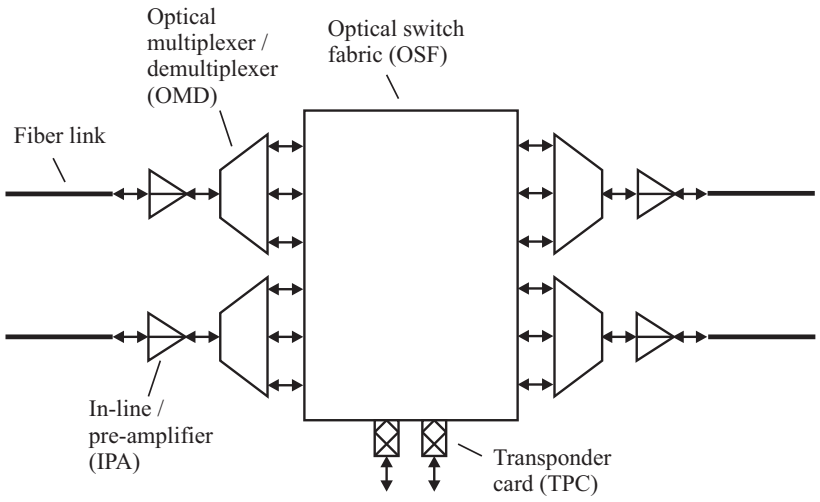

Figure 2.10: Bidirectional transparent node model.

demultiplexer (OD), they remain in the optical domain and are forwarded by an optical switch fabric (OSF). The optical switching functionality can be realized via small mirrors of a micro-electro-mechanical system (MEMS), for example. In order to compensate signal attenuation, all wavelength links traverse an IA after they are multiplexed on the

Table 2.10: Costs of inline and pre-amplifier for a transparent node.

Transmission range t	Inline amplifier cost c_t^{IA}	Transparent node pre-amplifier cost c^{TPA}
LH	3.0	1.25
ELH	3.8	1.25
ULH	4.7	1.25

Table 2.11: Optical switch fabric cost per fiber link and local port.

Wavelength channels $\lvert\mathcal{W}\rvert$	Optical switch cost per transit fiber link $c_{\lvert\mathcal{W}\rvert}^{\mathrm{OST}}$	Optical switch cost per local port c^{OSL}
40	5.3	0.1
80	8.0	0.1

outgoing fiber. Transponder cards are only allocated for local ingress/egress traffic. The corresponding bidirectional model of a transparent node is depicted in Figure 2.10

This node architecture permits wavelength paths (WPs) which are routed in optical shape from origin to destination node. The notion of transparency refers to the independence of the lightpath's protocol, bitrate, and modulation format. However, it excludes signal regeneration functionality that is offered by default in the former opaque scenario. As a consequence, long lightpaths experience severe signal degradation and the data cannot be correctly received at the destination node. Thus, the purely transparent node architecture is not regarded as practical approach in large-scale networks.

The component costs are again summarized in table format. Table 2.10 looks at the transmission range dependent inline/pre-amplifiers. The cost for the OSF in Table 2.11 is subject to the number of incident fibers and local ports for injecting and terminating lightpaths. We assume that variable optical attenuators to adjust the power level of the switched lightpaths are included in the price.

Translucent Node Architecture

Translucent nodes combine the merits of opaque and transparent nodes. The idea is to optically forward most of the lightpaths and only selectively regenerate wavelength signals if necessary. Figure 2.11 depicts the hybrid architecture of a translucent node. The basic structure resembles the transparent node model. However, two important building blocks are added. Firstly, an electrical switch fabric (ESF) is placed at the local ingress/egress side to interconnect signals between SLCs and long reach line cards (LLCs). Additionally, it can electrically multiplex lower bitrate client signals to higher bitrate wavelength signals. This processing step is often called grooming. A long reach line card can generate a narrow band transport signal at arbitrary wavelength. Moreover,

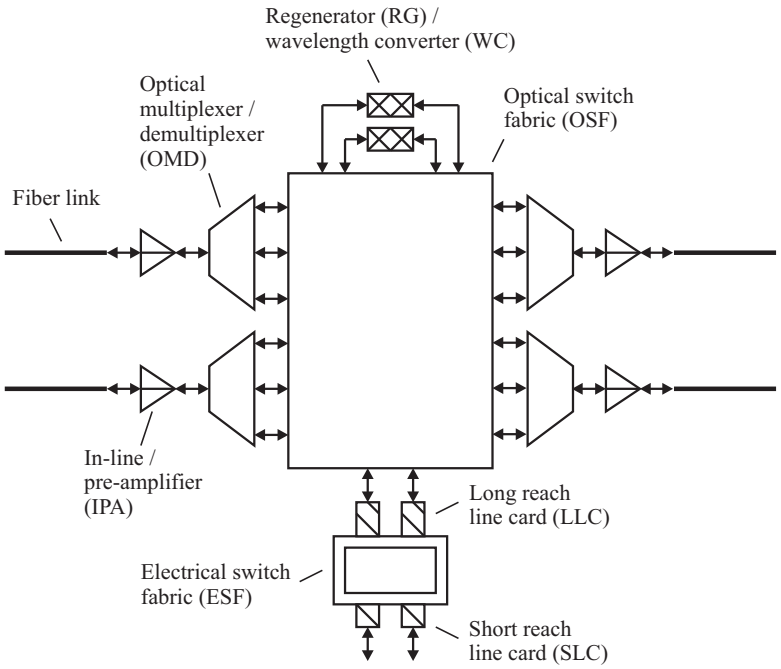

Figure 2.11: Bidirectional translucent node model.

Table 2.12: Long range line card cost depending on transmission range and bitrate.

Transmission range t	Bitrate b [Gbit/s]	Long range line card cost $c^{\mathrm{LLC}}_{b,t}$
LH	2.5	$0.9 \cdot q$
	10.0	0.9
ELH	2.5	$1.3 \cdot q$
	10.0	1.3
ULH	2.5	$1.8 \cdot q$
	10.0	1.8

regenerators (RGs) and wavelength converters (WCs) form a pool of resources that can be accessed via the optical switch fabric as needed. We consider electrical wavelength converters which translate the carrier frequency of an incoming wavelength signal and at the same time regenerate the signal.

The selective routing of lightpaths over wavelength converters gives rise to partial virtual wavelength paths (PVWPs). Figure 2.12 illustrates a routing configuration where lightpaths terminate at a translucent node. The option to regenerate and/or convert the wavelength is highlighted in Figure 2.13. Table 2.12 shows the long reach line card cost subject to transmission range and bitrate.

We note that a translucent network architecture can be either realized by employing the shown translucent node architecture at every node or via a heterogeneous environment

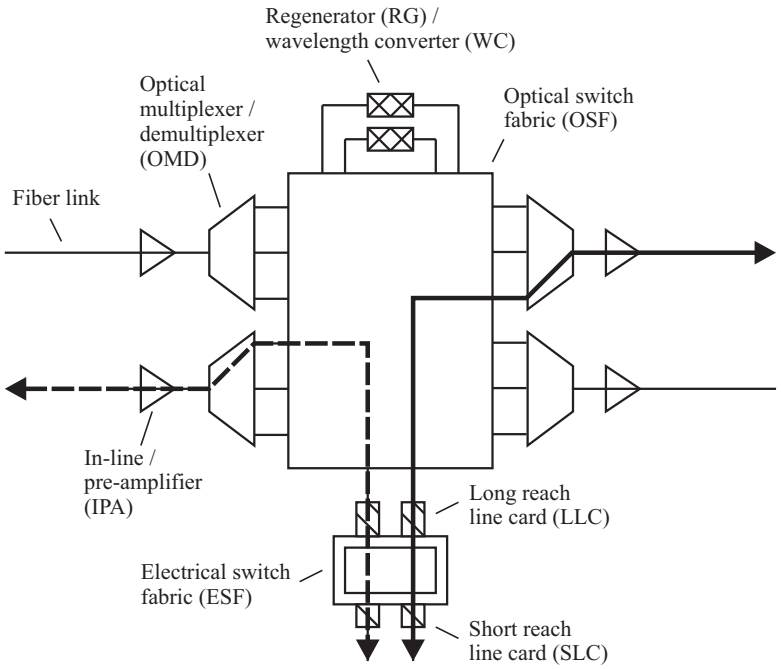

Figure 2.12: Locally adding and dropping translucent paths at a node.

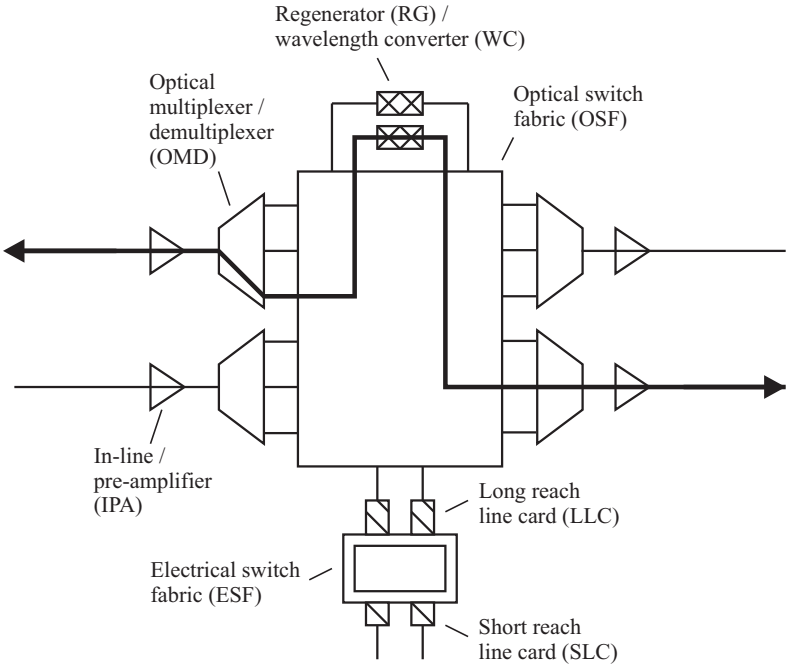

Figure 2.13: Electrical regeneration of a translucent path at a transit node.

consisting of opaque and transparent nodes [SG04] as described in the previous subsections. We focus on the former approach in the remainder of the work because it offers the fexibility to regenerate lightpaths at any node on demand.

2.4 Summary

In this chapter, we have presented an overview of optical core networks and related technologies. Fiber-optic communication offers attractive transmission characteristics by allowing for low signal attenuation and high transmission capacity due to a broadly usable frequency range in combination with wavelength division multiplexing (WDM). Network resilience is a crucial topic because a single network element failure may disrupt an enormous number of connections and cause high revenue loss due to violated service level agreement (SLA). A number of resilience schemes can be applied to recover from failures. Network operators must efficiently plan their networks to reduce costs. However, network design is a complex problem consisting of a number of interdependent tasks. Mathematical programming can be applied to solve such optimization problems and compute an optimal or near-optimal solution. It relies on an appropriate modeling of the network to form a realistic picture of the real world. Detailed node and link models were presented to reflect the characteristics of opaque, transparent, and translucent network architectures.

3 Topological Network Design

This chapter examines the topological network design. It is structured as follows. Section 3.1 discusses related work. In Section 3.2, we develop a heuristic that selects the best candidate edges from a fully meshed topology. Next, Section 3.3 formulates an optimization model for solving the topological design. In Section 3.4, the concept is demonstrated by means of case studies for realistic networks. Finally, the key findings are summarized in Section 3.5.

3.1 Related Work

Existing approaches for solving the topological design of optical transport networks can be classified into two groups, namely concepts based on integer linear programming formulations and heuristics or metaheuristics. The former category basically allows to determine optimal results. However, this is often not practical for large scenarios due to computational complexity. In contrast, the latter strategies are much faster and scale better but usually cannot identify the best solution. Most studies assume that the node locations are given and address a selective deployment of network links according to some optimization goal.

An early work on topological network design is presented in [GK77]. The authors discuss several planning aspects in the context of the Advanced Research Projects Agency Network (ARPANET), the first wide area packet switching network. They emphasize the relevance of choosing an appropriate design problem by identifying given characteristics, performance measures, variables, and constraints. An exact mathematical formulation is presented which minimizes the capacity-dependent link costs, routes all traffic demands subject to an upper limit on the average packet delay, and offers resilience via provisioning a two-connected topology. Alternative heuristics are examined in order to be able to efficiently solve the problem. One concept is a branch exchange method which starts from a random topology. After that, it sequentially performs local transformations by adding a new link and deleting an existing link. The resulting configuration is evaluated by solving the routing and dimensioning problem and comparing the costs to the initial setting. If there is a benefit, the modification is accepted and the next iteration step is performed until no further improvement can be achieved. Moreover, the authors highlight performance bounds to diagnose the efficiency of the heuristic.

In [PMdRP10] the authors analyze a number of real-world transport network topologies to identify the key characteristics. The most important parameters are nodal degree, the average number of hops according to a shortest path routing, and a clustering coefficient that reflects how densely the neighbors of a node are connected to each other. Furthermore, a link- and node-disjoint pairwise connectivity metric is introduced which specifies the average number of link- and node-disjoint paths for all node pairs. The authors develop a method which creates network topologies with similar properties. At first the network is partitioned into a number of regions where the nodes are placed. Then the nodes inside the same region are interconnected. Afterwards inter-region topology links are added and more links may be created to guarantee the nodal degree. The probability of connecting two nodes decreases exponentially subject to the ratio of their Euclidean distance and the maximum distance between any two nodes based on the Waxman model [Wax88].

The contribution in [LT08] investigates the physical topology design of all-optical networks. The authors formulate an ILP problem that minimizes the number of wavelengths allocated on each fiber link. This is motivated by the fact that costs of all-optical wavelength switches depend on the optical channel quantity. However, the optimization approach can only be applied to relatively small networks. Thus, the authors suggest a fast heuristic. It is based on a lower bound on the number of wavelengths by considering any combination of a first set of nodes and a second set of the remaining network nodes. The minimum wavelength quantity is determined by the number of lightpath demands between the two sets divided by the number of fiber links that interconnect the node sets. Starting from a minimum spanning tree topology, fiber links are iteratively added to increase the number of fiber links between any two node sets. A case study is carried out where the trade-off between link costs, estimated by the total fiber length, and the node costs, measured by the number of wavelengths, is investigated.

The study in [MKH09] examines the physical network topology design for Internet backbone networks. The authors consider a number of aspects in their design. The infrastructure costs are assumed to be dominated by the digging costs for laying fiber. In order to account for geographical restrictions, the fiber lengths are modeled via trip distances obtained from a route planner. Moreover, a combined performance metric for propagation and queuing delay is defined and survivability is addressed by providing disjoint routes. A corresponding ILP formulation turns out to be too complex from a computational point of view. The proposed heuristic starts from a full mesh graph. All demands are routed on shortest paths and the number of links is gradually reduced by removing the link which improves the cost function most, a weighted sum of the total link length and the performance metric.

In the article [MVZP06], the topological design and dimensioning of an all-photonic network is scrutinized. In order to allow for submicrosecond optical switching, the authors consider an agile network architecture based on synchronous switching of time slots. The global synchronization of all nodes relies on special switch configurations and network topologies to circumvent the necessity of optical memory. Thus, the

investigation focuses on composite star network topologies. The authors develop an appropriate integer linear programming model that places the core nodes and allocates interconnecting links.

The work in [CBFMF10] designs a physical topology using a multiobjective optimization. The goal is to minimize the total capital costs and network blocking at the same time. Physical layer effects are included in the design in terms of amplifier saturation power and noise figure. The evolutionary approach is based on genetic algorithms where the individuals of a population are assessed and selected based on their performance metric.

In [GD01a, GD01b] the authors propose a three-stage heuristic to create a network topology for an optical mesh-restorable network. Solving the complete problem of topological design, resilient routing, and network dimensioning turns out to be computationally intensive. The heuristic yields good solutions within relatively short time which is verified for some scenarios whose optimal solution could be determined.

3.2 Candidate Topology Computation

The network topology characterizes the physical fiber infrastructure. Each edge in the topological graph consists of a cable conduit that contains fiber cables for optical transmission. We assume that all edges are mutually disjoint and therefore fail independently of each other. Furthermore, we restrict to simple graphs without any loops and at most one edge between any node pair. The topological attributes strongly influence the routing and overall network design. In general, densely meshed networks permit shorter routes traversing fewer hops compared to sparse topologies. As a consequence, less capacity resources at the nodes and edges are necessary to route the traffic demands. Moreover, survivable network design can only compensate outages if the topology offers alternative routes to bypass the failure location. On the other hand, the provisioning of physical edges involves high investment costs. In addition to lighting the fibers, there are expenses for excavation work to lay the pipes and costs for rights-of-way. Thus, it is crucial to consider the trade-off between reduced capital investment due to capacity savings and the extra costs for additional edges.

The average node degree is a key parameter to classify the connectivity of the network topology. It specifies the mean number of edges at all nodes. Besides, the minimum node degree plays an important role to construct resilient networks. Any node with a single incident edge is already detached in case of a single failure of this edge. A subsequent edge outage before having repaired the initial one can isolate degree-two nodes. We aim to compute topologies with different average node degrees to allow for general statements of how the ratio of edge and node quantity affects the network capacity. Our goal is to identify design rules that reveal the optimal mesh degree of a network subject to the desired protection scheme.

In Section 3.3, we formulate an ILP to compute an optimal network topology regarding the shortest distance path routing of all demands in the network. In order to keep the computational complexity manageable, the number of eligible edges is restricted. If there is no upper limit on the edge quantity, all traffic would be routed over a direct edge between origin and destination node, yielding a fully meshed network. However, such a topology is not desirable for a number of reasons. Firstly, as stated before, the provisioning costs would be exorbitant. Secondly, fiber capacity is usually not used efficiently when routing the traffic between all node pairs on separate fibers. A high proportion of the fiber transmission equipment is necessary irrespective of the actual number of wavelengths used for data transport. This is true for optical amplifiers which boost the signal power of dozens of lightpaths within a relative broad frequency range as well as the compensation of dispersion effects. Thirdly, the computational complexity of a mathematical model based on a fully meshed graph is substantial since the number of edges grows quadratically with respect to the node quantity. Our approach assesses all edges of a fully meshed graph to create a suitable subgraph with edges that are eligible for the topological design.

We define a metric to quantify the potential of each edge to improve the shortest path routing in the network. The shorter the paths in terms of total route distances, the smaller the network resources. Let us consider a green field network scenario where only the set of nodes $\mathcal{N}$ and their locations are given. Our goal is to allocate edges and resources to route traffic between two randomly selected nodes n_1 and n_2. One may create the direct edge (n_1, n_2) and route the traffic over it. Another option is to transmit the data via another node n_3 by allocating edges (n_1, n_3) and (n_3, n_2). For the considered traffic demand, the direct edge solution is optimal with respect to resource consumption because it minimizes the transmission distance. The latter scheme necessitates two edges and requires more capacity, but additionally connects node n_3 to the network. Its attractiveness depends on the location of node n_3. If the transit node is situated close to edge (n_1, n_2), the two-hop solution (n_1, n_3) and (n_3, n_2) consumes only little extra capacity compared to the one-hop routing. The same holds true for the distance-dependent topological costs.

In order to detect such advantageous configurations, we introduce the edge eligibility score (EES) metric that quantifies an edge's potential to improve the shortest distance routing in the network. The metric is computed for each ordered node pair $(n_1, n_2) \subset \mathcal{N}^2 : n_1 \neq n_2$ according to Equation (3.1).

$$m^{\text{EES}}_{n_1,n_2} = \begin{cases} \min\limits_{n_3 \in \mathcal{N} \setminus \{n_1,n_2\}} \left(\frac{l_{n_1,n_3} + l_{n_3,n_2} - l_{n_1,n_2}}{l_{n_1,n_2}} \right) & \text{if } l_{n_1,n_2} + m^{\text{N}} \leq l^{\text{MTD}} \\ 0 & \text{else} \end{cases} \tag{3.1}$$

For each other node n_3 in the network, we determine the extra distance of the two-edge route compared to the direct edge length l_{n_1,n_2} and divide by the latter reference length. If node n_3 is closely situated to edge (n_1, n_2) we get a small positive EES. In case the route over the transit node involves a long detour, the metric yields high values.

The higher the discrepancy between the two routing configurations, the larger the metric. In other words, the higher the EES the better the routing can be improved by allocating edge (n_1, n_2) to the topology graph. The actual performance gain depends on the other edges that already have been included in the topology. We define the EES as minimum routing gain over all transit nodes n_3 so that the improvement is guaranteed irrespective of the existence of other edges. Additionally, we exclude network edges which are too long to enable optical transmission without electrical signal regeneration between the end nodes. This situation arises if the sum of edge length l_{n_1,n_2} and the equivalent node degradation length m^{N} exceeds the maximum transmission distance (MTD) length l^{MTD}.

We can thus interpret the EES as quantity that measures the relative routing metric improvement for routing traffic via a direct edge instead of provisioning two edges that connect one more node to the topology and using the corresponding two-hop route. A high EES value of a node pair indicates that the routing between the two nodes cannot be efficiently performed by any two-hop path. Consequently, the shortcut edge between the node pair is important for the shortest distance routing and should be eligible for the topological design. The following pseudo code describes the procedure of determining the eligible topology edges.

$$
\begin{aligned}
&\text{if}\big(m^{\mathrm{EES}}_{n_1,n_2} > \hat{m}^{\mathrm{EES}}\big)\ \{ \\
&\quad \mathcal{E}^{\mathrm{BD}} = \mathcal{E}^{\mathrm{BD}} \cup \{(n_1, n_2)\}; && \forall\, \{n_1, n_2\} \subset \mathcal{N} && (3.2)\\
&\}\\
&\text{while}\Big(\sum_{\substack{(n_2,n_3)\in\mathcal{E}^{\mathrm{BD}}:\\ n_2=n_1 \vee n_3=n_1}} 1 < \check{z}^{\mathrm{ND}}\Big)\ \{ \\
&\quad \mathcal{E}^{\mathrm{BD}} = \mathcal{E}^{\mathrm{BD}} \cup \big\{(n_2, n_3) : \{n_2, n_3\} \subset \mathcal{N} \wedge \\
&\qquad \wedge\, (n_2 = n_1 \ \vee\ n_3 = n_1) \wedge \\
&\qquad \wedge\, (n_2, n_3) \notin \mathcal{E}^{\mathrm{BD}} \wedge && \forall\, n_1 \in \mathcal{N} && (3.3)\\
&\qquad \wedge\, m^{\mathrm{EES}}_{n_2,n_3} = \max_{\substack{\{n_4,n_5\}\subset\mathcal{N}:\\ n_4=n_1 \vee n_5=n_1 \wedge \\ (n_4,n_5)\notin\mathcal{E}^{\mathrm{BD}}}} \big(m^{\mathrm{EES}}_{n_4,n_5}\big) \neq 0\big\}; \\
&\}
\end{aligned}
$$

The Commands (3.2) consider any unordered node pair to analyze each potential bidirected edge in the network. Initially, the set of bidirected topology edges $\mathcal{E}^{\mathrm{BD}}$ is empty. If the EES metric exceeds the threshold $\hat{m}^{\mathrm{EES}}$, the respective edge is added to $\mathcal{E}^{\mathrm{BD}}$ because it has a strong potential to improve the routing. The desired number of edges that should be taken into account can be controlled by varying the threshold.

Another crucial topological characteristic is the minimum nodal degree because it determines how many edge failures can be compensated until the node location is isolated. In order to guarantee a minimal connectivity per node, we allocate more edges by Commands (3.3) if necessary. As long as the actual number of incident edges is

smaller than the desired lower bound $\check{z}^{\mathrm{ND}}$ on the nodal degree, we choose the edge with maximum EES that is connected to the considered node from the remaining unselected edges.

3.3 Mathematical Program Formulation

In this section we develop the ILP for planning the network topology. A number of symbols are introduced to denote the relevant sets, elements, parameters, and variables. Furthermore, certain formulations are used to facilitate compact terms. A compilation of the syntax and symbols can be found in Appendix C.

The formulation $\{n_1, n_2\} \subset \mathcal{N}$ represents all distinct two-node subsets of the network nodes. A set represents a collection of objects that can be distinguished from each other. By definition the sequence of the elements of a set is irrelevant, i.e. sets $\{n_1, n_2\}$ and $\{n_2, n_1\}$ are identical. Furthermore, a set is determined by the members it contains irrespective of their frequency of occurrence ($\{n_1, n_1, n_2\} = \{n_1, n_2\}$). The notation $\{n_1, n_2\} \subset \mathcal{N}$ thus implicitly assumes that node n_1 is different from node n_2 ($n_1 \neq n_2$). We consider all unordered node pairs of the network and model the routing in a bidirectional way. Usually, the elements of a set are written in an intuitive sequence to improve readability which can be alphabetical order with respect to the node labels in our case. We adopt the node sequence of the set representation and apply it to the index of various parameters and variables that depend on the considered unordered node pair omitting the braces. It is worth to note that this sequence is not relevant and that no additional parameters and variables are required to consider the reverse node order.

We formulate the topological design optimization model using the flow approach for routing the traffic. This strategy requires a directed graph where adjacent nodes are connected by a pair of directed edges with opposite direction. The conceptual view of directed edges allows to analyze the outgoing and incoming traffic at each network node and thereby control the end-to-end routing. The physical network scenario is characterized by the set of nodes $\mathcal{N}$ and directed candidate edges $\mathcal{E}^{\mathrm{DI}}$. For each unordered node pair $\{n_1, n_2\} \subset \mathcal{N}$, the number of bidirectional traffic demands is given by d_{n_1,n_2}. We model the routing from node n_1 to node n_2 by a binary link variable $L_{n_1,n_2,e^{\mathrm{DI}}}$ for any directed network edge $e^{\mathrm{DI}} \in \mathcal{E}^{\mathrm{DI}}$ with geographical length $l^{\mathrm{ED}}_{e^{\mathrm{DI}}}$. Our aim is to design a network topology that optimizes the shortest path routing of all demands for a given maximum number of edges. This is motivated by the reduced network resource consumption as opposed to longer paths and thereby can reduce capital expenditures. The availability of short routes depends on the existence of network edges. The more nodes are connected via a direct edge, the fewer hops are necessary to reach the destination node. However, the provisioning of edges involves significant expenses for rights-of-way, construction work, and transmission equipment. Since all traffic requests will follow the shortest available route, they can be modeled by a single flow from origin to destination node. The actual capacity requirements of

this routing are given by d_{n_1,n_2}. Due to the same reason, although the network model is directed, it is sufficient to consider only one routing direction (from node n_1 to n_2) for each node pair. The optimization model can be formulated as follows.

Minimize

$$\sum_{\substack{\{n_1,n_2\}\subset\mathcal{N}:\\ n_1\neq n_2}} \sum_{e^{\mathrm{DI}}\in\mathcal{E}^{\mathrm{DI}}} L_{n_1,n_2,e^{\mathrm{DI}}} \cdot l^{\mathrm{ED}}_{e^{\mathrm{DI}}} \cdot d_{n_1,n_2} \tag{3.4}$$

subject to

$$\sum_{\substack{e^{\mathrm{DI}}\in\mathcal{E}^{\mathrm{DI}}:\\ \theta_{n_1,e^{\mathrm{DI}}}=1}} L_{n_1,n_2,e^{\mathrm{DI}}} = z^{\mathrm{DR}} \qquad \forall\,\{n_1,n_2\}\subset\mathcal{N}: n_1\neq n_2, \tag{3.5}$$

$$\sum_{\substack{e^{\mathrm{DI}}\in\mathcal{E}^{\mathrm{DI}}:\\ \iota_{n_1,e^{\mathrm{DI}}}=1}} L_{n_1,n_2,e^{\mathrm{DI}}} = 0 \qquad \forall\,\{n_1,n_2\}\subset\mathcal{N}: n_1\neq n_2, \tag{3.6}$$

$$\sum_{\substack{e^{\mathrm{DI}}\in\mathcal{E}^{\mathrm{DI}}:\\ \iota_{n_2,e^{\mathrm{DI}}}=1}} L_{n_1,n_2,e^{\mathrm{DI}}} = z^{\mathrm{DR}} \qquad \forall\,\{n_1,n_2\}\subset\mathcal{N}: n_1\neq n_2, \tag{3.7}$$

$$\sum_{\substack{e^{\mathrm{DI}}\in\mathcal{E}^{\mathrm{DI}}:\\ \theta_{n_2,e^{\mathrm{DI}}}=1}} L_{n_1,n_2,e^{\mathrm{DI}}} = 0 \qquad \forall\,\{n_1,n_2\}\subset\mathcal{N}: n_1\neq n_2, \tag{3.8}$$

$$\sum_{\substack{e^{\mathrm{DI}}\in\mathcal{E}^{\mathrm{DI}}:\\ \theta_{n_3,e}=1}} L_{n_1,n_2,e} = \sum_{\substack{e^{\mathrm{DI}}\in\mathcal{E}^{\mathrm{DI}}:\\ \iota_{n_3,e}=1}} L_{n_1,n_2,e^{\mathrm{DI}}} \qquad \forall\,\{n_1,n_2\}\subset\mathcal{N}: n_1\neq n_2,\ n_3\in\mathcal{N}\setminus\{n_1,n_2\}, \tag{3.9}$$

$$\sum_{\substack{e^{\mathrm{DI}}\in\mathcal{E}^{\mathrm{DI}}:\\ \mathcal{N}^{\mathrm{ED}}_{e^{\mathrm{DI}}}=\mathcal{N}^{\mathrm{ED}}_{e^{\mathrm{BD}}}}} L_{n_1,n_2,e} \leq E_{e^{\mathrm{BD}}} \qquad \forall\,\{n_1,n_2\}\subset\mathcal{N}: n_1\neq n_2,\ e^{\mathrm{BD}}\in\mathcal{E}^{\mathrm{BD}}, \tag{3.10}$$

$$\sum_{\substack{e^{\mathrm{DI}}\in\mathcal{E}^{\mathrm{DI}}:\\ \theta_{n,e^{\mathrm{DI}}}=1}} L_{n_1,n_2,e^{\mathrm{DI}}} \leq 1 \qquad \forall\,\{n_1,n_2\}\subset\mathcal{N}: n_1\neq n_2,\ n\in\mathcal{N}\setminus\{n_1,n_2\}, \tag{3.11}$$

$$\sum_{e^{\mathrm{BD}}\in\mathcal{E}^{\mathrm{BD}}} E_{e^{\mathrm{BD}}} \leq z^{\mathrm{ED}}, \tag{3.12}$$

$$L_{n_1,n_2,e^{\mathrm{DI}}} \in \{0,1\} \qquad \forall\,\{n_1,n_2\}\subset\mathcal{N}: n_1\neq n_2,\ e^{\mathrm{DI}}\in\mathcal{E}^{\mathrm{DI}}, \tag{3.13}$$

$$E_{e^{\mathrm{BD}}} \in \{0,1\} \qquad \forall\, e^{\mathrm{BD}}\in\mathcal{E}^{\mathrm{BD}}. \tag{3.14}$$

- The Objective (3.4) minimizes the total path metric of all routed traffic demands. We consider all unsorted origin/destination node pairs and summarize the path metrics by counting up the product of link variable, corresponding edge length, and the number of traffic demands for each directed path edge.
- Constraints (3.5) create the egress traffic flow at the origin node of each two-node set to route demands between them. The number of outgoing links depends on the

number of redundant paths in addition to the primary connection to compensate network failures. The total ingress flows at the demand's origin node must be zero according to Equation (3.6).

- The next two equations are the corresponding counterpart constraints at the destination node of each demand relation. Constraints (3.7) terminate the sink flow and Equations (3.8) prevent any egress traffic.
- Apart from the origin and destination node, the flow continuity must be guaranteed at each other node in the network. Constraints (3.9) create an equivalent number of incoming and outgoing links at the considered node.
- Equations (3.10) control the routing between each node pair per bidirectional network edge and combine two routing characteristics. Firstly, paths are allocated on edge-disjoint routes. Directed flows of the same demand relation cannot pass through any bidirected edge in forward and reverse direction at the same time, because the sum of links per edge on the left-hand side of the equation is limited by the binary edge variable. Secondly, candidate edges are allocated if they are traversed by any flow since the number of links serves as lower bound for the edge variable on the other hand.
- In order to yield node-disjoint path configurations Constraints (3.11) must be added. The formulation limits the number of incoming flows at each node other than origin or destination to one.
- Constraint (3.12) restricts the number of allocated edges in the network that may be used for the routing. It helps to adjust the topology to an appropriate subset of the highly meshed candidate topology.

3.4 Case Studies

In the following, we explore the topological design strategy by carrying out case studies for a German, European, and US reference network. This allows us to compare scenarios that differ in the number of network nodes and transmission distances. The network characteristics are taken from publications [HBB+04] and [BDH+99], respectively. However, our starting point is a green field where only the node locations and the traffic demands between the sites are given. In a first step, we pre-compute the set of all eligible edges according to the candidate topology assessment described in Section 3.2. The corresponding candidate network topologies are depicted in Figures 3.1, 3.5, and 3.9, respectively. Appendix A presents more detailed characteristics like geographical node sites and edge lengths. After that, the previously described mathematical model determines optimal toplogies and routing configurations. We design networks with various average node degrees by varying the maximum number of edges that may be allocated. Furthermore, we compensate single and dual failures by applying appropriate path protection schemes with one and two alternative paths, respectively.

3.4.1 Single Failure Compensation

At first we deal with single network failures by routing two disjoint end-to-end paths for each connection request. Depending on the failure type that should be recovered, the route pair must not traverse a common edge or transit node. The most sparsely meshed network that supports 1:1 path protection for any node pair is a ring network. In this case, the number of edges equals the node quantity.

German Reference Network Scenario

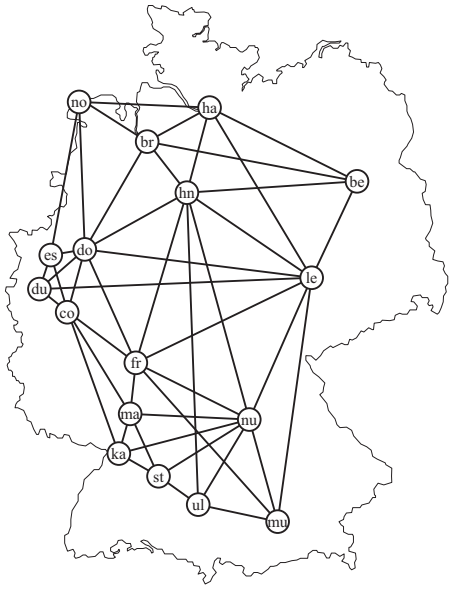

Figure 3.1: Candidate topology of the German reference network.

The candidate topology including all eligible edges for the German network scenario as presented in Figure 3.1 serves as starting point. Based on this structure, various topologies with a different number of edges are computed. Figure 3.3a shows the average connection capacity per demand for the resulting topologies in the German network scenario. It depicts the mean length of all links that must be provided to satisfy a demand offering 1:1 path protection. There are two curves for the edge-disjoint and node-disjoint routing, respectively. We can see that the resource requirements of both approaches do not differ significantly from each other. The maximum extra capacity of node-disjoint paths is less than 0.5%. Node-disjoint paths are also edge-disjoint because otherwise they would share the edge's end nodes. Therefore, a capacity-efficient node-disjoint routing is restricted to a subset of all edge-disjoint configurations achieving at most the same performance as the edge-disjoint scheme.

At least 17 edges are required to form a ring that interconnects all network nodes in the German scenario. The ring structure requires the highest amount of resources per connection. In order to satisfy a demand, the primary path may be routed on the shortest

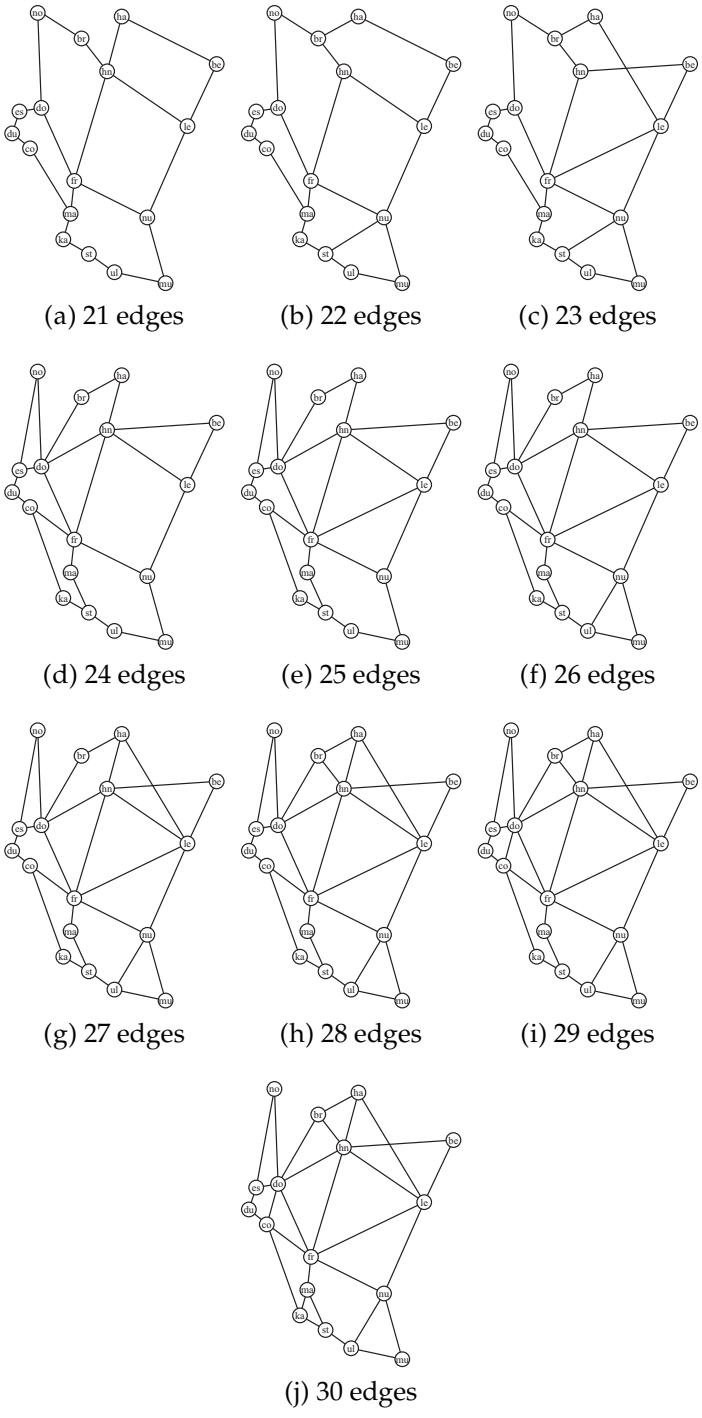

(a) 21 edges (b) 22 edges (c) 23 edges

(d) 24 edges (e) 25 edges (f) 26 edges

(g) 27 edges (h) 28 edges (i) 29 edges

(j) 30 edges

Figure 3.2: Network topologies computed for the German reference network designed for node-disjoint 1:1 path protection.

path option. However, even if the working path has a small length, the protection path must follow the remaining ring segment traversing all other network nodes. Thus, each demand requires link capacity on all network edges to configure 1:1 path protection.

There is notable capacity reduction of 28% by allowing just one more edge in the network. In this case two nodes can have three incident edges permitting a network topology of two overlapping rings. Increasing the number of eligible network edges to 19 and 20 further reduces the average link capacity by 16% and 12%, respectively. Paths involve fewer hops because more direct edges to reach the destination are available. However, the relative resource saving potential becomes smaller and smaller for more densely meshed networks. The higher the number of edges, the fewer demands benefit from an extra edge. This is due to the fact that routing configurations can only be improved for a narrow network region.

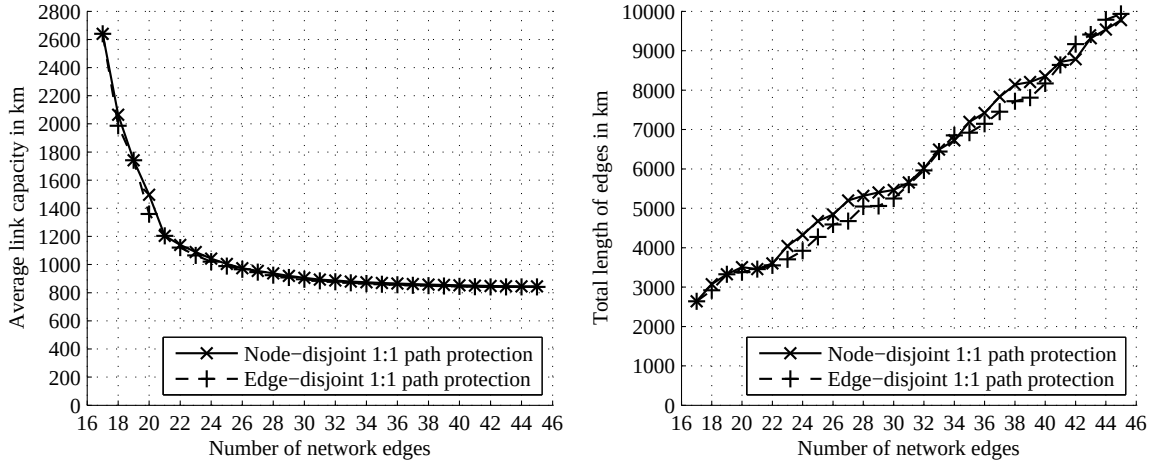

(a) Connection capacity (b) Topology dimension

Figure 3.3: Connection capacity and topology dimension for various German reference network topologies designed for 1:1 path protection.

Figure 3.3b shows the dimension of each resulting network topology in terms of total length of all inserted edges. If we assume that the costs to provide a fiber cable are proportional to the length of the edge, the diagram can be directly translated to topological costs. Node-disjoint path protection sometimes causes slightly higher overall edge lengths compared to the edge-disjoint scheme in the range of 5% to 10%, but it can also be the other way round.

The resulting network topologies are depicted in Figure 3.2. We observe that network topologies with similar average node degree can look quite different (see 3.2c and 3.2d). Consequently, a network provider should think carefully about the mesh intensity because a subsequent topological upgrade of the network by an additional edge may not necessarily represent the optimal solution.

European Reference Network Scenario

Figure 3.4 illustrates the corresponding results for the European network environment. The average link capacity is almost identical for node- and edge-disjoint 1:1 path

protection. The same holds true for the total extent of the designed topologies. Except for one case, the topologies for node- and edge-disjoint design are identical. It often seems to be preferable to prevent working and protection path from traversing a common intermediate node in order to minimize the total routing distance.

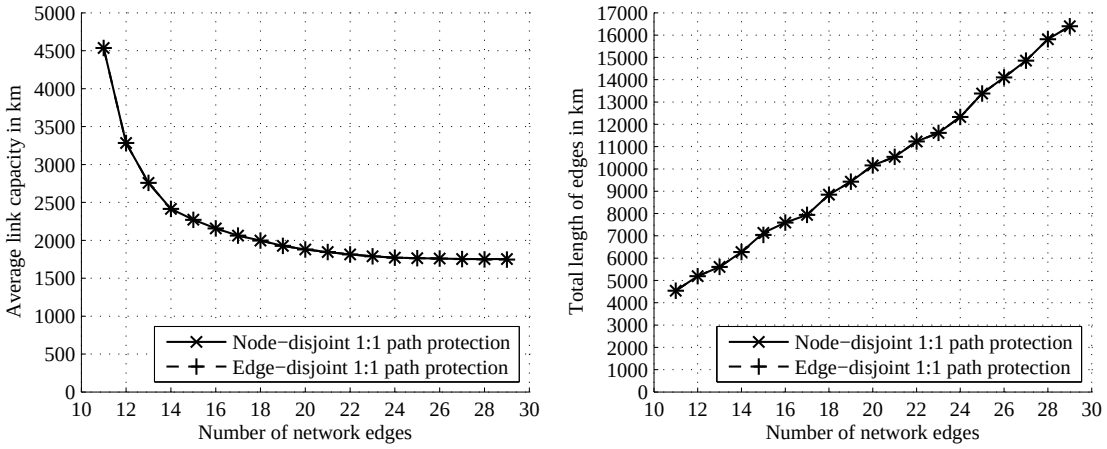

(a) Connection capacity (b) Topology dimension

Figure 3.4: Connection capacity and topology dimension for various European reference network topologies designed for 1:1 path protection.

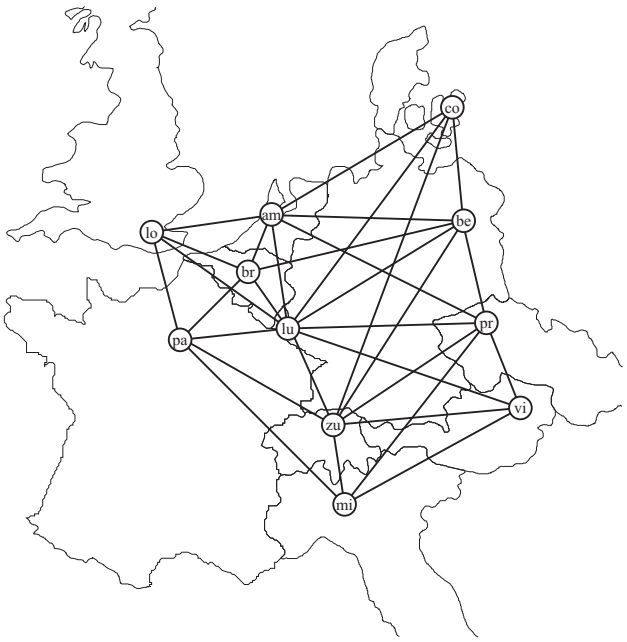

Figure 3.5: Candidate topology of the European reference network.

The corresponding network structures for the node-disjoint topological design are depicted in Figure 3.6. The graphs represent optimal topologies for a range of different average nodal degrees that restrict the number of edges which can be allocated from the candidate topology in Figure 3.5.

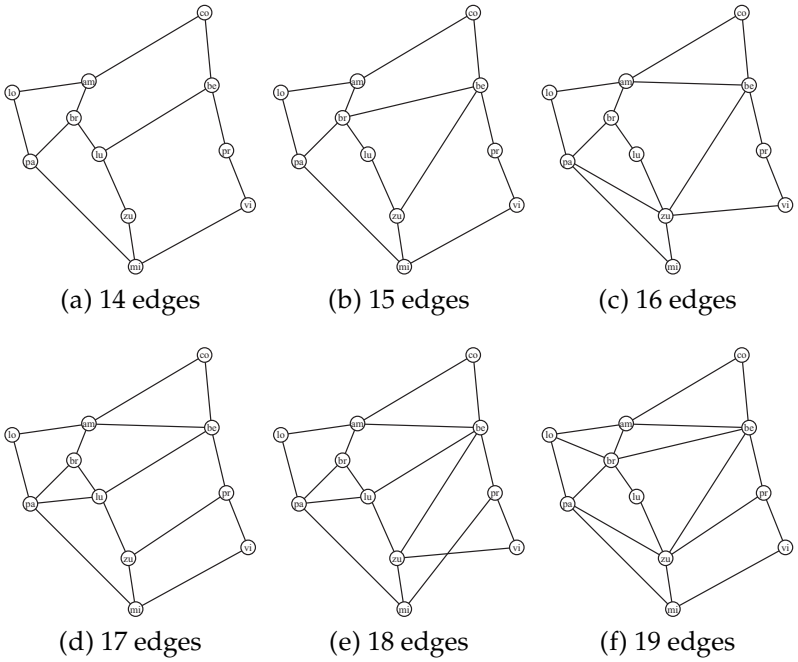

(a) 14 edges (b) 15 edges (c) 16 edges

(d) 17 edges (e) 18 edges (f) 19 edges

Figure 3.6: Network topologies computed for the European reference network designed for node-disjoint 1:1 path protection.

US Reference Network Scenario

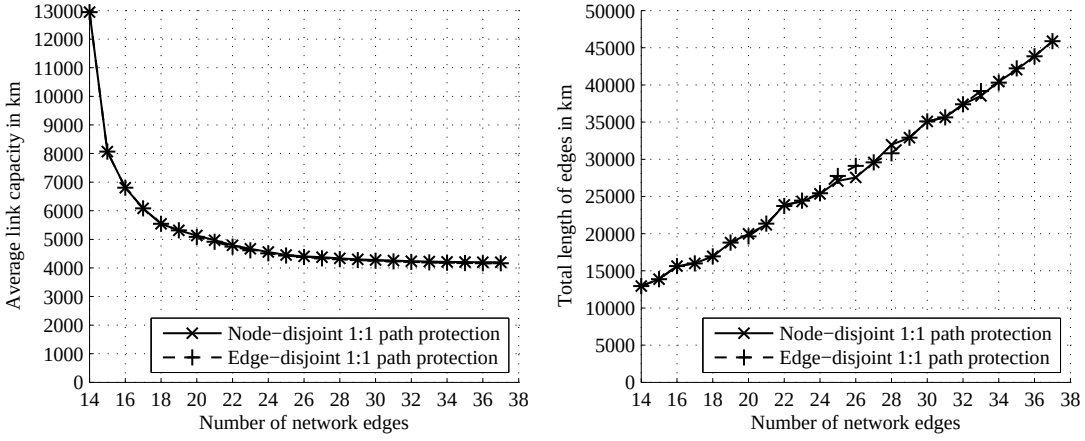

(a) Connection capacity (b) Topology dimension

Figure 3.7: Connection capacity and topology dimension for various US reference network topologies designed for 1:1 path protection.

The US network reference scenario is analyzed in Figure 3.7. Again, the network capacity significantly decreases when allowing a few more edges than are necessary to form a ring network. For an average node degree in the range of 4.0, the resource

consumption almost stagnates. On the other hand, the total length of all edges and by association the topological costs increase linearly with the number of edges.

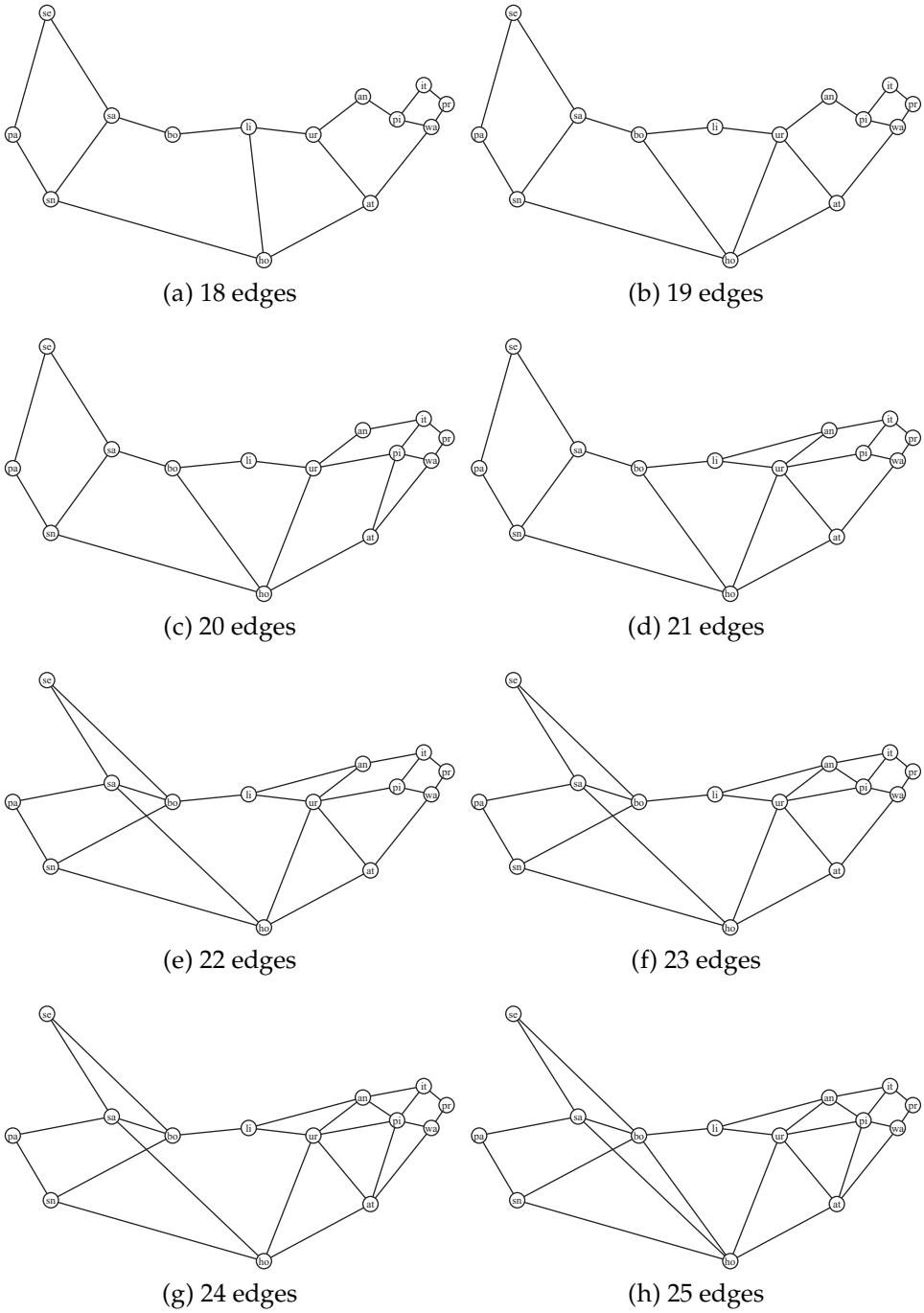

(a) 18 edges (b) 19 edges

(c) 20 edges (d) 21 edges

(e) 22 edges (f) 23 edges

(g) 24 edges (h) 25 edges

Figure 3.8: Network topologies computed for the European reference network designed for node-disjoint 1:1 path protection.

Figure 3.8 portrays the resulting network topologies for node-disjoint 1:1 path protection. The graphs are calculated based on the candidate topology in Figure 3.9 when

limiting the number of network links to values between 18 and 25. We observe that the edges tend to be allocated at a more central network position for increasingly meshed topologies.

Figure 3.9: Candidate topology of the US reference network.

3.4.2 Dual Failure Compensation

In order to reduce the impact of network outages, the topology and routing can be adapted to recover from dual failures. Two backup paths are necessary in addition to the primary path and all paths must be mutually disjoint so that any failure can disrupt the transmission along at most one of the paths. Such a routing configuration can only be met by a topology that offers at least three incident edges for each network node. In this case, no network node is isolated because of a dual failure affecting two edges that are connected to the same node. Considering a network with node set $\mathcal{N}$, the minimum total number of edges is given by $1.5 \cdot |\mathcal{N}|$. The factor 1.5 relates to three mandatory edges per node, where each edge is incident on two nodes (3/2).

German Reference Network Scenario

Figure 3.10a portrays the average capacity consumption per traffic request in terms of total link kilometers for a varying number of network edges. We notice that the mean capacity consumption of 2:1 path protection in a minimum network topology with 26 edges is smaller than the resources of 1:1 protection in a ring topology (see Section 3.4.1). The worst case relative extra capacity of a node-disjoint routing compared to the edge-disjoint scheme is at most 5%. Thus, this effect is more pronounced than for 1:1 path protection. It is due to a higher probability for a common transit node when routing three edge-disjoint paths in a capacity-efficient manner. Similar to the

single failure case, the relative capacity reduction decreases for more densely meshed topologies. When analyzing the topology with 30 edges, for example, the mean link capacity per demand for 2:1 protection exceeds the 1:1 requirements by 100% and 103% for edge- and node-disjoint routing, respectively. Three paths have less flexibility for a disjoint routing than two paths and consequently have to follow considerably longer routes.

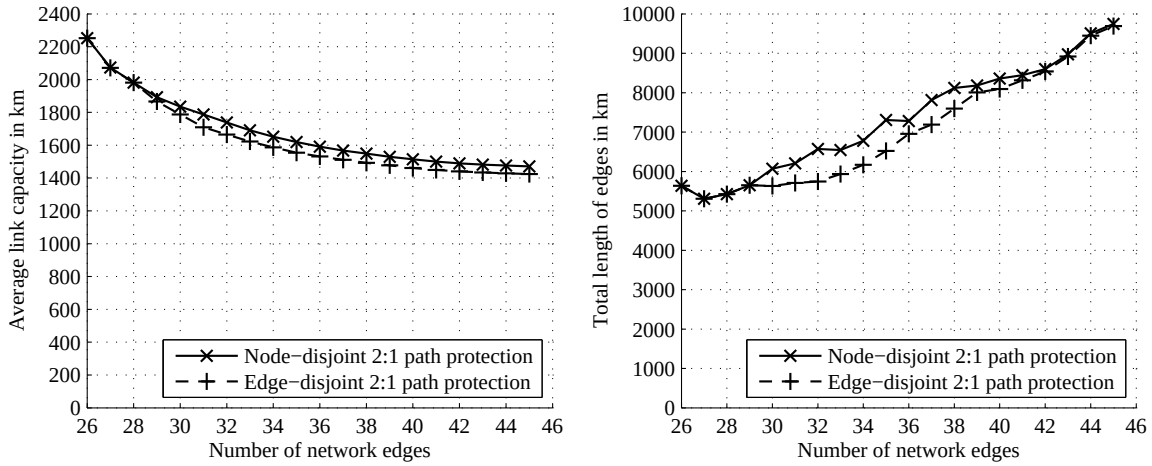

(a) Connection capacity (b) Topology dimension

Figure 3.10: Connection capacity and topology dimension for various German reference network topologies designed for 2:1 path protection.

The total extent of each network topology is displayed in Diagram 3.10b. Due to the minimum degree three for each node, the least meshed topology already causes an overall length of almost 6000 km. Compared to that, the 1:1 protection topology with a corresponding number of 26 edges has an overall edge length of less than 5000 km. However, we want to point out that the topology size is not included in the objective function. Instead, we emphasize the routing of all demands on shortest paths to minimize the overall network capacity. As a consequence, the total length of all network edges can even decline when increasing the number of edges because long edges may be replaced by shorter ones. This peculiarity occurs at the transition from 26 to 27 network edges, for example.

European Reference Network Scenario

The corresponding diagrams for the European network context are depicted in Figure 3.11. The results for node- and edge-disjoint path protection are again very similar deviating from each other by not more than 0.5%. This can be attributed to the small number of nodes rarely yielding shortest edge-disjoint routing configurations that have a common transit node. Therefore, the same topology and almost identical routing configuration is often optimal for node-disjoint path protection as well.

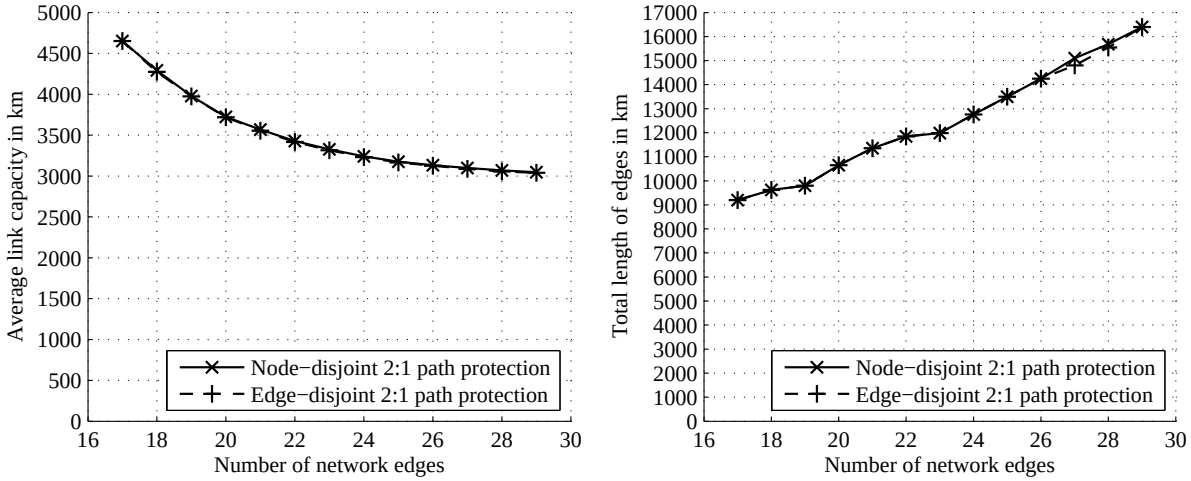

(a) Connection capacity (b) Topology dimension

Figure 3.11: Connection capacity and topology dimension for various European reference network topologies designed for 2:1 path protection.

US Reference Network Scenario

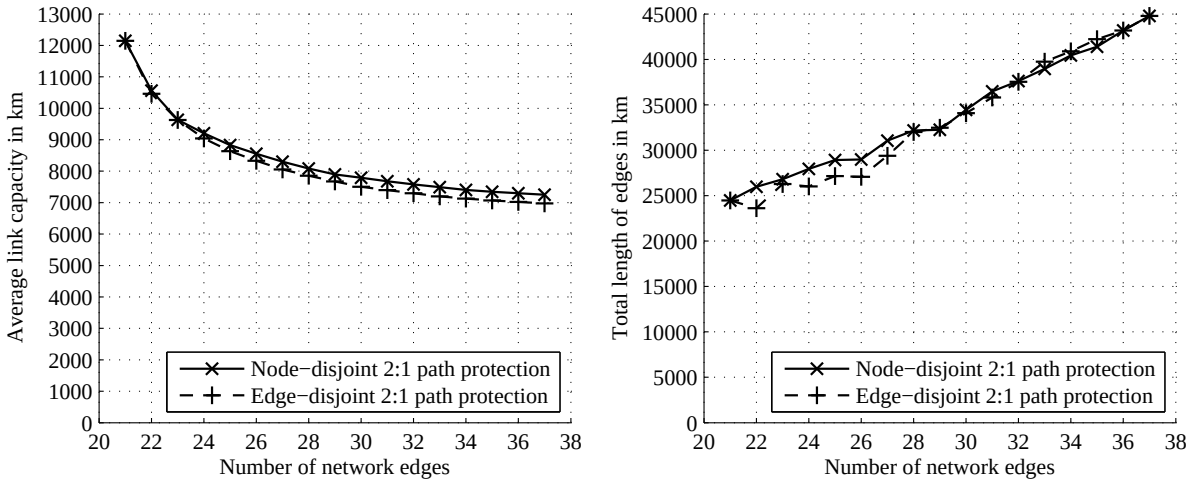

(a) Connection capacity (b) Topology dimension

Figure 3.12: Connection capacity and topology dimension for various US reference network topologies designed for 2:1 path protection.

The outcome for the US reference network scenario is shown in Figure 3.12. Except for the minimum possible edge number 21, the node-disjoint configuration continuously involves an additional capacity of 1% to 4%. In order to prevent the sharing of transit nodes for working and backup paths, the topology size increases by up to 10%.

The computational complexity of the topological design depends on the size of the network defined by the number of nodes and candidate edges. Furthermore, the desired edge quantity also plays an important role. For a small number of edges close to the limit of being able to find a feasible solution, it takes more time to solve the problem. This is because the decision whether to include an edge in the topology is strongly influenced by the decisions for other edges. All results for the European and US network are solved to optimality. The computation time per instance is less than 10 minutes for the 11-node European network and 4 hours for the 14-node US network. In the 17-node German reference scenario, optimality could not be proved for all topologies within a reasonable amount of time because the computation time is in the order of a few days.

3.5 Summary

In this chapter, we have investigated the topological network design of optical core networks. The geographical location of all network nodes was assumed to be given. In order to keep the computational complexity at a manageable level, we decomposed the design into two steps. Initially, a fully-meshed topology is considered. In a first phase, we reduce the number of edges to a reasonably large set by selecting the ones with the highest potential to improve a shortest path routing. Our motivation is to reduce the overall network capacity. For this purpose, we develop a novel EES performance metric. Moreover, minimum nodal degrees are to be met for resilience reasons with respect to failures. The resulting topology comprises a set of eligible edges which may be utilized in a subsequent routing step based on ILP. A number of case studies have been carried out for a German, European, and US network scenario. Our results show that capacity consumption can be notably lowered by adding few extra network links. An important finding is that a topology can be designed to support node-disjoint routing at little extra costs compared to a corresponding topology which only facilitates edge-disjoint routes.

4 Opaque Versus Translucent Network Design

This chapter explores the total capital expenditures for an opaque and a translucent network design. The next section presents related work in this context. Section 4.2 deals with an optimal translucent lightpath design by selectively provisioning regenerators. The routing and network dimensioning optimization model is developed for both scenarios in Section 4.3. Section 4.4 solves the wavelength assignment and converter allocation problem for the translucent architecture. A number of case studies are carried out in Section 4.5. Finally, Section 4.6 summarizes this chapter.

4.1 Related Work

An overview of translucent optical network design is presented in [ST07]. The authors show that translucent networks can be classified into three basic categories. Sparse signal regeneration may be realized by transparent network islands interconnected via border regeneration nodes, a small number of opaque nodes, or translucent node architectures. A number of key issues for network planning are described. Moreover, the authors motivate other interesting research topics in this context like sparse grooming or sparse fault detection.

The authors of [PHS+07] investigate an integrated design of a transparent optical network. They propose a concept of routing, fiber, and wavelength assignment which decomposes the overall traffic into sequentially arriving demands. Firstly, shortest routes between all nodes of the network topology are pre-calculated. In a second step, a first estimation of the required number of fibers is performed. After this, the next most critical lightpath request is selected and an ILP model is solved that routes the connection, selects the fibers, and assigns a free wavelength. Moreover, 1+1 path protection is implemented. The last step treats one request after another. However, blocking can occur due to lack of wavelength channels which makes it necessary to correct the initial guess of fiber capacity. The authors minimize the lightpath lengths in order to be able to allocate cheaper transmission systems with reduced transmission range. The resulting total costs include the expenses for transponders, switches, amplifiers, and dispersion compensating fiber.

When routing translucent or transparent lightpaths, it is essential to ensure signal quality in order to be able to correctly detect the signal at the receiver. The article [AKM+09] presents a survey on physical layer impairments aware routing and wavelength assignment algorithms. The authors explain the physical layer degradation effects and classify

available concepts to assess impairments into two categories. Analytical models yield formulas to characterize the impairments whereas hybrid approaches involve simulation or monitoring techniques. Various algorithmic approaches for solving the routing and wavelength assignment problem in the context of physical layer impairments are discussed.

In [PMD09] the authors examine opaque, transparent, and semi-transparent networks in terms of architecture and equipment costs. Integer linear programs are formulated for all network types. Given are the fiber topology and demand requests at different bitrates. The objective is to minimize the overall network equipment expenses according to a detailed cost model. The optimization models perform either an unprotected routing or consider 1+1 link-disjoint path protection. However, the authors state that the models are too complex to solve realistic network scenarios efficiently.

The work in [DGMK+10] investigates different translucent optical network architectures. The authors examine three node implementations with diverse capabilities and perform a thorough cost analysis considering capital expenditures as well as operational expenditures. Two alternative approaches for designing the network via an offline impairment-aware routing and wavelength assignment algorithm are developed. The exact algorithm evaluates the quality of transmission of each lightpath in detail whereas the relaxed algorithm adds a safety margin.

The article [MCL+03] examines the design of a pan-European fiber optic backbone network. For multiple topologies, a shortest path routing approach is applied to compare the capacity requirements, overall costs, and availability performance. The authors account for the traffic classes voice, transaction data, and Internet traffic which are either protected by 1+1 path protection or remain unprotected. The network model consists of IP routers that interface to optical crossconnects with wavelength conversion capability and WDM line systems. Moreover, given traffic demands are extrapolated via forecast to investigate future scenarios.

4.2 Translucent Lightpath Design

The following optimization model calculates an efficient design of translucent lightpaths. An explanation of the syntax and symbols can be found in Appendix C.

The mathematical program is based on the flow conservation formulation for the routing of traffic requests. However, in contrast to the flow concept applied to the topological network design in Section 3.3, we do not consider individual link flows per network edge. Instead, we deal with transparent wavelength path (WP) segments that are concatenated to form an end-to-end translucent partial virtual wavelength path (PVWP) path. Thus, the underlying routes of the WP segments are modeled as directed routes to differentiate their orientation. The set of all directed transparent routes starting at node n_1 and ending at node n_2 is given by $\mathcal{R}^{\mathrm{WP,DI}}_{1,n_1,n_2}$. It is a subset of all single

routes between the two nodes allowing lightpaths to be set up without electrical signal regeneration at any transit node. The number of transparent routes depends on the geographical distance between the considered node pair, the network topology, and the maximum transmission distance (MTD) dictated by the transmission technology. Nodes which are far apart from each other may only have few transparent routes between them or none. On the other hand, nodes situated close to each other usually offer a large variety of WPs. The decision whether a certain transparent route segment r^{WP} is chosen is indicated by binary variables $P_{r^{\mathrm{WP}}}$. Every corresponding transparent path is regenerated at the route's end nodes. If the wavelength path starts or ends at the origin or destination node of the translucent path, LLCs are responsible. Otherwise, this is performed by electrical signal regenerators at the translucent path's transit nodes. The associated costs depend on the actual transmission range $t_{r^{\mathrm{WP}}}$ which is required to support the WP along its route and are denoted by $c^{\mathrm{LLC}}_{t_{r,\mathrm{WP}}}$ and $c^{\mathrm{RG}}_{t_{r,\mathrm{WP}}}$, respectively. These costs per path node n are assigned to variable C^{NO}_n. The transmission equipment of all translucent paths on route r can be determined by the following ILP.

$\forall\, \{n_1, n_2\} \subset \mathcal{N} : n_1 \neq n_2,\ r \in \mathcal{R}_{1,n_1,n_2}$,

minimize

$$\sum_{n_3 \in \mathcal{N}_r^{\mathrm{DR}}} C^{\mathrm{NO}}_{n_3} \tag{4.1}$$

subject to

$$\sum_{\substack{n_3 \in \mathcal{N}_r^{\mathrm{DR}}:\\ n_3 \neq n_1}} \sum_{\substack{r^{\mathrm{WP}} \in \mathcal{R}^{\mathrm{WP,DI}}_{1,n_1,n_3}:\\ \psi_{r^{\mathrm{WP}},r}=1}} P_{r^{\mathrm{WP}}} = 1, \tag{4.2}$$

$$\sum_{\substack{n_3 \in \mathcal{N}_r^{\mathrm{DR}}:\\ n_3 \neq n_2}} \sum_{\substack{r^{\mathrm{WP}} \in \mathcal{R}^{\mathrm{WP,DI}}_{1,n_3,n_2}:\\ \psi_{r^{\mathrm{WP}},r}=1}} P_{r^{\mathrm{WP}}} = 1, \tag{4.3}$$

$$\sum_{\substack{n_4 \in \mathcal{N}_r^{\mathrm{DR}}:\\ n_4 \neq n_3}} \sum_{\substack{r^{\mathrm{WP}} \in \mathcal{R}^{\mathrm{WP,DI}}_{1,n_3,n_4}:\\ \psi_{r^{\mathrm{WP}},r}=1}} P_{r^{\mathrm{WP}}} = \sum_{\substack{n_4 \in \mathcal{N}_r^{\mathrm{DR}}:\\ n_4 \neq n_3}} \sum_{\substack{r^{\mathrm{WP}} \in \mathcal{R}^{\mathrm{WP,DI}}_{1,n_4,n_3}:\\ \psi_{r^{\mathrm{WP}},r}=1}} P_{r^{\mathrm{WP}}} \qquad \forall\, n_3 \in \mathcal{N}_r^{\mathrm{DR}} \setminus \{n_1, n_2\}, \tag{4.4}$$

$$C^{\mathrm{NO}}_{n_1} = \sum_{\substack{n_3 \in \mathcal{N}_r^{\mathrm{DR}}:\\ n_3 \neq n_1}} \sum_{\substack{r^{\mathrm{WP}} \in \mathcal{R}^{\mathrm{WP,DI}}_{1,n_1,n_3}:\\ \psi_{r^{\mathrm{WP}},r}=1}} c^{\mathrm{LLC}}_{t_{r,\mathrm{WP}}} \cdot P_{r^{\mathrm{WP}}}, \tag{4.5}$$

$$C^{\mathrm{NO}}_{n_2} = \sum_{\substack{n_3 \in \mathcal{N}_r^{\mathrm{DR}}:\\ n_3 \neq n_2}} \sum_{\substack{r^{\mathrm{WP}} \in \mathcal{R}^{\mathrm{WP,DI}}_{1,n_3,n_2}:\\ \psi_{r^{\mathrm{WP}},r}=1}} c^{\mathrm{LLC}}_{t_{r,\mathrm{WP}}} \cdot P_{r^{\mathrm{WP}}}, \tag{4.6}$$

$$C^{\mathrm{NO}}_{n_3} = \sum_{\substack{n_4 \in \mathcal{N}_r^{\mathrm{DR}}:\\ n_4 \neq n_3}} \sum_{\substack{r^{\mathrm{WP}} \in \{\mathcal{R}^{\mathrm{WP,DI}}_{1,n_3,n_4},\\ \mathcal{R}^{\mathrm{WP,DI}}_{1,n_4,n_3}\}:\\ \psi_{r^{\mathrm{WP}},r}=1}} 0.5 \cdot c^{\mathrm{RG}}_{t_{r,\mathrm{WP}}} \cdot P_{r^{\mathrm{WP}}} \qquad \forall\, n_3 \in \mathcal{N}_r^{\mathrm{DR}} \setminus \{n_1, n_2\}, \tag{4.7}$$

$$C^{\mathrm{NO}}_n \in \mathbb{R}^+_0 \qquad \forall\, n \in \mathcal{N}_r^{\mathrm{DR}}, \tag{4.8}$$

$$P_{r^{\mathrm{WP}}} \in \{0,1\} \qquad \forall\, n_3 \in \mathcal{N},\ n_4 \in \mathcal{N} : n_4 \neq n_3,\ r^{\mathrm{WP}} \in \mathcal{R}^{\mathrm{WP,DI}}_{1,n_3,n_4} : \psi_{r^{\mathrm{WP}},r} = 1. \tag{4.9}$$

- The Objective (4.1) performs a cost-optimal translucent path design with respect to the total long reach transmission equipment expenses at the nodes. The corresponding investment for line cards and regenerators at the path's nodes is determined in Equations (4.5)–(4.7).

- Constraint (4.2) allocates one egress wavelength path at the origin node of the translucent path. All considered candidate routes must enable transparent transmission to their destination node. In order to take into account potential intermediate regeneration at any node along the translucent path, we do not restrict to the longest possible path segment but also allow for any valid subpath.

- Equation (4.3) handles the ingress wavelength path at the translucent path's destination node in an equivalent manner.

- A closed sequence of wavelength paths from origin to destination is ensured by Constraints (4.4). At each intermediate node, the number of incoming paths must equal the number of outgoing paths. The number of regeneration iterations besides the electrical signal conversion at the translucent path's end nodes is given by the number of allocated path segments minus one.

- Constraints (4.5) and (4.6) determine the costs for long reach line card equipment at the end nodes n_1 and n_2. Depending on the selected egress path at the origin and the ingress path at the destination, line cards with appropriate transmission technology must be selected as calculated beforehand.

- Additional regeneration functionality is allocated at intermediate nodes where transparent path segments emerge or terminate. In contrast to the colored line cards at the origin and destination node which always have to offer symmetric transmission technology for both directions, the transmission range of intermediate regenerators may be different. From the viewpoint of an intermediate node with two incident WPs, the WP routes along which the signals are sent in both directions are usually unsymmetric, i.e. the transparently traversed fiber link distance and/or the number of transit nodes is different. As all cost values refer to bidirectional equipment, we multiply the regenerator cost by 0.5 in Constraints (4.7) to consider the two transmission directions along the path separately.

- The equipment costs of the path nodes may only take positive values according to Equations (4.8) and the path variables are defined as integer numbers in Constraints (4.9).

4.3 Routing and Network Dimensioning

The existence of disjoint routes that do not traverse any common physical edge or node except for the origin and destination plays a very important role to compensate network failures.

4.3.1 Computation of Disjoint Routes

Efficient algorithms for finding a list of simple routes in non-decreasing order of length are known [HMS07]. On the other hand, the author of [Bha99] formulates a fast algorithm for calculating the shortest pair of disjoint paths. However, depending on the network design strategy, it is advantageous to determine several disjoint route pairs and use the potential routing configurations as input data for the planning process. In contrast to the flow formulation where connections are provided by creating a continuous sequence of links from origin to destination node, the path approach based on pre-calculated routes can reduce the number of constraints and improve the ability to find optimal or near-optimal solutions. Whereas the former concept involves a directed graph to distinguish between ingress and egress flows at the nodes, a simpler bidirected (or equivalently undirected) graph suffices for the latter model. Moreover, one can easily create a set of eligible (disjoint) routes that fulfill certain criteria like maximum length as opposed to flows. Our aim is to calculate the shortest disjoint routes with respect to the total length of the primary and backup routes. This metric facilitates capacity-efficient network design. On the one hand, direct paths require fewer resources on the physical edges by passing through a smaller number of fiber kilometers. On the other hand, there is also a positive effect on the node equipment since shortest distance paths less frequently need signal regeneration and in general also have fewer transit nodes.

Given is a physical network graph characterized by its nodes $\mathcal{N}$ and edges $\mathcal{E}$. All single routes between any node pair $\{n_1, n_2\}$ in the network are summarized in $r \in \mathcal{R}_{1,n_1,n_2}$. They can be calculated by a breadth-first-search algorithm, for example. It starts at the origin node, explores all neighboring nodes, and creates a list of traversed edges for each node. In the next step, all neighbors of each of the previously identified nodes are visited and the sequences of edges to reach them are updated. When adding an edge, one must make sure that its target node is not already included in the list to avoid loops. This procedure is repeated until the destination node is reached or there are no further nodes to explore. Alternatively, one can apply an enumeration algorithm as presented in [Rub78]. The length of each route in terms of total transmission distance is denoted by l_r^{RO}. Binary parameters $\delta_{r,e}$ and $\epsilon_{r,n}$ indicate whether route r uses edge e and node n, respectively. The value of $z^{\mathrm{DR}} \in \mathbb{Z}^+$ determines the quantity of mutually disjoint routes that should be allocated per end-to-end connection, i.e. working path plus protection path(s). Which of these routes are chosen is revealed by the decision variables R_r and the resulting disjoint route configuration $r^{\parallel}$ is stored for each node pair in set $\mathcal{R}_{z^{\mathrm{DR}},n_1,n_2}$.

The following pseudo code and mathematical formulation describe the computation of $z^{\mathrm{DRC}} \in \mathbb{Z}^+$ disjoint route configurations. In a loop we consider each node pair and start with an empty set of disjoint routes. The optimization model calculates one disjoint route configuration. It is executed inside another loop until the desired number of disjoint routes is found or no further configuration exists.

forall $\left(\{n_1, n_2\} \subset \mathcal{N} : n_1 \neq n_2\right)$ {

$\mathcal{R}_{z^{\mathrm{DR}},n_1,n_2} = \emptyset$;

while $\left(\mathcal{R}_{z^{\mathrm{DR}},n_1,n_2} < z^{\mathrm{DRC}}\right)$ {

minimize

$$\sum_{r \in \mathcal{R}_{1,n_1,n_2}} R_r \cdot l_r^{\mathrm{RO}} \tag{4.10}$$

subject to

$$\sum_{r \in \mathcal{R}_{1,n_1,n_2}} R_r = z^{\mathrm{DR}}, \tag{4.11}$$

$$\sum_{r \in \mathcal{R}_{1,n_1,n_2}} R_r \cdot \delta_{r,e} \leq 1 \qquad \forall\, e \in \mathcal{E}, \tag{4.12}$$

$$\sum_{r \in \mathcal{R}_{1,n_1,n_2}} R_r \cdot \epsilon_{r,n_3} \leq 1 \qquad \forall\, n_3 \in \mathcal{N} \setminus \{n_1, n_2\}, \tag{4.13}$$

$$\sum_{r \in r^{\parallel}} R_r < z^{\mathrm{DR}} \qquad \forall\, r^{\parallel} \in \mathcal{R}_{z^{\mathrm{DR}},n_1,n_2}, \tag{4.14}$$

$$R_r \in \mathbb{Z}_0^+ \qquad \forall\, r \in \mathcal{R}_{1,n_1,n_2}; \tag{4.15}$$

if (infeasible) break;

$r^{\parallel} = \{r \in \mathcal{R}_{1,n_1,n_2} : R_r = 1\}$;

$\mathcal{R}_{z^{\mathrm{DR}},n_1,n_2} = \mathcal{R}_{z^{\mathrm{DR}},n_1,n_2} \cup \{r^{\parallel}\}$;

}

}

- The Objective (4.10) minimizes the total length of the disjoint routes R_r. Although the range of route variables is defined as non-negative integer values by Constraints (4.15), Equations (4.12) restrict feasible solutions to binary values so that any route can be selected at most once.
- Constraints (4.11) allocate the desired number of mutually disjoint routes per connection from the set of available single routes between the two nodes.

- For each edge, Constraints (4.12) guarantee that the selected routes do not share this single point of failure.
- If none of the routes should have a common transit node with any other route, Equations (4.13) must be added to the formulation.
- Constraints (4.14) prevent that the same set of disjoint routes as in a previous iteration is computed again. Compared to all already available disjoint route configurations, at least one route of the newly determined structure must be distinct. In other words, the sum of route variables indexed by the routes of an existing configuration must be smaller than the quantity of routes to be allocated.

All route variables with value one represent the selected routes of the computed disjoint route configuration. The first call of the ILP returns the absolute shortest disjoint routes or one of the shortest configurations if there is more than one optimal solution. After that, the resulting composition is added to the set of all previously determined disjoint paths. Thus, in each ILP step, the next best solution is computed and added to the set of all disjoint routes. If there is no other configuration left, the problem is infeasible and the computation terminates.

4.3.2 Opaque Network Design

In this section, we develop an ILP model which solves the combined routing and network dimensioning problem for the opaque network scenario.

The network topology is defined by the set of nodes $\mathcal{N}$ and eligible edges $\mathcal{E}$. If an edge e is incident on node n, the binary parameter $\alpha_{e,n}$ is one and zero otherwise. We assume symmetric demands between any node pair n_1, n_2 from node n_1 to Node n_2 and vice versa. Thus, the traffic requests are indexed by the unordered node pair $\{n_1, n_2\} \subset \mathcal{N}$, where n_1 is distinct from n_2. The network equipment supports different transmission bitrates $\mathcal{B}$ per wavelength channel. Consequently, the number of demands between n_1 and n_2 at bitrate b is denoted by $d_{n_1,n_2,b}$.

We consider a set of disjoint routing configurations between each unordered node pair $\{n_1, n_2\}$. A disjoint routing configuration is labeled $r^{\parallel}$ and consists of z^{DR} routes. Unprotected connections consist of a single path, two disjoint paths can compensate a single failure, and dual failures are addressed by three disjoint paths. The set of all eligible disjoint routing configurations is referred to as $\mathcal{R}_{z^{\mathrm{DR}},n_1,n_2}$. We want to emphasize that all paths belonging to the same configuration are mutually edge- or node-disjoint, so that at most one path is affected by the failure of an edge or node, respectively. A binary parameter $\delta_{r^{\parallel},e}$ indicates for each disjoint routing configuration $r^{\parallel}$ whether any route uses edge e.

Nonnegative integer path variables $P_{n_1,n_2,r^{\parallel},b}$ control the routing of demands between unordered node pair $\{n_1, n_2\}$ along disjoint routes $r^{\parallel}$ at bitrate b. In order to be able to aggregate traffic into higher bitrate wavelength channels, we introduce link variables $L_{e,b}$

for each network edge e and bitrate b. The number of fibers per edge e is modeled by variables F_e which can take nonnegative integer values. Each fiber offers a set of wavelength channels $\mathcal{W}$. Whether a network edge is used for transmission can be deduced from the binary variables E_e.

In order to compute the least expensive network configuration, we add up all the expenses per node and edge in variables C_n^{NO} and C_e^{ED}, respectively. The total costs per node are calculated by short reach line card costs C_n^{SLC}, electrical switch costs C_n^{ES}, transponder costs C_n^{TP}, optical multiplexer/demultiplexer costs C_n^{OMD}, and booster/pre-amplifier costs C_n^{BPA}. Concerning the edges, there are expenses for cable conduits (C_e^{CC}), fiber cables (C_e^{FC}), inline amplifiers (C_e^{IA}), dispersion compensating fibers (C_e^{DCF}), and dynamic gain equalizers (C_e^{DGE}). The cost values for all equipment types have been defined in Section 2.3.

Based on the above notations, we formulate the mathematical program for the opaque network design as follows.

Minimize

$$\sum_{n\in\mathcal{N}} C_n^{\mathrm{NO}} + \sum_{e\in\mathcal{E}} C_e^{\mathrm{ED}} \tag{4.16}$$

subject to

$$\sum_{r^{\parallel}\in\mathcal{R}_{z^{\mathrm{DR}},n_1,n_2}} P_{n_1,n_2,r^{\parallel},b} = d_{n_1,n_2,b} \qquad \begin{array}{l}\forall\,\{n_1,n_2\}\subset\mathcal{N}:\\ n_1\neq n_2,\ b\in\mathcal{B},\end{array} \tag{4.17}$$

$$\sum_{\substack{b_2\in\mathcal{B}:\\ b_2\geq b_1}} L_{e,b_2}\cdot b_2 \geq \sum_{\substack{\{n_1,n_2\}\subset\mathcal{N}:\\ n_1\neq n_2}} \sum_{\substack{r^{\parallel}\in\mathcal{R}_{z^{\mathrm{DR}},n_1,n_2}:\\ \delta_{r^{\parallel},e}=1}} \sum_{\substack{b_2\in\mathcal{B}:\\ b_2\geq b_1}} P_{n_1,n_2,r^{\parallel},b_2}\cdot b_2 \qquad \forall\, e\in\mathcal{E},\ b_1\in\mathcal{B}, \tag{4.18}$$

$$F_e\cdot|\mathcal{W}| \geq \sum_{b\in\mathcal{B}} L_{e,b} \qquad \forall\, e\in\mathcal{E}, \tag{4.19}$$

$$E_e\cdot \sum_{\substack{\{n_1,n_2\}\subset\mathcal{N}:\\ n_1\neq n_2}} \sum_{b\in\mathcal{B}} \frac{d_{n_1,n_2,b}}{|\mathcal{W}|} \geq F_e \qquad \forall\, e\in\mathcal{E}, \tag{4.20}$$

$$C_n^{\mathrm{SLC}} = \sum_{b\in\mathcal{B}} c_b^{\mathrm{SLC}}\cdot\Bigg(\sum_{\substack{\{n_1,n_2\}\subset\mathcal{N}:\\ n_1\neq n_2\,\wedge\\ (n_1=n\,\vee\,n_2=n)}} d_{n_1,n_2,b} + \sum_{\substack{e\in\mathcal{E}:\\ \alpha_{e,n}=1}} L_{e,b}\Bigg) \qquad \forall\, n\in\mathcal{N}, \tag{4.21}$$

$$C_n^{\mathrm{ES}} = \sum_{b\in\mathcal{B}} c_b^{\mathrm{ES}}\cdot\Bigg(\sum_{\substack{\{n_1,n_2\}\subset\mathcal{N}:\\ n_1\neq n_2\,\wedge\\ (n_1=n\,\vee\,n_2=n)}} d_{n_1,n_2,b} + \sum_{\substack{e\in\mathcal{E}:\\ \alpha_{e,n}=1}} L_{e,b}\Bigg) \qquad \forall\, n\in\mathcal{N}, \tag{4.22}$$

$$C_n^{\mathrm{TP}} = \sum_{b\in\mathcal{B}} \sum_{\substack{e\in\mathcal{E}:\\ \alpha_{e,n}=1}} c_{b,t_e}^{\mathrm{TP}}\cdot L_{e,b} \qquad \forall\, n\in\mathcal{N}, \tag{4.23}$$

$$C_n^{\mathrm{OMD}} = c_{|\mathcal{W}|}^{\mathrm{OMD}} \cdot \sum_{\substack{e \in \mathcal{E}: \\ \alpha_{e,n}=1}} F_e \qquad \forall\, n \in \mathcal{N}, \tag{4.24}$$

$$C_n^{\mathrm{BPA}} = c^{\mathrm{BPA}} \cdot \sum_{\substack{e \in \mathcal{E}: \\ \alpha_{e,n}=1}} F_e \qquad \forall\, n \in \mathcal{N}, \tag{4.25}$$

$$C_n^{\mathrm{NO}} = C_n^{\mathrm{SLC}} + C_n^{\mathrm{ES}} + C_n^{\mathrm{TP}} + C_n^{\mathrm{OMD}} + C_n^{\mathrm{BPA}} \qquad \forall\, n \in \mathcal{N}, \tag{4.26}$$

$$C_e^{\mathrm{CC}} = c^{\mathrm{CC}} \cdot l_e \cdot E_e \qquad \forall\, e \in \mathcal{E}, \tag{4.27}$$

$$C_e^{\mathrm{FC}} = c^{\mathrm{FC}} \cdot l_e \cdot E_e \qquad \forall\, e \in \mathcal{E}, \tag{4.28}$$

$$C_e^{\mathrm{IA}} = c_{t_e}^{\mathrm{IA}} \cdot \left(\left\lceil l_e / l^{\mathrm{IA}} \right\rceil - 1 \right) \cdot F_e \qquad \forall\, e \in \mathcal{E}, \tag{4.29}$$

$$C_e^{\mathrm{DCF}} = c_{t_e}^{\mathrm{DCF}} \cdot l_e / l^{\mathrm{DCF}} \cdot F_e \qquad \forall\, e \in \mathcal{E}, \tag{4.30}$$

$$C_e^{\mathrm{DGE}} = c^{\mathrm{DGE}} \cdot \left\lfloor l_e / l^{\mathrm{DGE}} \right\rfloor F_e \qquad \forall\, e \in \mathcal{E}, \tag{4.31}$$

$$C_e^{\mathrm{ED}} = C_e^{\mathrm{CC}} + C_e^{\mathrm{FC}} + C_e^{\mathrm{IA}} + C_e^{\mathrm{DCF}} + C_e^{\mathrm{DGE}} \qquad \forall\, e \in \mathcal{E}, \tag{4.32}$$

$$C_n^{\mathrm{SLC}}, C_n^{\mathrm{ES}}, C_n^{\mathrm{TP}}, C_n^{\mathrm{OMD}}, C_n^{\mathrm{BPA}}, C_n^{\mathrm{NO}} \in \mathbb{R}_0^+ \qquad \forall\, n \in \mathcal{N}, \tag{4.33}$$

$$C_e^{\mathrm{CC}}, C_e^{\mathrm{FC}}, C_e^{\mathrm{IA}}, C_e^{\mathrm{DCF}}, C_e^{\mathrm{DGE}}, C_e^{\mathrm{ED}} \in \mathbb{R}_0^+ \qquad \forall\, e \in \mathcal{E}, \tag{4.34}$$

$$P_{n_1,n_2,r^{\parallel},b} \in \mathbb{Z}_0^+ \qquad \begin{array}{l} \forall\, \{n_1, n_2\} \subset \mathcal{N} : n_1 \neq n_2, \\ \quad r^{\parallel} \in \mathcal{R}_{z^{\mathrm{DR}},n_1,n_2},\ b \in \mathcal{B}, \end{array} \tag{4.35}$$

$$L_{e,b} \in \mathbb{Z}_0^+ \qquad \forall\, e \in \mathcal{E},\ b \in \mathcal{B}, \tag{4.36}$$

$$F_e \in \mathbb{Z}_0^+ \qquad \forall\, e \in \mathcal{E}, \tag{4.37}$$

$$E_e \in \{0, 1\} \qquad \forall\, e \in \mathcal{E}. \tag{4.38}$$

- The Objective (4.16) minimizes the total opaque network costs. It summarizes the equipment expenses for all nodes and the edge costs. The actual investments per node and edge depend on the routing and network dimensioning which is performed in Constraints (4.17)–(4.20). Based on the resulting configuration the costs for nodes and edges are calculated in Equations (4.21)–(4.32).

- Constraints (4.17) route the demands by constructing lightpaths. For each unordered node pair $\{n_1, n_2\}$ and each wavelength channel bitrate b, the traffic quantity $d_{n_1,n_2,b}$ must be satisfied. We assume that all demands should be protected against the same failure scenario, i.e. the number of disjoint paths per routing configuration z^{DR} and the edge- or node-disjoint option are set globally. Nevertheless, traffic classes with different protection conditions can easily be included in the formulation by adding extra indexes for the demands that allow to distinguish the requirements. The paths $P_{n_1,n_2,r^{\parallel},b}$ can be set up along any eligible disjoint routing configuration $r^{\parallel}$. Moreover, demands are initially transported via paths at their

native bitrate, i.e. requests are not multiplexed into higher bitrate channels. We note that the paths $P_{n_1,n_2,r^{\|},b}$ do not define the link configuration on the network edges because they still can be multiplexed with each other into higher bitrate signals.

- This grooming functionality is addressed in Constraints (4.18) which map the end-to-end virtual wavelength paths (VWPs) onto wavelength links. For each edge e and any bitrate b_1, the right-hand side of the equation calculates the total bitrate of all paths that traverse the considered edge and whose bitrate is at least b_1. The overall bitrate of all wavelength links with bitrate b_1 or higher on the left-hand side of the equation must be accordingly dimensioned. Paths at bitrate b_1 can be aggregated by selecting links with higher bitrates instead of an equivalent link quantity at the same bitrate. As a prerequisite, each bitrate must be an integer multiple of all other smaller bitrates. This condition prevents the multiplexing of smaller bitrate signals into different higher bitrate signals. Let us assume the set of available transmission bitrates $\mathcal{B}$ including 2.5 Gbit/s, 10 Gbit/s, and 40 Gbit/s. Examining the constraints for an arbitrary edge yields the following scenario. Traffic at 40 Gbit/s can only be routed via 40 Gbit/s wavelength links. However, the greater-than-or-equal relation allows that more links at 40 Gbit/s are provisioned than necessary for the native demands at 40 Gbit/s. These links can be used for grooming paths at 2.5 Gbit/s and 10 Gbit/s because they are taken into consideration on the left-hand side of the equations when setting bitrate b_1 to these two values. Paths at 10 Gbit/s may be mapped directly onto links at 10 Gbit/s or groomed to 40 Gbit/s links. However, it is not sufficient to restrict the right-hand side of the equation to 10 Gbit/s paths since the 40 Gbit/s links must additionally support the 40 Gbit/s paths by all means. Paths at the lowest bitrate 2.5 Gbit/s can be transported in any link. In the case of b_1 amounting to 2.5 Gbit/s, the constraints yield the fundamental condition that the total bitrate offered by the links must not be lower than the overall bitrate of all paths. However, this constraint on its own would not prevent from splitting 10 Gbit/s traffic demands into 2.5 Gbit/s wavelength channels and 40 Gbit/s requests into 2.5 Gbit/s and 10 Gbit/s wavelengths, respectively. Thus, the other constraints where the two higher bitrates are assigned to b_1 are mandatory.

- Equations (4.19) derive the number of fibers F_e that is necessary to provide the required wavelength links per edge e. In the opaque case, the color of a path can be changed at each node along its route via OEO conversion. Thus, no wavelength blocking occurs and the number of usable wavelengths is only limited by the fiber quantity and the supported number of wavelengths per fiber. The actual wavelength of each link can be selected arbitrarily and does not have to be considered in the model.

- Constraints (4.20) detect whether any transmission occurs on the eligible physical edges. A network edge e must be allocated in terms of cable conduit and fibers as soon as at least one lightpath traverses it. This circumstance is indicated by a positive fiber quantity F_e. The quotient of the total demands in the network and

the wavelength channel quantity per fiber on the left-hand side of the equations calculates the maximum possible number of fibers on any network edge. It represents the worst case routing configuration from a fiber capacity point of view where all the traffic demands are routed on the same edge. We multiply the physical edge variable E_e by this factor and specify the fiber variable as lower bound. By this means, the edge variable is set to one for a non-zero fiber variable and we guarantee that the left-hand side of the equation can be greater than or equal to the fiber quantity despite the binary edge variable.

Constraints (4.21)–(4.26) determine the network equipment costs for each node.

- In order to insert a non-colored optical signal at an opaque node, it is converted into electrical form by a short reach line card (SLC). The number of SLCs for local add/drop on the tributary side is predefined by the number of traffic requests. Since the price of a short reach line card depends on the traffic bitrate b, we distinguish between the respective demands $d_{n_1,n_2,b}$ for each unordered node pair $\{n_1, n_2\}$. Moreover, SLCs are necessary at the WDM line side of the electrical switch for all wavelength links $L_{e,b}$ on any adjacent edge e. These two cost terms are added up in Equations (4.21). The same holds true for the electrical switch (ES) costs in Constraints (4.22) which are calculated accordingly.

- Long reach transponders (TPs) establish the wavelength links on the edges. The applied transponder transmission technology depends on the distance the signal must travel. Since the lightpaths are regenerated at each node, the transmission technology can be pre-calculated per edge by t_e based on the edge length l_e. The total TP costs can then be expressed by Constraints (4.23).

- The channels of each lit fiber must be multiplexed/demultiplexed at the adjacent nodes by optical multiplexer/demultiplexer (OMD) units. Equations (4.24) accumulate all fibers incident on node n and multiply with the respective cost $c^{\mathrm{OMD}}_{|\mathcal{W}|}$.

- Before being demultiplexed and after being multiplexed on the fiber, booster/pre-amplifiers (BPAs) at the nodes strengthen the signal power of all lightpaths. Their number corresponds to the OMD quantity and is calculated for all nodes by Constraints (4.25).

- Equations (4.26) assess the total node costs by adding up the individual equipment investments.

The following constraints calculate the costs that are associated with the physical network edges.

- Expenses for the cable conduits (CCs) and fiber cables (FCs) depend on the length of the allocated network edges. Equations (4.27) and (4.28) determine the respective cost terms per network edge. We expect that a cable consisting of dozens of fibers will be installed to account for growing traffic demands. Usually, only a fraction of all installed fibers will be used for transmission in the considered traffic

scenario. However, if the total traffic is very high, additional constraints may be added to ensure sufficient fiber resources for each edge.

- In order to compensate the fiber attenuation, the optical signals are amplified after regular distances. The length-dependent costs for IAs are calculated in Constraints (4.29).
- Similarly, Equations (4.30) and (4.31) compute the DCF investments and DGE expenses, respectively.
- All these cost terms per edge are accumulated in Constraints (4.32).

4.3.3 Translucent Network Design

The results of the translucent lightpath design serve as input parameters for the translucent network design. The binary parameter $\chi_{r,n,t}$ specifies for every translucent connection along route r whether a long reach line card (LLC) with transmission range t is required at node n. We note that LLCs are only used at the origin and destination node of a translucent path. The number of regenerators (RGs) with transmission range t at transit node n of translucent route r is available via $z^{\mathrm{RG}}_{r,n,t}$.

In order to guarantee a fair comparison with the opaque scenario, we allocate a long reach line card (LLC) for every path in the disjoint routing configuration. In order to reduce costs, one can restrict to a single line card per demand by choosing the one with longest transmission range. However, this would not permit a flexible simultaneous transmission along working and protection path, because one must utilize the same wavelength. Furthermore, the LLC would represent a single point of failure. Nevertheless, the single LLC approach is an interesting option to decrease equipment costs which is only available in the translucent network scenario.

Minimize

$$\sum_{n\in\mathcal{N}} C^{\mathrm{NO}}_{n} + \sum_{e\in\mathcal{E}} C^{\mathrm{ED}}_{e} \tag{4.39}$$

subject to

$$\sum_{r^{\parallel}\in\mathcal{R}_{z^{\mathrm{DR}},n_1,n_2}} \sum_{\substack{b_2\in\mathcal{B}:\\ b_2\geq b_1}} P_{n_1,n_2,r^{\parallel},b_2}\cdot b_2 \geq \sum_{\substack{b_2\in\mathcal{B}:\\ b_2\geq b_1}} d_{n_1,n_2,b_2}\cdot b_2 \qquad \begin{array}{l}\forall\,\{n_1,n_2\}\subset\mathcal{N}:\\ n_1\neq n_2,\\ b_1\in\mathcal{B},\end{array} \tag{4.40}$$

$$F_e\cdot|\mathcal{W}| \geq \sum_{\substack{\{n_1,n_2\}\subset\mathcal{N}:\\ n_1\neq n_2}} \sum_{\substack{r^{\parallel}\in\mathcal{R}_{z^{\mathrm{DR}},n_1,n_2}:\\ \delta_{r^{\parallel},e}=1}} \sum_{b\in\mathcal{B}} P_{n_1,n_2,r^{\parallel},b} \qquad \forall\, e\in\mathcal{E}, \tag{4.41}$$

$$E_e\cdot \sum_{\substack{\{n_1,n_2\}\subset\mathcal{N}:\\ n_1\neq n_2}} \sum_{b\in\mathcal{B}} \frac{d_{n_1,n_2,b}}{|\mathcal{W}|} \geq F_e \qquad \forall\, e\in\mathcal{E}, \tag{4.42}$$

$$C_n^{\mathrm{SLC}} = \sum_{b \in \mathcal{B}} c_b^{\mathrm{SLC}} \cdot \sum_{\substack{\{n_1,n_2\} \subset \mathcal{N}: \\ n_1 \neq n_2 \wedge \\ (n_1 = n \vee n_2 = n)}} d_{n_1,n_2,b} \qquad \forall\, n \in \mathcal{N}, \tag{4.43}$$

$$C_n^{\mathrm{ES}} = \sum_{b \in \mathcal{B}} c_b^{\mathrm{ES}} \cdot \Bigg(\sum_{\substack{\{n_1,n_2\} \subset \mathcal{N}: \\ n_1 \neq n_2 \wedge \\ (n_1 = n \vee n_2 = n)}} d_{n_1,n_2,b} + \\ + \sum_{\substack{\{n_1,n_2\} \subset \mathcal{N}: \\ n_1 \neq n_2 \wedge \\ (n_1 = n \vee n_2 = n)}} \sum_{\substack{r^{\parallel} \in \mathcal{R}_{\mathrm{zDR},n_1,n_2} \\ r \in \mathcal{R}_{1,n_1,n_2}: \\ r \in r^{\parallel}}} P_{n_1,n_2,r^{\parallel},b} \Bigg) \qquad \forall\, n \in \mathcal{N}, \tag{4.44}$$

$$C_n^{\mathrm{LLC}} = \sum_{\substack{\{n_1,n_2\} \subset \mathcal{N}: \\ n_1 \neq n_2 \wedge \\ (n_1 = n \vee n_2 = n)}} \sum_{\substack{r^{\parallel} \in \mathcal{R}_{\mathrm{zDR},n_1,n_2} \\ r \in \mathcal{R}_{1,n_1,n_2}: \\ r \in r^{\parallel}}} \sum_{b \in \mathcal{B}} \sum_{\substack{t \in \mathcal{T}: \\ \chi_{r,n,t} = 1}} c_{b,t}^{\mathrm{LLC}} \cdot P_{n_1,n_2,r^{\parallel},b} \qquad \forall\, n \in \mathcal{N}, \tag{4.45}$$

$$C_n^{\mathrm{OSL}} = c^{\mathrm{OSL}} \cdot \Bigg(\sum_{\substack{\{n_1,n_2\} \subset \mathcal{N}: \\ n_1 \neq n_2 \wedge \\ (n_1 = n \vee n_2 = n)}} \sum_{\substack{r^{\parallel} \in \mathcal{R}_{\mathrm{zDR},n_1,n_2} \\ r \in \mathcal{R}_{1,n_1,n_2}: \\ r \in r^{\parallel}}} \sum_{b \in \mathcal{B}} P_{n_1,n_2,r^{\parallel},b} + \\ + \sum_{\substack{\{n_1,n_2\} \subset \mathcal{N}: \\ n_1 \neq n_2 \wedge \\ (n_1 \neq n \vee n_2 \neq n)}} \sum_{\substack{r^{\parallel} \in \mathcal{R}_{\mathrm{zDR},n_1,n_2} \\ r \in \mathcal{R}_{1,n_1,n_2}: \\ r \in r^{\parallel} \wedge \\ \epsilon_{r,n} = 1}} \sum_{b \in \mathcal{B}} \sum_{t \in \mathcal{T}} z_{r,n,t}^{\mathrm{RG}} \cdot P_{n_1,n_2,r^{\parallel},b} \Bigg) \qquad \forall\, n \in \mathcal{N}, \tag{4.46}$$

$$C_n^{\mathrm{RG}} = \sum_{b \in \mathcal{B}} \sum_{t \in \mathcal{T}} 0.5 \cdot c_{b,t}^{\mathrm{RG}} \cdot \\ \cdot \sum_{\substack{\{n_1,n_2\} \subset \mathcal{N}: \\ n_1 \neq n_2 \wedge \\ (n_1 \neq n \vee n_2 \neq n)}} \sum_{\substack{r^{\parallel} \in \mathcal{R}_{\mathrm{zDR},n_1,n_2} \\ r \in \mathcal{R}_{1,n_1,n_2}: \\ r \in r^{\parallel} \wedge \\ \epsilon_{r,n} = 1}} z_{r,n,t}^{\mathrm{RG}} \cdot P_{n_1,n_2,r^{\parallel},b} \qquad \forall\, n \in \mathcal{N}, \tag{4.47}$$

$$C_n^{\mathrm{OST}} = c^{\mathrm{OST}} \cdot \sum_{\substack{e \in \mathcal{E}: \\ \alpha_{e,n} = 1}} F_e \qquad \forall\, n \in \mathcal{N}, \tag{4.48}$$

$$C_n^{\mathrm{OMD}} = c_{|\mathcal{W}|}^{\mathrm{OMD}} \cdot \sum_{\substack{e \in \mathcal{E}: \\ \alpha_{e,n} = 1}} F_e \qquad \forall\, n \in \mathcal{N}, \tag{4.49}$$

$$C_n^{\mathrm{TPA}} = c_{t^{\mathrm{MAX}}}^{\mathrm{TPA}} \cdot \sum_{\substack{e \in \mathcal{E}: \\ \alpha_{e,n} = 1}} F_e \qquad \forall\, n \in \mathcal{N}, \tag{4.50}$$

$$C_n^{\mathrm{NO}} = C_n^{\mathrm{SLC}} + C_n^{\mathrm{ES}} + C_n^{\mathrm{LLC}} + C_n^{\mathrm{OSL}} + C_n^{\mathrm{RG}} + \\ + C_n^{\mathrm{OST}} + C_n^{\mathrm{OMD}} + C_n^{\mathrm{TPA}} \qquad \forall\, n \in \mathcal{N}, \tag{4.51}$$

$$C_e^{\mathrm{CC}} = c^{\mathrm{CC}} \cdot l_e \cdot E_e \qquad \forall\, e \in \mathcal{E}, \tag{4.52}$$

$$C_e^{\mathrm{FC}} = c^{\mathrm{FC}} \cdot l_e \cdot E_e \qquad \forall\, e \in \mathcal{E}, \tag{4.53}$$

$$C_e^{\mathrm{IA}} = c_{t^{\mathrm{MAX}}}^{\mathrm{IA}} \cdot \left\lceil l_e / l^{\mathrm{IA}} \right\rceil \cdot F_e \qquad \forall\, e \in \mathcal{E}, \tag{4.54}$$

$$C_e^{\mathrm{DCF}} = c_{t^{\mathrm{MAX}}}^{\mathrm{DCF}} \cdot l_e / l^{\mathrm{DCF}} \cdot F_e \qquad \forall\, e \in \mathcal{E}, \tag{4.55}$$

$$C_e^{\mathrm{DGE}} = c^{\mathrm{DGE}} \cdot \left\lfloor l_e / l^{\mathrm{DGE}} \right\rfloor \cdot F_e \qquad \forall\, e \in \mathcal{E}, \tag{4.56}$$

$$C_e^{\mathrm{ED}} = C_e^{\mathrm{CC}} + C_e^{\mathrm{FC}} + C_e^{\mathrm{IA}} + C_e^{\mathrm{DCF}} + C_e^{\mathrm{DGE}} \qquad \forall\, e \in \mathcal{E}, \tag{4.57}$$

$$C_n^{\mathrm{NO}}, C_n^{\mathrm{SLC}}, C_n^{\mathrm{ES}}, C_n^{\mathrm{LLC}}, C_n^{\mathrm{OSL}}, C_n^{\mathrm{RG}}, C_n^{\mathrm{OST}}, C_n^{\mathrm{OMD}}, C_n^{\mathrm{TPA}} \in \mathbb{R}_0^+ \qquad \forall\, n \in \mathcal{N}, \tag{4.58}$$

$$C_e^{\mathrm{ED}}, C_e^{\mathrm{CC}}, C_e^{\mathrm{FC}}, C_e^{\mathrm{IA}}, C_e^{\mathrm{DCF}}, C_e^{\mathrm{DGE}} \in \mathbb{R}_0^+ \qquad \forall\, e \in \mathcal{E}, \tag{4.59}$$

$$P_{n_1,n_2,r^{\parallel},b} \in \mathbb{Z}_0^+ \qquad \forall\, \{n_1, n_2\} \subset \mathcal{N} : n_1 \neq n_2,\ r^{\parallel} \in \mathcal{R}_{z^{\mathrm{DR}},n_1,n_2},\ b \in \mathcal{B}, \tag{4.60}$$

$$F_e \in \mathbb{Z}_0^+ \qquad \forall\, e \in \mathcal{E}, \tag{4.61}$$

$$E_e \in \{0, 1\} \qquad \forall\, e \in \mathcal{E}. \tag{4.62}$$

- The Objective (4.39) minimizes the overall design costs subdivided into node and network expenses
- Constraints (4.40) make sure that all traffic demands are satisfied by a translucent protected path P. A request at bitrate b can be served by a path at the same bitrate or any higher transmission rate. This is supported by the electrical switch fabric (ESF) at the demand's origin and destination node which allows for end-to-end grooming. Again, we make sure that no higher-bitrate connections are distributed over lower-bitrate flows.
- The number of required fibers F_e for each network edge is calculated in Constraints (4.41). One wavelength is required for every selected translucent path traversing the considered edge. Thus, fibers are allocated such that the total number of wavelength channels is not smaller than the path quantity.
- Constraints (4.42) detect whether an edge is utilized. This is an essential step in order to be able to identify the edge related costs.

The following nine equations calculate the total node costs for the translucent network design.

- The short reach line cards (SLCs) only appear at the tributary side. Based on the demand matrix, their type and quantity are known a priori. The related costs are calculated by Constraints (4.43)
- Constraints (4.44) evaluate the electrical switch fabric costs which depend on the number of ports and their bitrate. The first term analyzes the interfaces to the short reach line cards and the second term deals with the long reach line card ports.

- Constraints (4.45) examine the long reach line card (LLC) costs at each node. All translucent paths starting or ending at the considered node need an LLC to transform the short reach to a long reach optical signal.

- A portion of the costs for the optical switch fabric is caused by local ports. Local ports are either used for adding and dropping translucent lightpaths or for accessing the pool of regenerators. Both options are considered accordingly in Constraints (4.46).

- Constraints (4.47) calculate the regenerator (RG) costs. The location and transmission range of regenerators is known for every translucent path from the previously performed translucent lightpath design.

- The remaining portion of optical switch fabric costs stems from the transit ports to forward signals on the fiber links. The related expenses are specified in Constraints (4.48). Although the number of lightpaths may be smaller than the available wavelengths in the fibers, it makes sense to provide full switching functionality for all channels to prevent from routing limitations. Otherwise one would have to comply with node-specific rules that a certain set of wavelengths cannot be utilized for lightpath routing.

- Similarly, the costs for optical multiplexers and demultiplexers occur per incident fiber link. They are summarized in Constraints (4.49)

- Constraints (4.50) determine the investments for transparent node pre-amplifiers (TPAs) which are needed per ingress/egress fiber link, too.

- All above cost terms are added up in Constraints (4.51) for each node.

The following six equations specify the equipment costs at the network edges.

- Constraints (4.52) and (4.53) consider the expenses for cable conduits (CCs) and fiber cables (FCs), respectively.

- The number of inline amplifiers (IAs) per fiber link is calculated by rounding up the fraction of link length l_e and IA spacing l^{IA}. As a result, Constraints (4.54) include all amplifiers along the fiber links as well as the inline amplifiers situated at the translucent nodes.

- Constraints (4.55) and (4.56) cover the dispersion compensating fiber (DCF) segments and the dynamic gain equalizers (DGEs), respectively.

- Eventually, all these individual network edge cost terms are summarized in Constraints (4.57).

4.4 Wavelength Assignment and Converter Allocation

In the opaque network scenario, all lightpaths are converted into electrical form at each node. Before sending out the signal on the next hop, it is translated back into optical form by a transponder. Opaque nodes provision transponder cards for every wavelength. Thus, it is possible to change the incoming wavelength arbitrarily at each node by switching the electrical signal to the transponder operating at the desired transmission frequency. As long as a single free wavelength channel is available on all the edges of a lightpath, the wavelength connection can be established.

For the translucent network model, the situation is different because the lightpaths are only selectively terminated electrically at some nodes. This is due to the fact that wavelength connections are kept in optical form as far as possible to reduce expensive OEO signal conversion. Only when exceeding the maximum transmission distance, lightpaths are regenerated at intermediate nodes. Thus, lightpaths may pass through a number of edges where the wavelength cannot be changed. In order to enable valid routing configurations for these transparent path segments, the same wavelength must be assigned to all links. When assuming a single fiber per network edge, this means that all wavelength paths and transparent segments of virtual wavelength paths traversing a common edge must be transmitted at a different color. In case of multiple fibers per edge, the actual fiber quantity restricts the number of overlapping lightpaths which can be assigned the same wavelength. A number of studies have shown that it is not necessary to perform wavelength conversion at every node in order to reach lightpath blocking as low as for the opaque network case (see [SGCB02], for example).

Wavelength conflicts occur if one cannot find any wavelength that is available on all the edges of a transparent route. Such lightpaths are blocked and cannot be established. Although a significant number of wavelength channels may still be available on every traversed fiber link, the wavelength continuity constraint prevents a utilization of these resources. Thus, it is crucial to resolve wavelength conflicts by an intelligent wavelength assignment strategy. However, this problem is very complex and cannot be solved in polynomial time because the decisions of assigning wavelengths to transparent paths highly influence each other [ZJM00]. Different approaches to deal with the wavelength assignment problem are conceivable. One option is to include the wavelength decision in the ILP-based routing and dimensioning process. However, this strategy is only practicable for small networks with a limited number of lightpaths due to computational complexity. Our strategy is to solve the wavelength assignment task separately in a subsequent step.

The preceding routing and network dimensioning process determines the routes of all lightpaths and creates sufficient link capacity in terms of the number of fibers per edge based on the traffic demands and the number of available wavelength channels per fiber. Nevertheless, lightpath blocking can occur as explained before. In order to guarantee valid wavelength assignments for all paths, we allow for extra wavelength converters to resolve conflicts. By default, the transmission frequency can be selected at the lightpath's

end nodes and altered at every transit node where the signal is regenerated. We assume that the same wavelength is chosen for both transmission directions of any wavelength link to preserve a consistent bidirectional network architecture. Further wavelength converters (WCs) can be provided at optically bypassed nodes to truncate transparent lightpaths overlapping with many other wavelength paths. Otherwise it might be impossible to set up the paths at different wavelengths or use alternative fibers on the same network edge.

The allocation of extra converters can be combined with a careful overdimensioning of the link capacity in the previous routing and network dimensioning task. Usually, the number of fibers per edge is defined by rounding up the ratio of the number of lightpaths over the edge and the number of usable wavelength channels per fiber. In order to allow for more wavelength flexibility, one can define a small wavelength margin per fiber that initially cannot be used for the routing of connections although the channels exist. In the subsequent wavelength assignment and converter allocation phase, these wavelengths are made eligible again. As a result, fibers are not entirely filled with lightpaths because of the spare channels. Such a routing configuration facilitates the wavelength continuity of transparent lightpaths.

The following equations show the preliminary calculations that are necessary to evaluate the results of the previously conducted routing and network dimensioning ILP in the translucent network scenario.

$$z^{\mathrm{WP}}_{n_1,n_2,r^{\mathrm{WP}}} = \sum_{\substack{\{n_3,n_4\}\subset\mathcal{N}:\\ n_3\neq n_4}} \sum_{\substack{r^{\parallel}\in\mathcal{R}^{\mathrm{DR}}_{z,n_3,n_4}:\\ \phi_{r^{\mathrm{WP}},r^{\parallel}}=1}} \sum_{b\in\mathcal{B}} P_{n_3,n_4,r^{\parallel},b} \qquad \begin{array}{l}\forall\,\{n_1,n_2\}\subset\mathcal{N}: n_1\neq n_2,\\ r^{\mathrm{WP}}\in\mathcal{R}^{\mathrm{WP}}_{1,n_1,n_2}\end{array} \tag{4.63}$$

$$\mathcal{I}^{\mathrm{WP}}_{n_1,n_2,r^{\mathrm{WP}}} = \{1,2,3,...z^{\mathrm{WP}}_{n_1,n_2,r^{\mathrm{WP}}}\} \qquad \begin{array}{l}\forall\,\{n_1,n_2\}\subset\mathcal{N}: n_1\neq n_2\\ r^{\mathrm{WP}}\in\mathcal{R}^{\mathrm{WP}}_{1,n_1,n_2}\end{array} \tag{4.64}$$

$$f_e = F_e \qquad \forall\, e\in\mathcal{E} \tag{4.65}$$

- The routing of all traffic requests between two nodes n_3, n_4 is given by the values of the path variables $P_{n_3,n_4,r^{\parallel},b}$ that show how many paths have been selected along disjoint routes $r^{\parallel}$ at bitrate b. Now we are interested in the corresponding transparent path segments that are strung together to form these end-to-end paths. The set of all single transparent wavelength paths between two nodes n_1, n_2 is denoted by $r^{\mathrm{WP}} \in \mathcal{R}^{\mathrm{WP}}_{1,n_1,n_2}$. Equations (4.63) calculate the quantity $z^{\mathrm{WP}}_{n_1,n_2,r^{\mathrm{WP}}}$ of each WP segment r^{WP}. All disjoint end-to-end paths $r^{\parallel}$ between any unordered node pair n_3, n_4 are examined and hits are identified by the binary parameter $\phi_{r^{\mathrm{WP}},r^{\parallel}}$. The specific bitrates of the connections do not matter for the wavelength assignment procedure.

- Based on the number of allocated transparent paths, Equations (4.64) define a set of identification numbers $\mathcal{I}^{\mathrm{WP}}_{n_1,n_2,r^{\mathrm{WP}}}$ to be able to distinguish all WPs between nodes n_1, n_2 that follow the same route r^{WP}.

- The number of fibers for every network edge e has been calculated by the variable F_e in the routing and dimensioning optimization. Corresponding input parameters f_e for the wavelength design are determined by Equations (4.65).

The following mathematical formulation details the wavelength identification task. At best, each transparent path can be assigned a continuous wavelength between its end nodes. If some lightpaths are blocked because no common wavelength is available on all routing hops, wavelength converters can be allocated at intermediate path nodes. In this case, the transmission frequency can be altered at the respective locations. Nevertheless, the resulting transparent subsegments are still subject to wavelength continuity. In order to support extra wavelength modifications, we evaluate the transmission frequency of each transparent path r^{WP} between nodes n_1, n_2 per link. The set of edges and nodes of route r^{WP} are denoted by $\mathcal{E}^{\mathrm{DR}}_{r^{\mathrm{WP}}}$ and $\mathcal{N}^{\mathrm{DR}}_{r^{\mathrm{WP}}}$, respectively. Since there may exist multiple paths along the same route, the binary variables $L_{n_1,n_2,r^{\mathrm{WP}},i,e,w}$ are also indexed over the set of path identifiers $\mathcal{I}^{\mathrm{WP}}_{n_1,n_2,r^{\mathrm{WP}}}$ and reveal whether wavelength w is assigned on edge e. Wavelength converters are potentially allocated per path with identifier i on wavelength path route r^{WP} at any intermediate path node n_3. The end nodes of each path are excluded because the wavelength can be selected there anyway. We represent converters by binary variables $W_{r^{\mathrm{WP}},i,n_3}$. The optimization model for wavelength assignment and converter allocation can be formulated as follows.

Minimize

$$\sum_{\substack{\{n_1,n_2\}\subset\mathcal{N}:\\ n_1\neq n_2}} \sum_{r^{\mathrm{WP}}\in\mathcal{R}^{\mathrm{WP}}_{1,n_1,n_2}} \sum_{i\in\mathcal{I}^{\mathrm{WP}}_{n_1,n_2,r^{\mathrm{WP}}}} \sum_{\substack{n_3\in\mathcal{N}^{\mathrm{DR}}_{r^{\mathrm{WP}}}:\\ n_3\neq n_1\,\wedge\, n_3\neq n_2}} W_{r^{\mathrm{WP}},i,n_3} \tag{4.66}$$

subject to

$$\sum_{w\in\mathcal{W}} L_{n_1,n_2,r^{\mathrm{WP}},i,e,w} = 1 \qquad \begin{array}{l}\forall\,\{n_1,n_2\}\subset\mathcal{N}: n_1\neq n_2,\\ r^{\mathrm{WP}}\in\mathcal{R}^{\mathrm{WP}}_{1,n_1,n_2},\ i\in\mathcal{I}^{\mathrm{WP}}_{n_1,n_2,r^{\mathrm{WP}}},\\ e\in\mathcal{E}:\delta_{r^{\mathrm{WP}},e}=1,\end{array} \tag{4.67}$$

$$\sum_{\substack{\{n_1,n_2\}\subset\mathcal{N}:\\ n_1\neq n_2}} \sum_{\substack{r^{\mathrm{WP}}\in\mathcal{R}^{\mathrm{WP}}_{1,n_1,n_2}:\\ \delta_{r^{\mathrm{WP}},e}=1}} \sum_{i\in\mathcal{I}^{\mathrm{WP}}_{n_1,n_2,r^{\mathrm{WP}}}} L_{n_1,n_2,r^{\mathrm{WP}},i,e,w} \leq f_e \qquad \forall\, e\in\mathcal{E},\ w\in\mathcal{W}, \tag{4.68}$$

$$W_{r^{\mathrm{WP}},i,n_3} \geq L_{n_1,n_2,r^{\mathrm{WP}},i,e_1,w} - L_{n_1,n_2,r^{\mathrm{WP}},i,e_2,w} \qquad \begin{array}{l}\forall\,\{n_1,n_2\}\subset\mathcal{N}: n_1\neq n_2,\\ r^{\mathrm{WP}}\in\mathcal{R}^{\mathrm{WP}}_{1,n_1,n_2},\ i\in\mathcal{I}^{\mathrm{WP}}_{n_1,n_2,r^{\mathrm{WP}}},\\ n_3\in\mathcal{N}^{\mathrm{DR}}_{r^{\mathrm{WP}}}\setminus\{n_1,n_2\},\\ \{e_1,e_2\}\subset\mathcal{E}^{\mathrm{DR}}_{r^{\mathrm{WP}}}:\ e_1\neq e_2\,\wedge\\ \alpha_{e_1,n_3}=\alpha_{e_2,n_3}=1,\ w\in\mathcal{W},\end{array} \tag{4.69}$$

$$W_{r^{\mathrm{WP}},i,n_3}\in\{0,1\} \qquad \begin{array}{l}\forall\,\{n_1,n_2\}\subset\mathcal{N}: n_1\neq n_2,\\ r^{\mathrm{WP}}\in\mathcal{R}^{\mathrm{WP}}_{1,n_1,n_2},\ i\in\mathcal{I}^{\mathrm{WP}}_{n_1,n_2,r^{\mathrm{WP}}},\\ n_3\in\mathcal{N}^{\mathrm{DR}}_{r^{\mathrm{WP}}}\setminus\{n_1,n_2\},\end{array} \tag{4.70}$$

$$L_{n_1,n_2,r^{\mathrm{WP}},i,e,w} \in \{0,1\} \qquad \begin{array}{l} \forall\, \{n_1,n_2\} \subset \mathcal{N} : n_1 \neq n_2, \\ r^{\mathrm{WP}} \in \mathcal{R}^{\mathrm{WP}}_{1,n_1,n_2},\ i \in \mathcal{I}^{\mathrm{WP}}_{n_1,n_2,r^{\mathrm{WP}}}, \\ e \in \mathcal{E} : \delta_{r^{\mathrm{WP}},e} = 1,\ w \in \mathcal{W}. \end{array} \tag{4.71}$$

- The objective function presented in Equation (4.66) aims to reduce additional network costs by minimizing the number of supplementary wavelength converters. The color of transparent lightpath with identifier i along route r^{WP} may be altered at any intermediate node by OEO conversion.
- Constraints (4.67) assign one wavelength to each lightpath link. The sum of all allocated links $L_{n_1,n_2,r^{\mathrm{WP}},i,e,w}$ over all wavelengths w per traversed edge e must equal one.
- The number of available wavelengths is limited by the fiber link quantity since each wavelength may be used at most once per fiber. This restriction is analyzed by Constraints (4.68) which provide the fiber number per network edge as upper bound for all lightpaths passing through at identical wavelength.
- Equations (4.69) detect any wavelength transformation on the links of a transparent path. For this purpose, we examine the transit nodes n_3 of each WP with identifier i separately. The two consecutive path edges incident on node n_3 are denoted by e_1 and e_2, respectively. The right-hand side of the constraints subtracts the respective wavelength link variables on both edges from each other for all fiber wavelengths w. If the links have the same wavelength, the resulting value is zero for all available wavelengths. On the other hand, if the links are assigned different transmission frequencies, the outcome is plus one for the wavelength used on edge e_1 and minus one when analyzing the wavelength on edge e_2. This difference serves as lower bound for the converter allocation on the right-hand side of the equations. In the former case of identical wavelengths, the number of wavelength converters $W_{r^{\mathrm{WP}},i,n_3}$ can be zero, whereas it must be at least one for the latter case of different wavelengths. The sequence of subtracting both link variables is irrelevant.
- Constraints (4.70) and (4.71) define the wavelength converter and link variables as binary variables. The variables may equivalently be restricted to nonnegative integers only, because the number of links per transparent path cannot exceed the value one according to Equations (4.67) and the quantity of wavelength converters is minimized in the objective.

4.5 Case Studies

This section presents the network design studies that have been carried out for our three reference network scenarios. In a first preparatory step, we calculate all simple routes for any given network topology. After that, the translucent lightpath design is applied

to determine the transceiver equipment for each route. In order to account for signal degradation at translucent nodes, we assume an 80 km distance penalty per optically bypassed transit node. Moreover, the set of eligible disjoint routing configurations is pre-calculated and limited to the 250 shortest ones for each node pair. The network and cost key parameters are shown in Table 4.1 and Table 4.2, respectively.

Table 4.1: Network key parameters and their default values.

Wavelength channels per fiber $\lvert\mathcal{W}\rvert$	Maximum long haul transmission distance $l_{\text{LH}}^{\text{MTD}}$ [km]	Span length l^{FS} [km]
80	1500	80

Table 4.2: Cost key parameters and their default values.

Cost ratio 10 Gbit/s / 2.5 Gbit/s q	Cable conduit cost $c_{l_e}^{\text{CC}}$
3.0	0.05

4.5.1 Network Dimensioning Analysis

At first we examine the network dimensioning results by evaluating the total network costs and the expenses for the individual network component types.

German Reference Network

This subsection presents the results for the German reference scenario. Figure 4.1 depicts the equipment costs of all network elements and the infrastructure expenses for the network topology with 21 edges which was designed for node-disjoint path protection. Cable conduits and fiber cables are considered as basic infrastructure because they provide the framework for optical networking. We compare opaque and translucent network design side-by-side.

According to Figure 4.1a, the equipment investments in the opaque case are clearly dominated by the transponder (TP) costs representing 55% of the overall costs. The other most relevant portions come from the electrical switch (ES), short reach line card (SLC), and optical multiplexer/demultiplexer (OMD) components representing 18%, 16%, and 6% of the equipment expenses, respectively. The influence of the remaining network elements booster/pre-amplifier (BPA) (2%), inline amplifier (IA) (2%), and dispersion compensating fiber (DCF) (1%) is only very small. For the translucent network design, long reach line cards (LLCs) implicate the highest cost term producing 26% of the

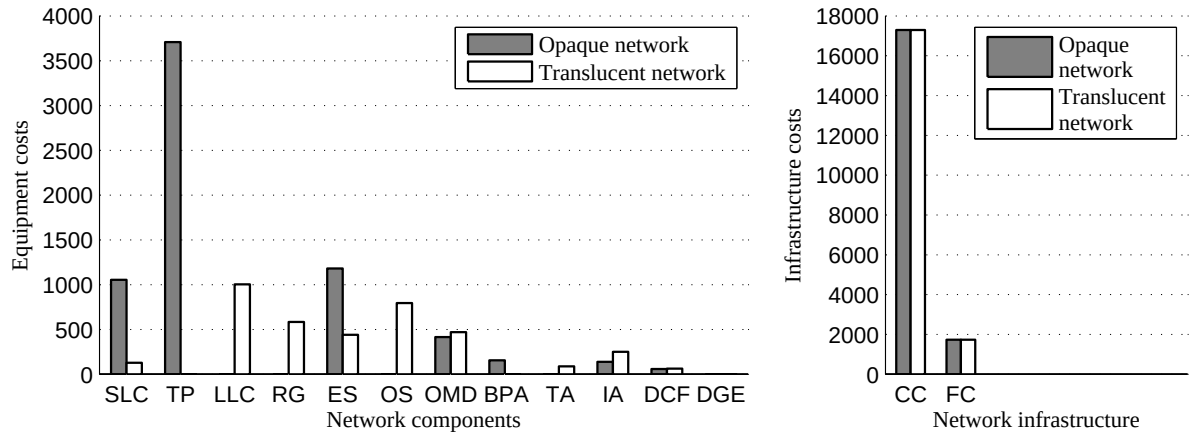

(a) Equipment (b) Infrastructure

Figure 4.1: Equipment and infrastructure costs of the opaque and translucent network design for the 21-edge German reference network designed for node-disjoint 1:1 path protection.

overall expenditures. However, the costs for optical switch (21%), regenerator (15%), optical multiplexer/demultiplexer (12%), and electrical switch (12%) components are in a similar range. Except for the inline amplifier (7%), the remaining matters of expense (short reach line card (3%), transparent node pre-amplifier (2%), and dispersion compensating fiber (2%)) are below five percent. The infrastructure costs are shown in Figure 4.1b. All existing topology edges are used for transmission in both the opaque and the translucent network setting. Thus, the expenditures for cable conduits and fiber cables are equivalent.

The following diagrams illustrate the dependency of the network costs on the topology. We consider all physical networks obtained from the topological design with an average node degree between 2.5 and 3.5. Figure 4.2a shows the total network equipment costs over the number of network edges. For 21 network edges, the overall element costs of the network can be brought down to 57% when applying the translucent instead of the opaque network design. More densely meshed network topologies further reduce the equipment expenses because the demands can be routed on shorter paths traversing fewer hops. The curves demonstrate that the relative benefit in the opaque scenario is a little higher than for the translucent case. Nevertheless, the selective allocation of regenerators in the 30-edge network reduces the total equipment costs to 66%.

The total infrastructure costs usually increase for a larger amount of network edges according to Figure 4.2b. After identical expenses for topologies up to 26 edges, the opaque and translucent infrastructure costs diverge for more densely meshed physical networks. While the opaque design utilizes all network edges, the translucent counterpart selects only 26 edges although the topologies offer 27 and 28 edges. Furthermore, the 29- and 30-edge topologies are reduced to 27 edges. From this, one can infer that an opaque network relies on a higher average node degree in order to reduce the number

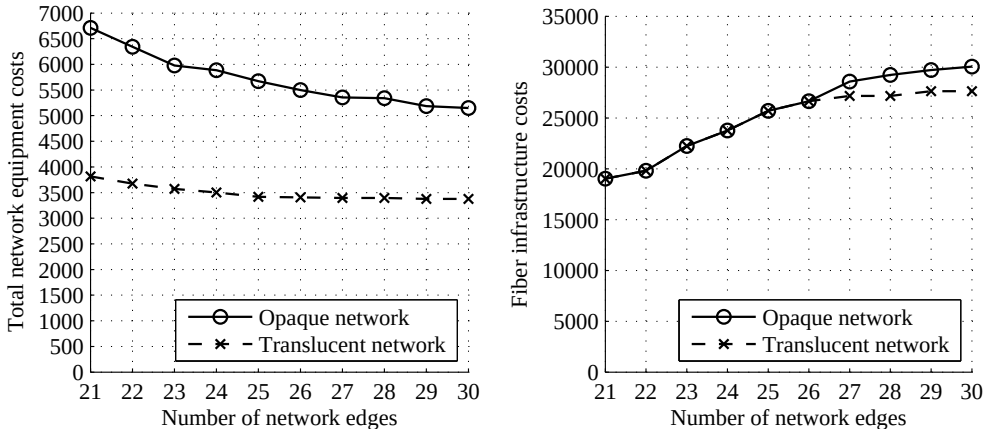

(a) Equipment (b) Infrastructure

Figure 4.2: Total equipment and infrastructure costs of the opaque and translucent network design for various German reference network topologies designed for node-disjoint 1:1 path protection.

of routing hops. Each additional hop of a path yields high extra costs due to mandatory TP, SLC, and ES equipment. A translucent network on the other hand provides long range transmission equipment at the demand's end nodes and regenerates the signal at intermediate nodes only if necessary. Another reason is that the available transmission range of the transceiver equipment allows some flexibility to choose longer paths. Additionally, optical switch (OS) costs do not arise for each lightpath individually but on a per fiber basis. Thus, it is often possible to find a number of paths which follow different routes but involve the same costs in terms of transponders and regenerators.

Figure 4.3 compares the individual transceiver cost terms and their overall costs for the opaque and translucent network solutions. In both scenarios short reach line cards (SLCs) must be allocated to add and drop lightpaths at the origin and destination node. Besides, they are a prerequisite to convert each wavelength channel to electrical/ optical form at the input/output of the electrical switch in the opaque case. The same holds true for the transponders (TPs) leading to an enormous number and high costs. Due to the short length of many edges in the German network, the maximum transmission distance of the transponders is often not exploited in the opaque solution. In contrast, translucent lightpaths can optically bypass transit nodes and keep the signal in the optical domain as long as the signal quality is adequate. The limited physical distances between the nodes often permit to establish end-to-end transparent paths or necessitate at most one intermediate regeneration step.

The switching and multiplexing costs are presented in Figure 4.4. The OMD expenses are proportional to the number of allocated fibers and similar for opaque and translucent design. In the opaque scenario, all lightpaths are switched electronically whereas the translucent approach arranges ESs for local ingress and egress traffic, solely. Most

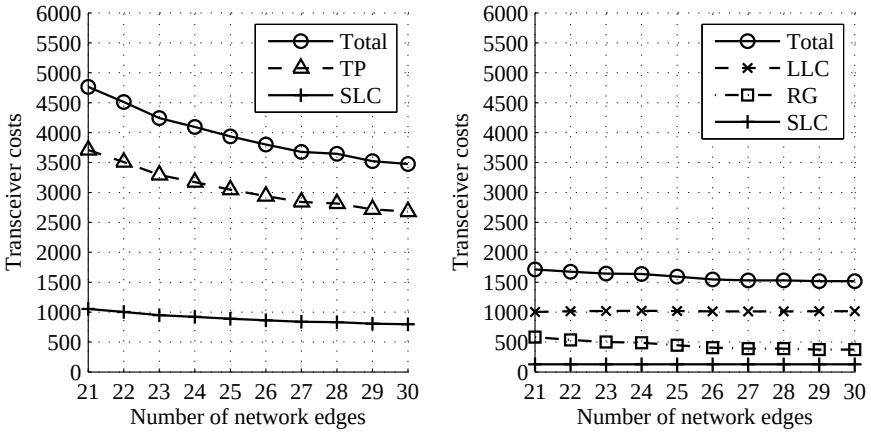

(a) Opaque network (b) Translucent network

Figure 4.3: Transceiver costs of the opaque and translucent network design for various German reference network topologies designed for node-disjoint 1:1 path protection.

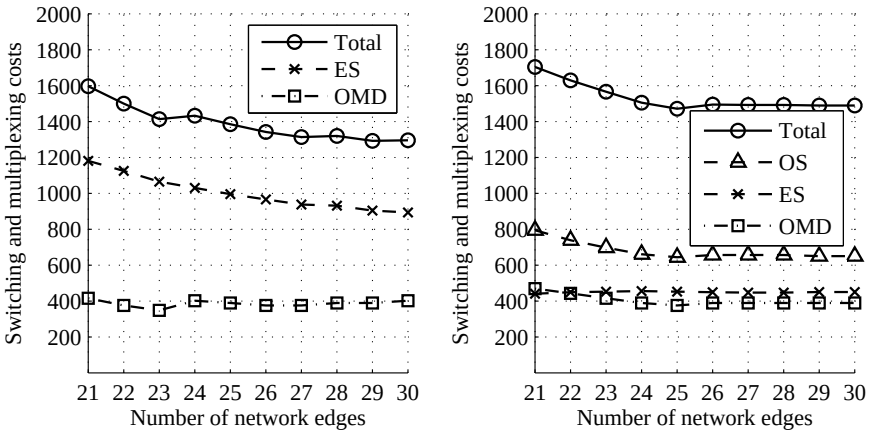

(a) Opaque network (b) Translucent network

Figure 4.4: Switching and multiplexing cost evaluation of the opaque and translucent network design for various German reference network topologies designed for node-disjoint 1:1 path protection.

transit traffic is routed transparently at a translucent node by optical switching. Since the nodes should be able to process any wavelength on an incident fiber, the OS must provide ports for the entire set of available wavelengths no matter how many channels are actually active. Thus, the total switching costs of the translucent networks slightly exceed the respective investments in the opaque case. The allocation of optical switch ports for all wavelengths per fiber is the reason why the requirement to fully utilize the wavelength channel capacity of the fibers is more pronounced in the translucent approach.

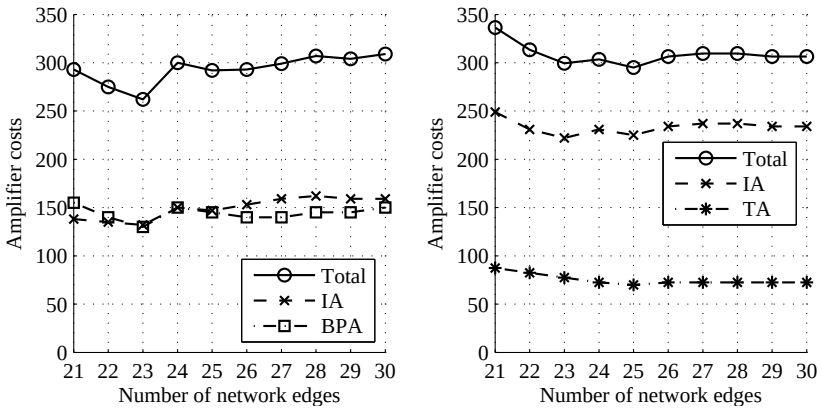

(a) Opaque network (b) Translucent network

Figure 4.5: Amplifier costs of the opaque and translucent network design for various German reference network topologies designed for node-disjoint 1:1 path protection.

Figure 4.5 portrays the amplifier costs. The total expenses for signal amplification in the translucent network are up to 15% higher than for the opaque design but may also be very similar. This is due to identical costs for all inline amplifiers placed after a recurring 80 km distance along all fiber links. Only the amplifier configurations at the nodes differ. In the opaque case, a booster/pre-amplifier with cost 2.5 terminates both ends of each fiber link whereas the translucent design involves one transparent node pre-amplifier with cost 1.25 per end node and an additional inline amplifier with cost 3.0 at the sender side. Thus, the amplification investment of a translucent fiber link (5.5) is only marginally higher than for an opaque link (5.0) in the German network. Another important influence is the specific set of fiber links allocated by the design. Longer fiber links necessitate a higher number of amplification stages and increase the amplifier expenditures although the link quantity may be identical.

European Reference Network

In order to account for longer distances in the European network scenario we incorporate extended long haul transceiver technology with a transmission length of 1500 km. All the equipment in the translucent design is of ELH type to establish a consistent network scenario. The opaque approach on the other hand may comprise long haul technology on short edges because all wavelength connections are terminated electrically at each network node.

Figure 4.6 shows the equipment and infrastructure expenditures for the network topology consisting of 14 edges. The distribution of the cost terms is comparable to the results of the German network. Again, the infrastructure costs far exceed the network element costs.

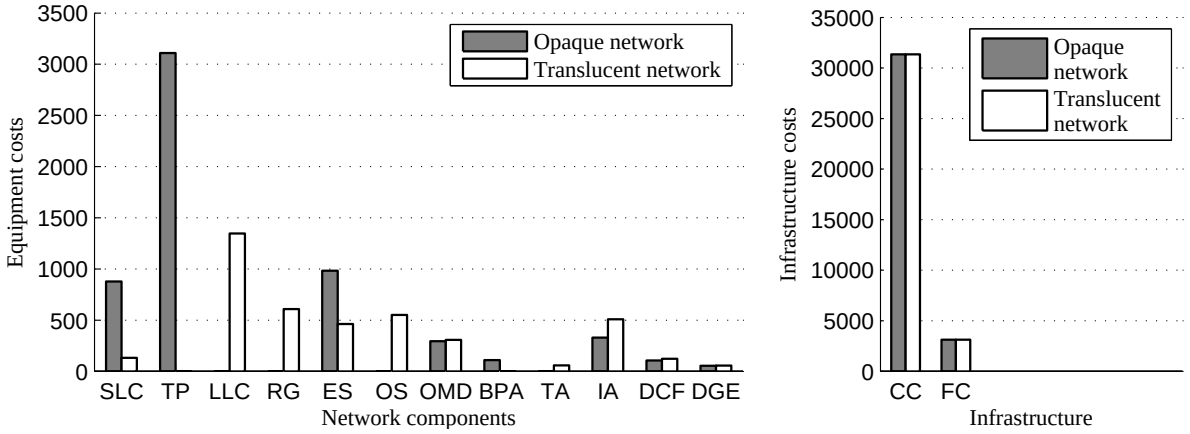

(a) Equipment (b) Infrastructure

Figure 4.6: Equipment and infrastructure costs of the opaque and translucent network design for the 14-edge European reference network designed for node-disjoint 1:1 path protection.

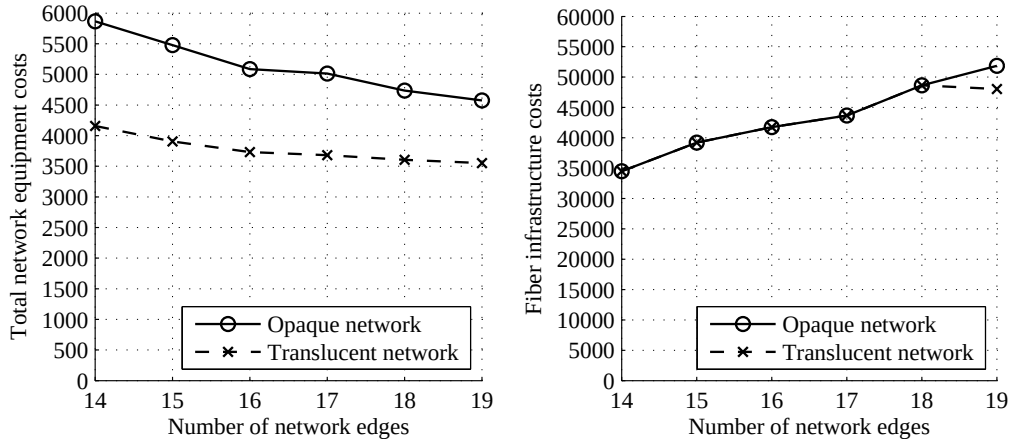

(a) Equipment (b) Infrastructure

Figure 4.7: Total equipment and infrastructure costs of the opaque and translucent network design for various European reference network topologies designed for node-disjoint 1:1 path protection.

The influence of the topology on the equipment and infrastructure investments are depicted in Figure 4.7. The equipment cost savings of the translucent network solution with respect to the opaque design are between 22% and 29% with an average of 26%.

Figure 4.8 evaluates the transceiver expenses for both network architectures. While the cost penalty for the 14-edge network is 91% for the opaque scenario, it decreases to 69% for the 19-edge topology. In the translucent scenario, the transceiver costs reduction

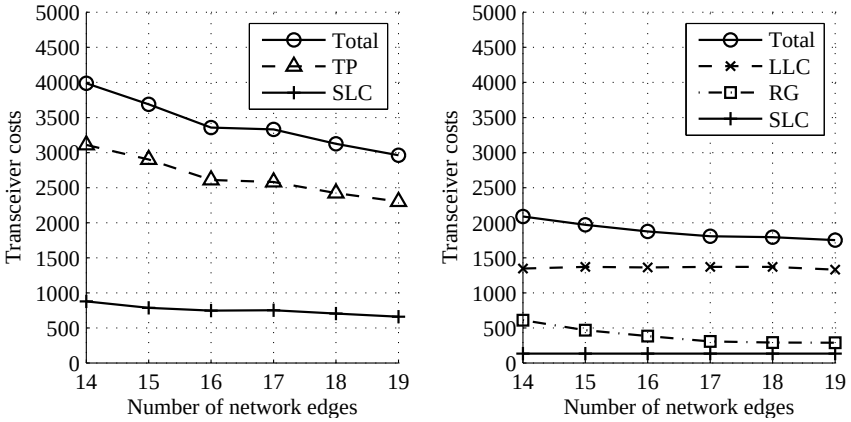

(a) Opaque network (b) Translucent network

Figure 4.8: Transceiver costs of the opaque and translucent network design for various European reference network topologies designed for node-disjoint 1:1 path protection.

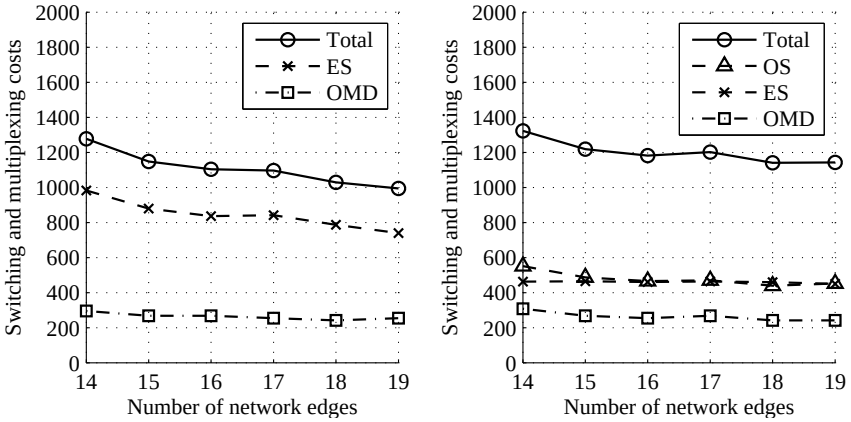

(a) Opaque network (b) Translucent network

Figure 4.9: Switching and multiplexing costs of the opaque and translucent network design for various European reference network topologies designed for node-disjoint 1:1 path protection.

for increasing edge quantity can be attributed to savings on regenerators because the topologies provide shorter routes.

The overall switching and multiplexing expenditures portrayed in Figure 4.9 are comparable for both network scenarios. For a sparsely meshed network, the opaque design is more expensive because the routing involves a relatively high number of hops and electrical switching ports must be allocated per hop.

Figure 4.10 compares the amplifier investments. The cost discrepancy between both approaches is more pronounced than in the German network because the opaque

network design allows to equip all network edges shorter than the maximum LH transmission distance with LH amplifiers whereas the translucent scenario stipulates ELH amplifiers on any edge.

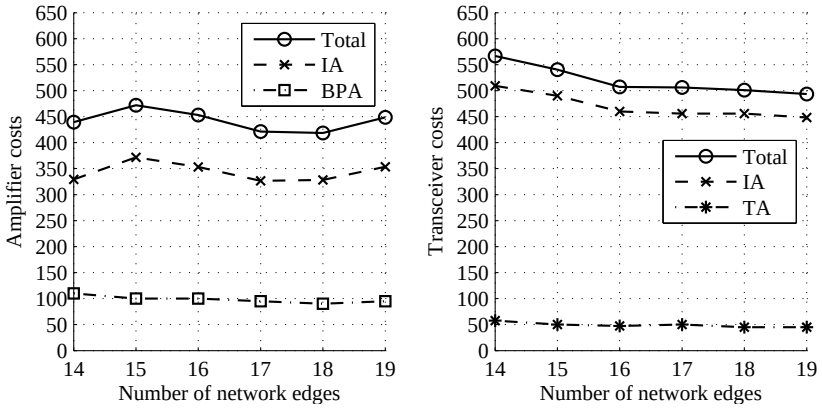

(a) Opaque network (b) Translucent network

Figure 4.10: Amplifier costs of the opaque and translucent network design for various European reference network topologies designed for node-disjoint 1:1 path protection.

US Reference Network

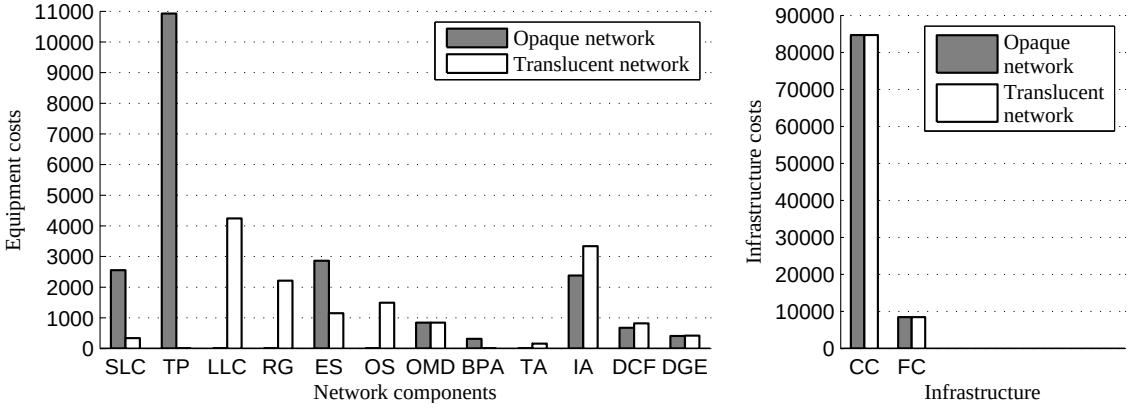

(a) Equipment (b) Infrastructure

Figure 4.11: Equipment and infrastructure costs of the opaque and translucent network design for the 18-edge US reference network designed for node-disjoint 1:1 path protection.

Very long edge distances in the US network above one thousand kilometers demand for ultra long haul technology. We assume a maximum transparent transmission range of 3000 km in the fiber medium.

Figure 4.11 gives an overview of the network equipment costs and the infrastructure expenses. Again, the transponders yield the major cost contribution of all network components and the infrastructure costs outweigh the equipment expenses.

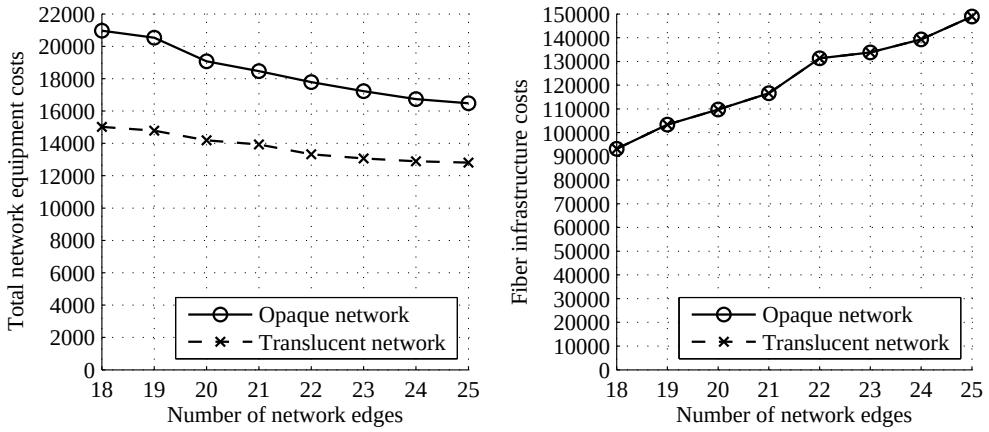

(a) Equipment (b) Infrastructure

Figure 4.12: Total equipment and infrastructure costs of the opaque and translucent network design for various US reference network topologies designed for node-disjoint 1:1 path protection.

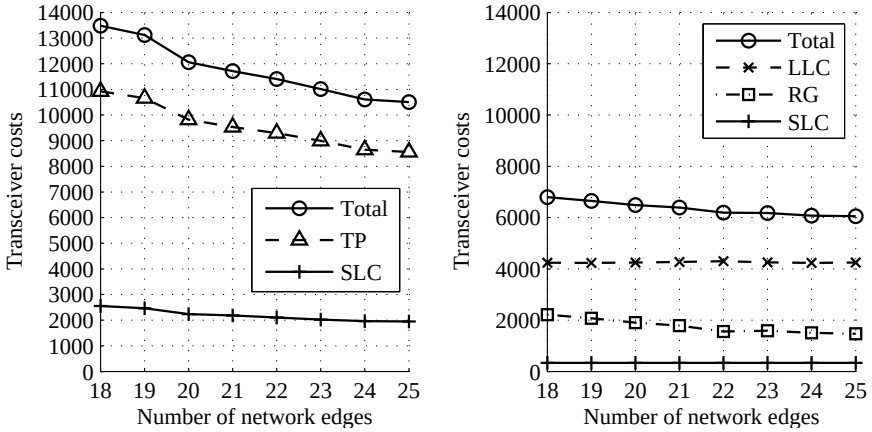

(a) Opaque network (b) Translucent network

Figure 4.13: Transceiver costs of the opaque and translucent network design for various US reference network topologies designed for node-disjoint 1:1 path protection.

The average cost savings for the translucent solution with respect to the entire network equipment is in the range of 25% of the opaque equipment expenditures for all considered topologies. Figure 4.12 shows detailed curves for the total equipment and fiber infrastructure investments over the number of network edges. As with the other

networks, the translucent design's cost reduction arises from the selective provisioning of electrical signal regeneration.

Figure 4.13 shows a massive reduction of transceiver costs by 46% on average compared to the opaque concept.

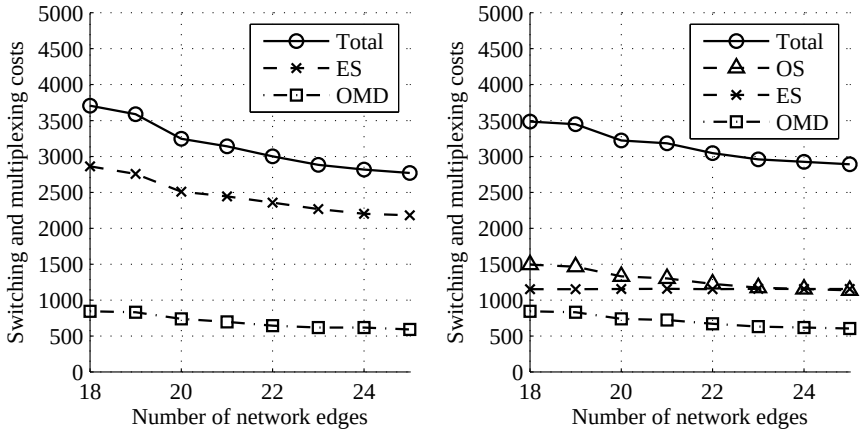

(a) Opaque network (b) Translucent network

Figure 4.14: Switching and multiplexing costs of the opaque and translucent network design for various US reference network topologies designed for node-disjoint 1:1 path protection.

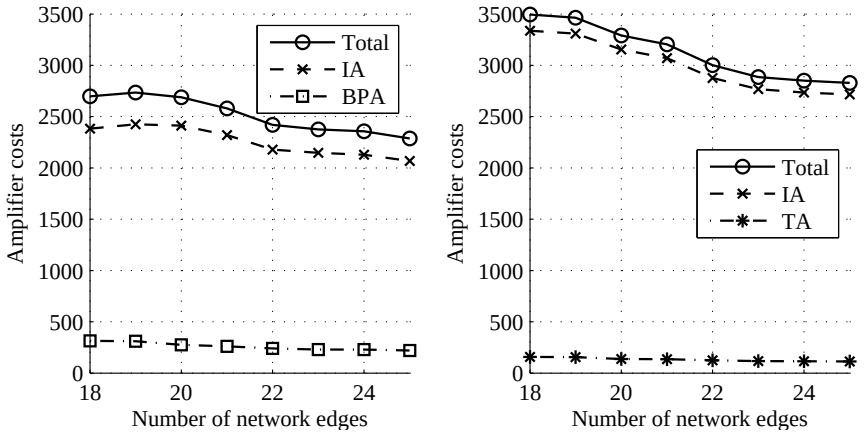

(a) Opaque network (b) Translucent network

Figure 4.15: Amplifier costs of the opaque and translucent network design for various US reference network topologies designed for node-disjoint 1:1 path protection.

The total switching and multiplexing costs of both approaches are compared in Figure 4.14. There is not that much difference between the resulting values with a minor advantage of the translucent design compared to the opaque solution for more sparsely meshed topologies and vice versa for networks with a larger edge set.

Figure 4.15 visualizes the amplifier expenditures. The electrical signal termination at each node in the opaque design allows to adapt the amplifier type with respect to the supported transmission range. Long haul technology is sufficient for a number of short edges in the US network and most other edges can be equipped with extended long haul technology.

4.5.2 Routing Analysis

This subsection discusses the routing characteristics of the opaque and translucent network design.

German Reference Network

Figure 4.16a shows the number of allocated fiber links for the German network topologies. We observe that the variation between both approaches is quite small, especially for more densely meshed topologies. The distribution of all wavelength links is depicted in Figure 4.16b.

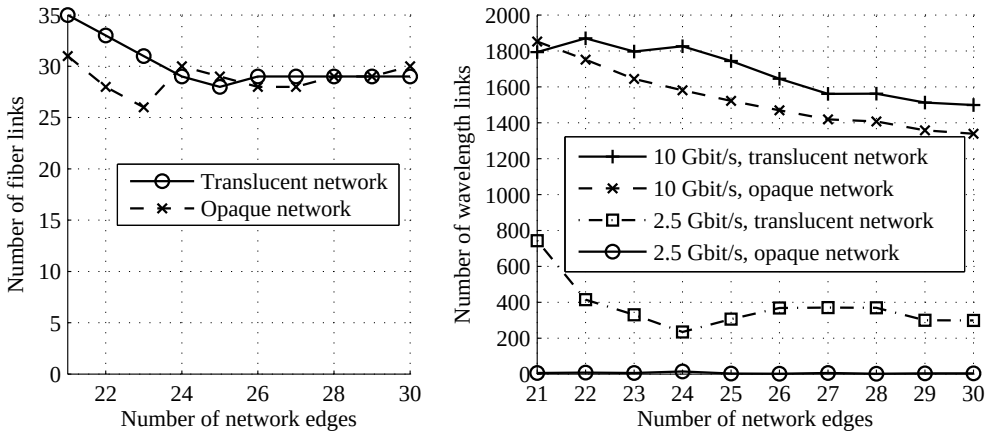

(a) Fiber links (b) Wavelength links

Figure 4.16: Allocated fiber and wavelength links of the opaque and translucent network design for various German reference network topologies designed for node-disjoint 1:1 path protection.

In an opaque network, all 2.5 Gbit/s links can be multiplexed to higher bitrate links on each network edge at no extra cost due to the grooming capability of the electrical switch. Since transponder costs can be reduced via this aggregation, 10 Gbit/s links are prevalent. The number of 2.5 Gbit/s links is insignificant and varies between 2 and 14. In contrast, the translucent network design only allows for end-to-end grooming between origin and destination node by default. This implies a reduced flexibility and manifests by a relevant number of 2.5 Gbit/s links. However, the 10 Gbit/s links in the

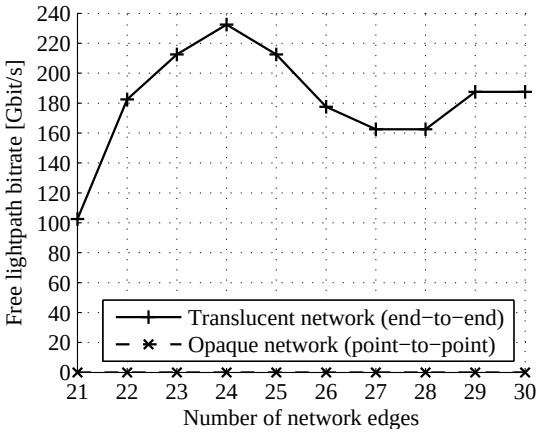

Figure 4.17: Unexploited lightpath capacity of the opaque and translucent network design for various German reference network topologies designed for node-disjoint 1:1 path protection.

translucent scenario outnumber the 2.5 Gbit/s links in the opaque case except for one topology.

At first glance it may seem surprising that such a configuration is optimal but the answer is given by Figure 4.17. The diagram portrays the unused bitrate of all lightpaths in gigabit per second for both approaches. In the translucent case, we measure the idle bitrate in an end-to-end manner per lightpath because the capacity cannot be easily used by other connections without extra equipment at the nodes. In the opaque scenario, the unused bitrate is counted per link due to the flexible accessibility for other connections. While the opaque design utilizes 100% of the bitrate of all links, some of the translucent paths at 10 Gbit/s offer free capacity. From a cost point of view, it is advantageous to establish a 10 Gbit/s lightpath instead of three 2.5 Gbit/s connections due to the savings on transponder costs. Furthermore, each 2.5 Gbit/s lightpath blocks one wavelength channel per hop just like 10 Gbit/s paths do. This effect would reduce the overall bitrate that can be achieved per fiber. On the other hand, high initial costs for lighting an extra fiber by providing switching functionality, amplifiers, and multiplexers prevent the excessive allocation of new fibers. This is another motivation for setting up 10 Gbit/s lightpaths instead of 2.5 Gbit/s connections.

European Reference Network

The corresponding routing results for the European network scenario are depicted in the following two figures. The characteristics known from the German scenario can be confirmed.

The total number of all provided fiber links is almost identical as can be seen in Figure 4.18a. In two topologies, the opaque and the translucent network require the same

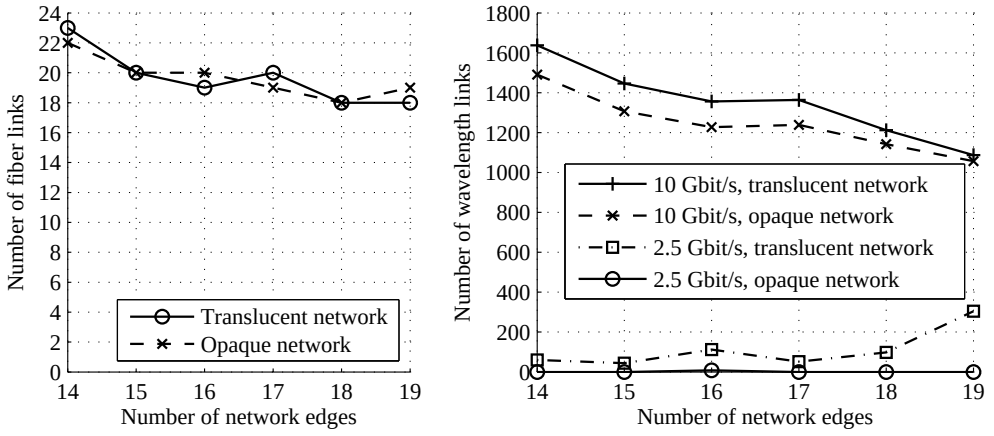

(a) Fiber links (b) Wavelength links

Figure 4.18: Allocated fiber and wavelength links of the opaque and translucent network design for various European reference network topologies designed for node-disjoint 1:1 path protection.

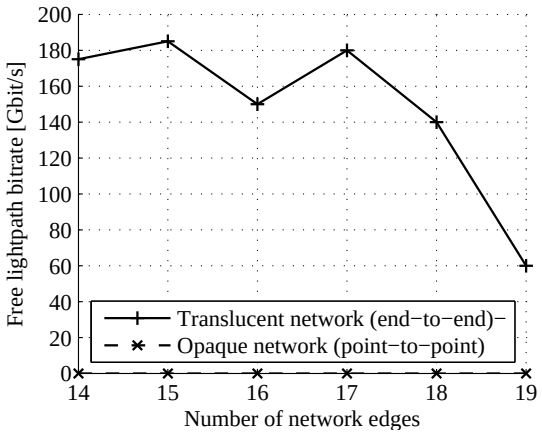

Figure 4.19: Unexploited lightpath capacity of the opaque and translucent network design for various European reference network topologies designed for node-disjoint 1:1 path protection.

number of fibers. The remaining four topologies differ by one link with a 50/50 distribution between the opaque and the translucent design. In terms of allocated lightpaths, 10 Gbit/s wavelength links clearly dominate in the opaque network according to Figure 4.18b. The translucent design on the other hand consists of a relevant portion of 2.5 Gbit/s links and requires more 10 Gbit/s links.

When examining the established lightpaths in Figure 4.19, we observe that the available lightpath capacity of 10 Gbit/s connections is not completely exploited in the translucent scenario. This is in contrast to the opaque case where no idle resources remain.

US Reference Network

The lightpath routing in the US reference networks can be analyzed based on Figure 4.20. It shows diagrams for the number of fiber and wavelength links over different topologies, respectively. Again, we conclude that a similar number of fiber links for both architectures is utilized in a different manner. The translucent design involves a higher number of 10 Gbit/s links compared to the opaque case and the former approach also yields 2.5 Gbit/s connections which are negligible in the latter architecture.

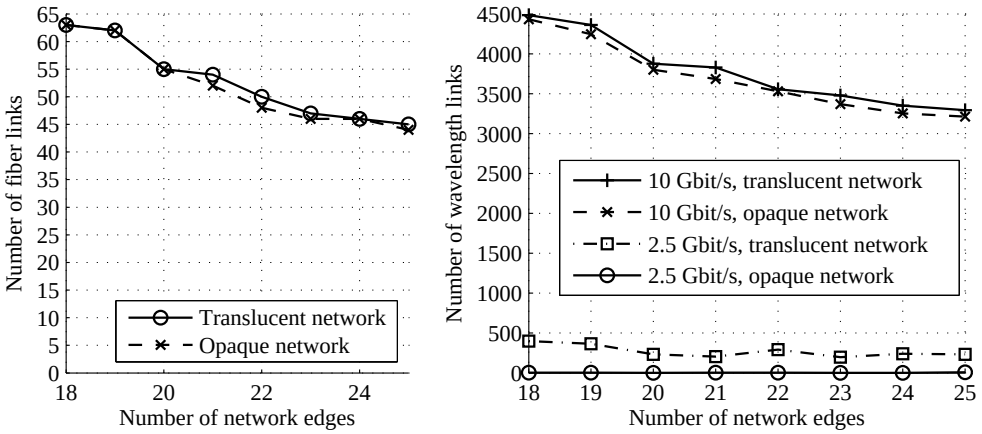

(a) Fiber links (b) Wavelength links

Figure 4.20: Allocated fiber and wavelength links of the opaque and translucent network design for various US reference network topologies designed for node-disjoint 1:1 path protection.

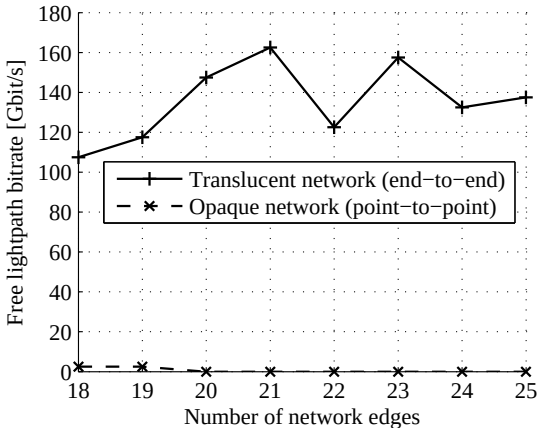

Figure 4.21: Unexploited lightpath capacity of the opaque and translucent network design for various US reference network topologies designed for node-disjoint 1:1 path protection.

Spare bitrate capacity in 10 Gbit/s lightpaths is presesented Figure 4.21. The opaque design can almost completely exploit the wavelength channels while there are unused

resources in the translucent design. We want to remark that both designs are optimal and that this effect arises from the availability of electrical signal multiplexing at no extra cost in the opaque node architecture.

4.5.3 Wavelength Assignment and Converter Allocation Analysis

In the opaque network scenario, the wavelength assignment task can be performed by simply choosing an arbitrary available wavelength for each lightpath link. This is due to the fact that the opaque network architecture enables wavelength conversion at each node by default. In the translucent scenario, one must identify a wavelength which is available on all of the edges of a transparent lightpath. Only if the lightpath is regenerated at an intermediate node to refresh the signal quality, the wavelength can be translated.

Our case studies show that the wavelength assignment and converter allocation problem in the translucent network scenario essentially reduces to a wavelength assignment task. For all presented network designs in every reference scenario, it was possible to compute a valid wavelength configuration that fulfills the wavelength continuity constraint. The available number of wavelengths per edge is given by the fiber quantity allocated during the routing and network dimensioning process and the number of wavelength channels per fiber. By experimenting with longer maximum transmission distances, we were able to create a translucent network design for the European scenario with 17 edges whose wavelength assignment ILP yielded infeasible status when excluding wavelength converters. However, the wavelength converter allocation model could not find any solution within a reasonable time frame.

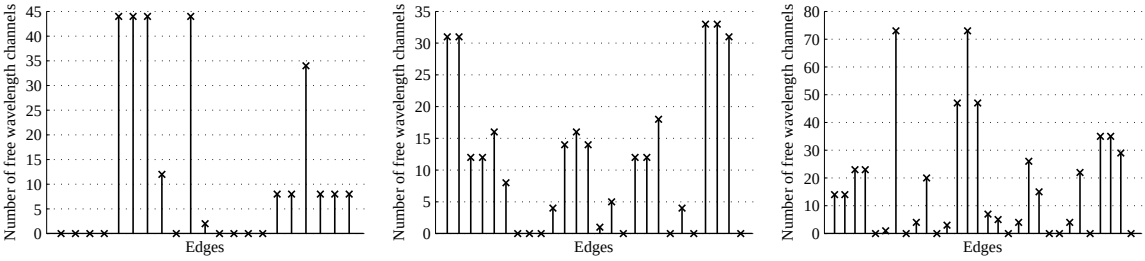

(a) 21 edges (b) 26 edges (c) 30 edges

Figure 4.22: Free wavelength channels of the translucent network design for selected German reference network topologies designed for node-disjoint 1:1 path protection.

We conclude that the characteristical structure of translucent lightpaths helps to prevent wavelength conflicts to a great extent. Translucent paths without intermediate signal regeneration traverse only few hops. Consequently, the overlapping potential with other wavelength paths is restricted. In case of long translucent lightpaths, wavelength conversion functionality is available due to the necessity to regenerate the signal at one

or more transit nodes. These circumstances often facilitate a wavelength assignment for the static routing and dimensioning problem without supplementary converters.

Figures 4.22, 4.23, and 4.24 analyze the number of free wavelength channels on the edges for selected topologies of the German, European, and US reference network scenario, respectively. The diagrams illustrate the number of free wavelength channels for all edges. We observe very high wavelength loads up to 100% for most edges. Thus, we can rule out the possibility, that the wavelength assignment problem is alleviated due to inefficient wavelength channel utilization.

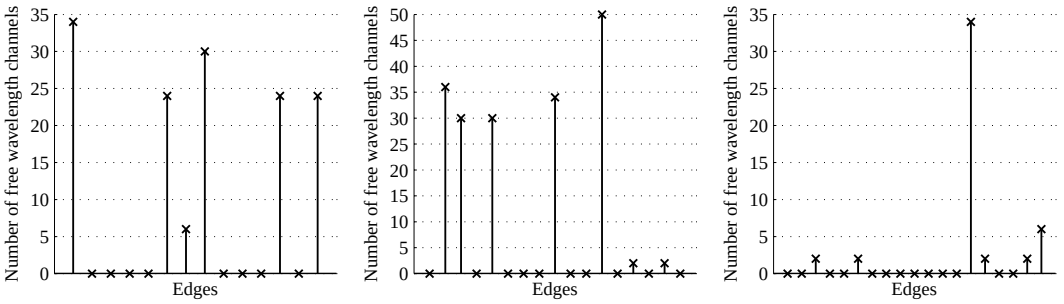

(a) 14 edges (b) 17 edges (c) 19 edges

Figure 4.23: Free wavelength channels of the translucent network design for selected European reference network topologies designed for node-disjoint 1:1 path protection.

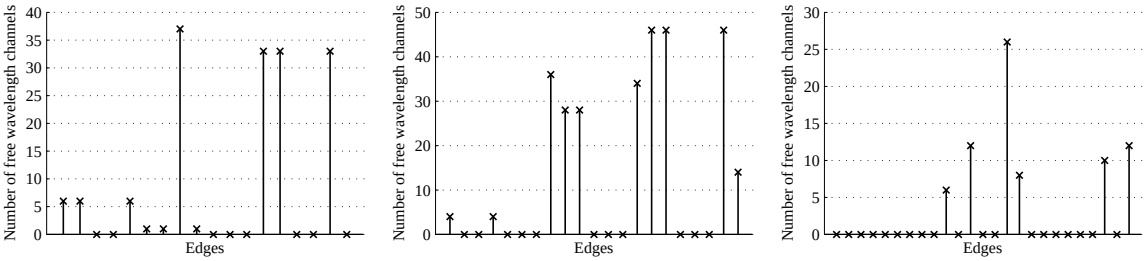

(a) 18 edges (b) 21 edges (c) 25 edges

Figure 4.24: Free wavelength channels of the translucent network design for selected US reference network topologies designed for node-disjoint 1:1 path protection.

4.6 Summary

In this chapter, we investigated the routing and network dimensioning problem for an opaque and a translucent network scenario. The former architecture offers electrical signal regeneration at every lightpath hop by providing point-to-point links. In contrast, the translucent architecture enables lightpaths to optically bypass transit nodes and

selectively regenerate the signal in case of degraded signal quality. For each scenario, we developed a novel mathematical optimization formulation that minimizes the total capital expenditures based on a realistic node and link architecture using a detailed cost model. Our approach enables profound insights in the cost terms of all network equipment. Numerous case studies were carried out to assess the network designs for different network topologies in terms of geographical size and mesh degree. Our investigations show that a translucent network design can significantly cut down network investments due to reduced transceiver hardware.

5 Availability-Aware Routing Design

This chapter deals with a novel availability-based routing strategy. The next section takes a look at related work. In Section 5.2, we present metrics for the performance evaluation of network resilience strategies. Section 5.3 introduces the virtual link concept and analyzes corresponding reliability block diagrams. In Section 5.4, we formulate a mathematical program that computes connections offering a guaranteed end-to-end availability while minimizing the utilized network resources. Next, Section 5.5 discusses the results of case studies. Finally, Section 5.6 concludes the chapter by giving a brief summary.

5.1 Related Work

The importance of a clear understanding of the relationship between survivable network design and the respective performance in terms of availability has been recognized a long time ago [TN94]. Various resilience schemes have been proposed since then. However, many studies restricted themselves to investigating the ability to recover from certain network failures. Only a few years ago, the availability awareness has gained momentum. Related work can be roughly grouped into two categories. The first group stands for survivability-oriented network designs whose availability performance is evaluated in a subsequent step. In case the target performance is not met, the configuration may be adapted optionally. The second category of studies aims to create routing configurations that implicitly fulfill certain availability requirements by taking availability metrics into account. Moreover, many publications refer to link failures neglecting the influence of node reliability.

The article [HWHM04] introduces a dynamic link-state parameter which reflects the availability of network components and the resources, i.e. the link is intact and has free capacity. The authors suggest to apply this metric to link-state routing protocols. An algorithm is developed to guarantee reliable connections by allocating a working path and an optional protection path. A conceptually similar approach in the context of dedicated and shared path protection is described in [TMP05]. The publication [AM08] describes a different availability-aware provisioning framework based on probing techniques.

The work in [CG02] analyzes the availability of span-restorable mesh networks. The authors show that the network design can tolerate a high percentage of all dual failures although it targets only single failures. This circumstance is facilitated by capacity

modularity offering some extra resources that can be efficiently used in an adaptive way in case of a second network edge failure. An enhanced network design with respect to dual failure restorability is presented in [CG05].

In [AMP+03, SCV+08] the authors investigate the connection availability of dedicated and shared path protection. The latter study compares the results with unprotected connections evaluating heterogeneous network scenarios with different geographic coverage, node degree, and number of hops along the shortest path. Event-based simulations are carried out to represent a dynamic environment where connections are requested and released according to a Poisson process. The online routing algorithm establishes the connections along shortest distance paths. An integration of availability constraints is beyond the scope of this work.

Reference [TMP06] examines the trade-off between availability and capacity for path protection. The authors develop a two-stage heuristic. In the first phase, the requests are routed with a minimization of connection unavailability in mind. The unavailability of each link is applied as metric for a shortest path routing to approximate the total unavailability of the connection. Working and protection path are calculated in two different ways. On the one hand, an algorithm that finds the minimum total metric of both disjoint paths is applied. On the other hand, a shortest path algorithm first computes the most direct path and afterwards the shortest remaining disjoint path by removing the network links that were used by the former path. The total connection availability of both solutions is calculated and the best one is selected. In a subsequent phase, the network resources are minimized. Based on the given routing configuration and the supported wavelength channel quantity, the number of fibers can be determined. In order to reduce the fiber capacity, rerouting of connections is granted by tolerating a defined degradation of the availability. In a greedy manner, the fibers with the smallest number of utilized wavelengths are selected and an attempt to reroute all traversing connections is made. In [CLE04] the authors propose a different iterative heuristic to integrate availability awareness into cost modeling and analyze the trade-off between availability and network costs. A decoupled concept of evaluating the availability and cost performance of networks separately based on genetic algorithms is presented in [GKG+10]. Publication [Sch05] probes the availability performance of path protection with one and two alternative paths and compares the results with the unprotected case. The author develops respective ILP formulations to minimize the overall edge costs of a connection while ensuring a given availability.

The study [DCG03] investigates the availability and capacity consumption of shared path protection. This network survivability scheme allows multiple working paths to share protection resources if they are mutually disjoint. The authors consider an approach that establishes the working paths via shortest path routing in an initial step. A shared path protection design to compensate any single link failure is performed afterwards based on ILP. The objective is to minimize the protection capacity measured in terms of total length of all allocated wavelength links. Case studies are carried out which analyze the restorability of dual failures. The authors prove that the fraction of restored connections can significantly be increased by limiting the sharing degree of

protection links, i.e. restricting the number of working paths which can utilize the same backup link. In [KMO09] the authors develop a heuristic and an ILP-based scheme to enable availability-aware connection provisioning based on calculating a feasible sharing degree. A similar scenario is analyzed in [LTMP09], where the shareability level of the backup capacity is dynamically adjusted in an online manner based on the actual downtime experienced by the connection. The interdependency of availability guarantees and capacity-efficient grooming of subwavelength connections is addressed in [TML+09]. Publication [Kos06] compares the connection availability and network costs of dedicated path protection, shared path protection, and demand-wise shared protection. The authors of [SM08] relax the disjoint routing constraint of classical path protection by allowing link sharing between a primary and one or more backup paths. A dynamic provisioning algorithm is developed in order to enable availability warranties and service differentiation. Other resilience mechanism variants, namely shared segment protection and shared subpath protection, are examined in [KM10].

The work [ZKZM03] describes a framework to enable availability-guaranteed services in wavelength division multiplexing networks. It consists of a connection availability evaluation and a suitable provisioning scheme. The authors analyze the service availability of unprotected paths, dedicated path protection, and shared path protection. It is shown that the multiplication of link availabilities to calculate a path's availability can be transformed to a summation by applying the logarithm. This facilitates a maximum availability path computation via simple shortest path routing. The authors present an ILP model that minimizes the network resources in terms of wavelength links subject to the routing of all connection requests whose availability requirements can be satisfied with a single path. Dedicated path protection is considered in case a single path connection does not offer the desired availability. The authors formulate a corresponding mathematical program. However, this involves nonlinear constraints for ensuring the end-to-end availability. Thus, the model cannot be solved by ILP without applying an approximation.

5.2 Performance Criteria for Network Resilience

5.2.1 Survivability

Typical resilience mechanisms such as path protection are designed to fulfill certain survivability requirements, for example the compensation of any single node or edge failure. In order to survive any single failure scenario, an alternative backup path is supplied in addition to the primary connection. The routes therefore must not traverse a common edge or node, as a failure can affect both transmission options otherwise. Network capacity is reserved for both paths so that, after the failure detection, affected connections are switched to the backup path (1:1 protection). Alternatively, both paths may be used for transmission simultaneously (1+1 protection).

However, on the other hand, network operators commit to a short maximum service downtime per year when defining service level agreements (SLAs) with their business customers. A violation of the stipulated requirements causes high contract penalties. From a customer perspective, the costs of a failure include direct and indirect loss of business, reduced productivity, data loss, damaged public image, and legal issues [Sem08].

Common resilience schemes have been analyzed with respect to their resulting availability. However, a capacity consuming end-to-end disjoint routing of all traffic demands may not be necessary to ensure specific availabilities. Especially for short transmission distances and depending on the probability of node failures, more efficient routing configurations might be possible.

5.2.2 Reliability and Availability

In the course of normal language use, terms like reliability and availability intuitively refer to a status in which something is working as desired. Both words are often used interchangeably. However, from an engineering perspective, reliability and availability address different characteristics. In the following we summarize the most important definitions and formulas to provide a clear understanding of the topic. A comprehensive description of reliability theory and engineering is presented in [Sta09]. Reference [Def08] explains a number of related terms in the context of telecommunication.

The term *reliability* refers to the probability of a component or system to provide its required service during a certain time interval in the presence of failures. Thus, reliability is a function of the operating time. It commences with reliability one and declines to reliability zero. The reliability at a given point in time expresses the likelihood that the component or system is still in functional state after being put into operation at point in time zero. Consequently, maintenance operations cannot improve the reliability of a device because reliability considers a continuous period of being fully operational. Reliability plays an important role for critical applications that do not tolerate any short interruption of the service.

Availability is another related term in this context. It expresses the probability of a component or system to serve its purpose at a particular point of time. In contrast to reliability, repairing a device after a failure improves the availability because it can perform its function again. Figure 5.1 depicts the operational state of an example device over time. We assume that the device has been put into operation at time t_0 and functions properly. At time t_1 a defect causes the unavailability of the service. The device's life time consists of a sequence of up and down states.

Usually, availabilities are considered for the steady-state, i.e. assuming that the observation time is long enough to reach stable values for time to failure (TTF) and time to repair (TTR). In this case, the availability does not depend on time. The device's life can then be modeled as a fixed repetitive cycle of constant mean time to failure (MTTF)

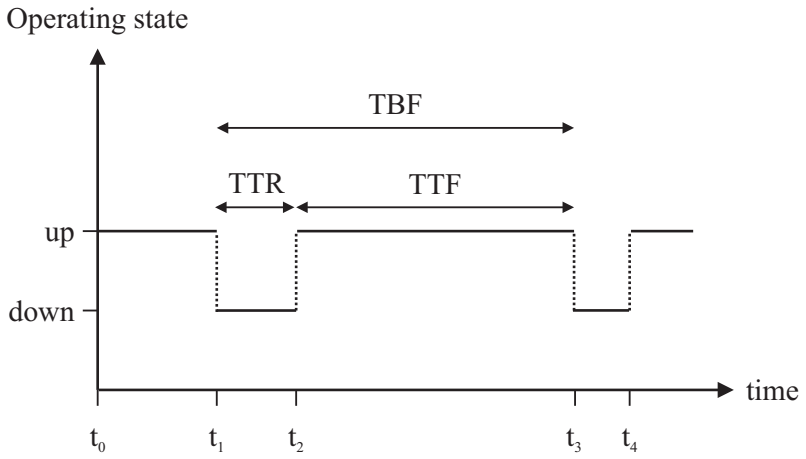

Figure 5.1: Visual representation of time to repair (TTR), time to failure (TTF), and time between failures (TBF) based on the operational state of a component or system over time.

and constant mean time to repair (MTTR). The mean time between failures (MTBF) is calculated according to Equation (5.1). A so called interval availability for shorter observation periods and its application is presented in [WM10].

$$\text{MTBF} = \text{MTTF} + \text{MTTR} \tag{5.1}$$

In the transport network context, the availability of services is a crucial topic because strict maximum service outage times must not be exceeded in order to fulfill the SLAs for business customers. Providing for short maintenance intervals in case of a failure can significantly ameliorate the availability of this long-term task.

The availability a of a component providing a service characterizes the probability that it is in functional state. The unavailability u refers to the probability that the component is down, which is the contrary event. In order to calculate the probabilities, the following two attributes must be known. The mean time to repair (MTTR) represents the mean time it takes to fix the module after an outage. On the other hand, the average time of fault-free operation is denoted by mean time to failure (MTTF). Equations (5.2) and (5.3) show the formulas for availability a and unavailability u, respectively.

$$a = \frac{\text{MTTF}}{\text{MTTF} + \text{MTTR}} \tag{5.2}$$

$$u = 1 - a = \frac{\text{MTTR}}{\text{MTTF} + \text{MTTR}} \tag{5.3}$$

When dealing with availabilities the term *nines* is often used for quantification. It is preceded by a number that represents the quantity of consecutive nines after the decimal

point. Table 5.1 presents various nines of availability and the corresponding downtimes per year. Two nines still correspond to almost four days outage time and four nines must be reached to reduce the downtime to less than one hour, for example.

Table 5.1: Availabilities ranging from one nine to six nines and corresponding downtimes per year.

Availability	Downtime per year
0.9	36.50 days
0.99	3.65 days
0.999	8.76 hours
0.9999	52.56 minutes
0.99999	5.26 minutes
0.999999	31.54 seconds

If the mean time to repair is much smaller than the mean time to failure, the unavailability can be approximated by the ratio of MTTR and MTTF. The inverse of the MTTF is denoted as failure rate. It is usually measured in failure in time (FIT) reflecting the total number of failures happening in a billion (10^9) hours of operation. Typically, electronic hardware failure rates follow a bathtub curve over time. During the early operating phase after the initial startup, the failure rate continuously decreases. The reason for this behavior is infant mortality. Next, the failure rate remains at a low, almost constant level during the useful life. Finally, the failure rate continuously rises at the end of life phase due to so-called wear out failures. Thus, the overall shape of the curve resembles a bathtub from a horizontal point of view. During the normal life interval, the failure rate can be well-approximated by a constant value.

The unavailability of a complex system can be calculated from the individual component unavailabilities. Reliability circuits model the logical relationship between the modules. In case the failure of a single element leads to an outage of the whole system, the components form a serial circuit. If there are redundant components that can be used alternatively to keep the system functional, the respective elements compose a parallel circuit.

5.3 Virtual Link Concept

5.3.1 Functional Principle

A regular network link represents a single channel between two neighboring nodes. We extend the notion of links to adjacent or non-adjacent nodes interconnected by redundant paths by defining *virtual links*. A virtual link forms a routing configuration

of node-disjoint paths between two arbitrary nodes representing the link's end nodes. Thus, a virtual link consists of multiple sequences of normal links that go from source node to target node, potentially traversing a number of intermediate nodes. All paths associated with a virtual link are mutually disjoint.

In contrast to a normal link enabling a single connection over one edge between neighboring nodes, a virtual link facilitates redundant connections. Virtual links may be provisioned by means of various path configurations. A dual (virtual) link consists of a 1:1 or 1+1 path protection constellation between a node pair. Triple (virtual) links add another link sequence and offer three node-disjoint paths. The concept can be further extended to quadruple (virtual) links and beyond that. However, the network topology often restricts the applicability because four or more node-disjoint paths are rarely available. In the following, we therefore restrict to dual and triple links.

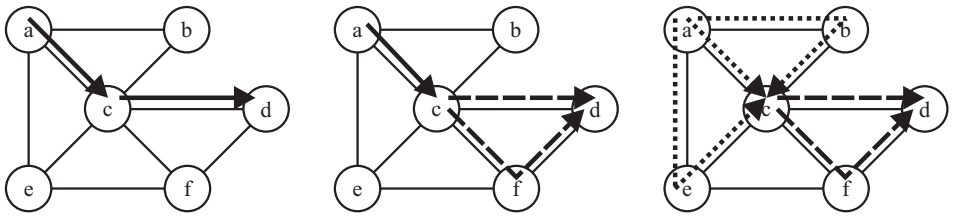

Figure 5.2: Virtual link routing using a concatenation of standard links, dual virtual links, and triple virtual links.

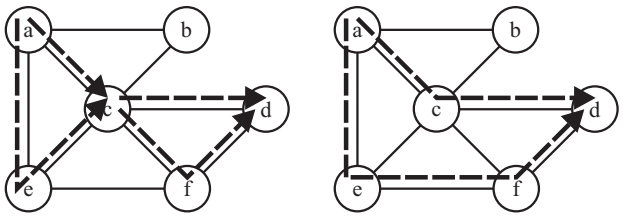

Figure 5.3: Consideration of link and path protection by virtual link protection.

A single end-to-end path is made up of adjacent links. The connection is cut off as soon as one of the links fails. As the paths of a virtual link do not traverse a common node except for the link's source and target node, virtual links can be incorporated into an unprotected routing configuration to increase the end-to-end availability of the connection. In case of a failure on a path of a virtual link, one or two alternative paths remain functional for a dual and triple link, respectively. This redundancy enables an intact connection between the end nodes. Contrary to traditional resilience schemes, an arbitrary sequence of normal links and virtual links from the traffic origin to the destination node can be formed to adapt to the desired end-to-end availability. As a supplemental measure to allocating extra network resources, monitoring the signal quality and forecasting failures can be employed to improve the availability [WH04]. Figure 5.2 shows three example configurations for a connection from node "a" to node "d" consisting of standard links and dual or triple virtual links.

We note that the virtual link resilience scheme inherently includes path protection and link protection scheme as can be seen in Figure 5.3. However, all virtual links belonging to the same connection are assumed to be node-disjoint except for the links' end nodes. Such a constraint does not exist for link protection. The reason for this configuration is an improved total availability which will be explained in the next subsection. The main advantage of the virtual link concept is its flexible configuration that adapts to a desired availability and can reduce network resource consumption.

5.3.2 Reliability Block Model

In order to calculate the availability of a complex system, one must analyze how failures of the individual components affect the total availability. Reliability block diagrams represent a method of visualizing these interdependencies. Based on this structure, one can formalize the problem and compute the overall availability. If the failure of a single element leads to an outage of the entire system, then the respective critical components form a serial circuit. In this case, the total availability is given by the product of the components' availabilities. Redundant components where only a single element must work for the system to be available are modeled by a parallel circuit. The overall unavailability is then calculated by the product of the element unavailabilities, i.e. all elements must be unavailable to stop the system from functioning.

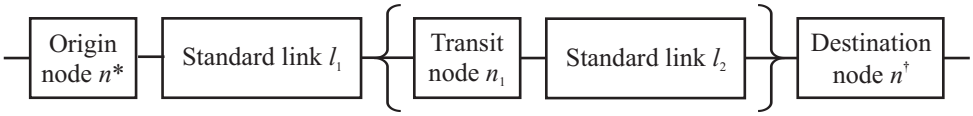

Figure 5.4: Reliability block diagram of a single path connection.

The reliability block diagram of a single path is displayed in Figure 5.4. All nodes and links of the path are arranged as serial circuit because any single failure interrupts the connection. The transit node and standard link segment is surrounded by curly braces to indicate that these blocks may be repeated zero or multiple times. An analysis of the individual elements inside a node or link is beyond the scope of this work. More detailed reliability models can become quite complex, especially when multiple network technologies are involved [JJU02, VCD+05, MH06, PTFW06, WS07].

$$\begin{aligned} u_r^{\mathrm{RO}} &= 1 - \prod_{\substack{n\in\mathcal{N}:\\ \epsilon_{r,n}=1}} a_n^{\mathrm{NO}} \cdot \prod_{\substack{e\in\mathcal{E}:\\ \delta_{r,e}=1}} a_e^{\mathrm{ED}} \\ &\approx \sum_{\substack{n\in\mathcal{N}:\\ \epsilon_{r,n}=1}} u_n^{\mathrm{NO}} + \sum_{\substack{e\in\mathcal{E}:\\ \delta_{r,e}=1}} u_e^{\mathrm{ED}}, \qquad \text{if } u_n^{\mathrm{NO}} \ll 1,\ \forall\, n \in \mathcal{N} \ \wedge\ u_e^{\mathrm{ED}} \ll 1,\ \forall\, e \in \mathcal{E} \end{aligned} \tag{5.4}$$

The corresponding unavailability u_r^{RO} of a single path is shown in Equation (5.4). In the first line, the unavailability is calculated by subtracting the overall availability from

one. For small element unavailabilities, the total unavailability of a serial reliability circuit can be approximated by the sum of the element unavailabilities. This is a valid assumption for the nodes and links of a transport network. Thus, a path's unavailability corresponds to the sum of all node and link unavailabilities according to the second line of the formula.

Figure 5.5 analyzes the reliability block diagrams for two and three disjoint paths representing a dual and a triple link, respectively. All paths constituting a virtual link consist of at least one standard link. Every extra link along a path additionally inserts another intermediate node. All the links and transit nodes of a path form a serial reliability circuit because they represent single points of failure. Curly braces around the sequence of transit node and normal link symbolize that this part may be absent or be repeated any number of times. In order to be able to consider the paths as a parallel circuit and to increase the total availability, all paths of a virtual link must not have any common transit node or edge. If links do not fail independently of each other due to sharing a common resource, one would have to deal with shared risk link groups [KMES09]. When adding the origin and destination node of a connection in a serial manner, we get the reliability diagram of an end-to-end 1:1 and 2:1 path protection scheme.

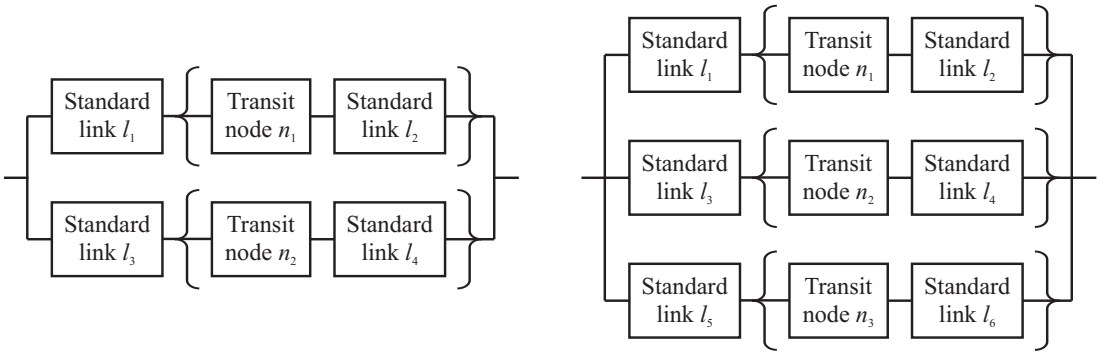

Figure 5.5: Reliability block diagram of a dual and triple virtual link.

The unavailability $u_{r^{\parallel}}^{\mathrm{VL}}$ of a virtual link along disjoint routes $r^{\parallel}$ can be calculated according to Equation (5.5). The part in brackets represents the unavailability of one path of the virtual link excluding the origin and destination node. Again, we utilize the approximation known from Equation (5.4). The product of all path unavailabilities corresponds to the total virtual link unavailability.

$$u_{r^{\parallel}}^{\mathrm{VL}} \approx \prod_{r \in r^{\parallel}} \Bigg(\sum_{\substack{n \in \mathcal{N}: \\ \epsilon_{r,n}=1 \wedge \\ \kappa_{r,n}=0 \wedge \\ \lambda_{r,n}=0}} u_n^{\mathrm{NO}} + \sum_{\substack{e \in \mathcal{E}: \\ \delta_{r,e}=1}} u_e^{\mathrm{ED}} \Bigg), \qquad \text{if } u_n^{\mathrm{NO}} \ll 1, \forall\, n \in \mathcal{N} \wedge u_e^{\mathrm{ED}} \ll 1, \forall\, e \in \mathcal{E} \quad (5.5)$$

The concatenation of normal links and virtual links from origin node to destination node results in the overall reliability diagram portrayed in Figure 5.6. Again, curly

braces indicate that the sequence of transit node and standard link or virtual link may be existent arbitrary times. We note that normal and virtual link building blocks can only be arranged in a serial way if these links do not overlap at any node or edge except for the links' end nodes. Otherwise, a failure may disrupt not just one path of a single virtual link but affect multiple virtual links. This would deteriorate the availability of the virtual links.

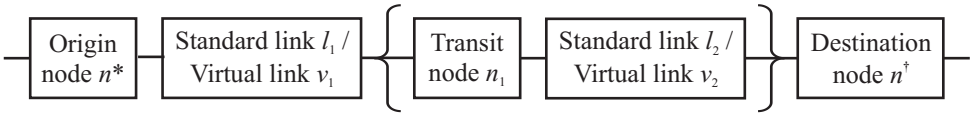

Figure 5.6: Reliability block diagram of a virtual link protected end-to-end connection.

5.4 Mathematical Program Formulation

In the following, we develop a mixed integer linear program to compute optimal availability-oriented routing configurations based on the virtual link strategy. The best solution fulfills the desired end-to-end connection availability while demanding a minimum amount of network capacity. The given network graph is characterized by the set of Nodes $\mathcal{N}$ and interconnecting directed edges $\mathcal{E}^{\mathrm{DI}}$. We consider a directed graph in order to be able to distinguish incoming and outgoing traffic flows at the network nodes. Traffic requests at wavelength granularity between any unordered origin/destination node pair $\{n_1, n_2\}$ are denoted by $d_{n_1,n_2} \in \mathbb{Z}_0^+$. An end-to-end wavelength connection is adaptively created by a sequence of standard and virtual links. We assume that all traffic between the same node pair follows the optimal route, i.e. we route a single flow and weight it according to the number of wavelength requests. Hence, binary standard link variables $L_{n_1,n_2,e}$ are indexed by unordered node pairs and normal links on edge e. Binary virtual link variables $V_{n_1,n_2,r^{\parallel}}$ are characterized by the constituting disjoint routes $r^{\parallel}$, respectively. We note that routes are also directed to model incoming and outgoing flows at the network nodes.

The capacity consumption of the routing is measured by the accumulated distance of all allocated wavelength links. Standard link metrics l_e^{ED} are directly derived from the length of the respective edge whereas virtual link metrics $l_{r^{\parallel}}^{\mathrm{RO}}$ summarize the distance of all involved edges. One may bring forward the argument that it is sufficient to restrict the set of considered disjoint routes to a single dual and triple virtual link, namely the ones that provide the highest connection availability. However, they are not necessarily the ones with minimum overall distance because the links' transit nodes do not add to the routing metric but influence the resulting availability. As a result, shorter virtual links with a minor unavailability penalty are better suited for demands that do not require the highest possible connection availability. Another advantage of having several virtual links between every node pair arises when concatenating virtual links. As explained before, virtual link sequences must not have any common intra-link

transit node in order to fail independently of each other. If the eligible virtual links to and from a certain node access the node via the same edge, it is impossible to combine them.

The unavailability of each standard link is given by the corresponding edge unavailability u_e^{ED} from which the virtual link unavailabilities $u_{r^{\parallel}}^{\mathrm{VL}}$ of the disjoint routes $r^{\parallel}$ can be calculated in conjunction with the node unavailability u^{NO}. A maximum end-to-end unavailability of $\hat{u}^{\mathrm{CO}}$ must not be exceeded for any connection. Using the given definitions we formulate the optimization model via the following equations.

Minimize

$$\sum_{\substack{\{n_1,n_2\}\subset\mathcal{N}:\\ n_1\neq n_2}} \Big(\sum_{e\in\mathcal{E}^{\mathrm{DI}}} L_{n_1,n_2,e}\cdot d_{n_1,n_2}\cdot l_e^{\mathrm{ED}} + \sum_{r^{\parallel}\in\mathcal{R}^{\mathrm{DI}}_{z\mathrm{RO}}} V_{n_1,n_2,r^{\parallel}}\cdot d_{n_1,n_2}\cdot l_{r^{\parallel}}^{\mathrm{RO}} \Big) \tag{5.6}$$

subject to

$$\sum_{\substack{e\in\mathcal{E}^{\mathrm{DI}}:\\ \theta_{n_1,e}=1}} L_{n_1,n_2,e} + \sum_{\substack{n_3\in\mathcal{N}:\\ n_3\neq n_1}} \sum_{r^{\parallel}\in\mathcal{R}^{\mathrm{DI}}_{z\mathrm{RO},n_1,n_3}} V_{n_1,n_2,r^{\parallel}} = 1 \qquad \forall\,\{n_1,n_2\}\subset\mathcal{N}: n_1\neq n_2, \tag{5.7}$$

$$\sum_{\substack{e\in\mathcal{E}^{\mathrm{DI}}:\\ \iota_{n_1,e}=1}} L_{n_1,n_2,e} + \sum_{\substack{n_3\in\mathcal{N}:\\ n_3\neq n_1}} \sum_{r^{\parallel}\in\mathcal{R}^{\mathrm{DI}}_{z\mathrm{RO},n_3,n_1}} V_{n_1,n_2,r^{\parallel}} = 0 \qquad \forall\,\{n_1,n_2\}\subset\mathcal{N}: n_1\neq n_2, \tag{5.8}$$

$$\sum_{\substack{e\in\mathcal{E}^{\mathrm{DI}}:\\ \iota_{n_2,e}=1}} L_{n_1,n_2,e} + \sum_{\substack{n_3\in\mathcal{N}:\\ n_3\neq n_2}} \sum_{r^{\parallel}\in\mathcal{R}^{\mathrm{DI}}_{z\mathrm{RO},n_3,n_2}} V_{n_1,n_2,r^{\parallel}} = 1 \qquad \forall\,\{n_1,n_2\}\subset\mathcal{N}: n_1\neq n_2, \tag{5.9}$$

$$\sum_{\substack{e\in\mathcal{E}^{\mathrm{DI}}:\\ \theta_{n_2,e}=1}} L_{n_1,n_2,e} + \sum_{\substack{n_3\in\mathcal{N}:\\ n_3\neq n_2}} \sum_{r^{\parallel}\in\mathcal{R}^{\mathrm{DI}}_{z\mathrm{RO},n_2,n_3}} V_{n_1,n_2,r^{\parallel}} = 0 \qquad \forall\,\{n_1,n_2\}\subset\mathcal{N}: n_1\neq n_2, \tag{5.10}$$

$$\begin{aligned}\sum_{\substack{e\in\mathcal{E}^{\mathrm{DI}}:\\ \theta_{n_3,e}=1}} L_{n_1,n_2,e} + \sum_{\substack{n_4\in\mathcal{N}:\\ n_4\neq n_3}} \sum_{r^{\parallel}\in\mathcal{R}^{\mathrm{DI}}_{z\mathrm{RO},n_3,n_4}} V_{n_1,n_2,r^{\parallel}} = \\ = \sum_{\substack{e\in\mathcal{E}^{\mathrm{DI}}:\\ \iota_{n_3,e}=1}} L_{n_1,n_2,e} + \sum_{\substack{n_4\in\mathcal{N}:\\ n_4\neq n_3}} \sum_{r^{\parallel}\in\mathcal{R}^{\mathrm{DI}}_{z\mathrm{RO},n_4,n_3}} V_{n_1,n_2,r^{\parallel}}\end{aligned} \qquad \begin{aligned}&\forall\,\{n_1,n_2\}\subset\mathcal{N}: n_1\neq n_2,\\ &n_3\in\mathcal{N}\setminus\{n_1,n_2\},\end{aligned} \tag{5.11}$$

$$\begin{aligned}1 \geq 0.5\cdot\Big(\sum_{\substack{e\in\mathcal{E}^{\mathrm{DI}}:\\ \theta_{n_3,e}=1\,\vee\\ \iota_{n_3,e}=1}} L_{n_1,n_2,e} + \sum_{\substack{n_4\in\mathcal{N}:\\ n_4\neq n_3}} \sum_{\substack{r^{\parallel}\in\{\mathcal{R}^{\mathrm{DI}}_{z\mathrm{RO},n_3,n_4},\\ \mathcal{R}^{\mathrm{DI}}_{z\mathrm{RO},n_4,n_3}\}}} V_{n_1,n_2,r^{\parallel}} \Big) + \\ + \sum_{\substack{n_4,n_5\in\mathcal{N}\setminus n_3:\\ n_4\neq n_5}} \sum_{\substack{r^{\parallel}\in\mathcal{R}^{\mathrm{DI}}_{z\mathrm{RO},n_4,n_5}:\\ n_3\in\mathcal{N}^{\mathrm{RO}}_{r^{\parallel}}}} V_{n_1,n_2,r^{\parallel}}\end{aligned} \qquad \begin{aligned}&\forall\,\{n_1,n_2\}\subset\mathcal{N}: n_1\neq n_2,\\ &n_3\in\mathcal{N},\end{aligned} \tag{5.12}$$

$$\begin{aligned}\hat{u}^{\mathrm{CO}} \geq \sum_{e\in\mathcal{E}^{\mathrm{DI}}} L_{n_1,n_2,e}\cdot u_e^{\mathrm{ED}} + \sum_{r^{\parallel}\in\mathcal{R}^{\mathrm{DI}}_{z\mathrm{RO}}} V_{n_1,n_2,r^{\parallel}}\cdot u_{r^{\parallel}}^{\mathrm{VL}} + \\ + \Big(\sum_{e\in\mathcal{E}^{\mathrm{DI}}} L_{n_1,n_2,e} + \sum_{r^{\parallel}\in\mathcal{R}^{\mathrm{DI}}_{z\mathrm{RO}}} V_{n_1,n_2,r^{\parallel}} + 1 \Big)\cdot u^{\mathrm{NO}}\end{aligned} \qquad \forall\,\{n_1,n_2\}\subset\mathcal{N}: n_1\neq n_2, \tag{5.13}$$

$$L_{n_1,n_2,e} \in \{0,1\} \qquad \forall \{n_1,n_2\} \subset \mathcal{N} : n_1 \neq n_2, \; e \in \mathcal{E}^{\mathrm{DI}}, \tag{5.14}$$

$$V_{n_1,n_2,r^{\parallel}} \in \{0,1\} \qquad \forall \{n_1,n_2\} \subset \mathcal{N} : n_1 \neq n_2, \; r^{\parallel} \in \mathcal{R}^{\mathrm{DI}}_{z^{\mathrm{RO}}}. \tag{5.15}$$

- The Objective (5.6) minimizes the overall network resources by routing the wavelength connections on shortest paths with respect to the geographical extent. It summarizes all utilized standard and virtual links of the routing flows weighted by the demand quantity and the distance metric for all allocated links.
- The following five equations perform the routing of all traffic requests between each node pair. Flow conservation constraints are formulated for each node. The end-to-end flow may consist of a sequence of normal links and virtual links. Constraints (5.7) and (5.8) create an outgoing normal or virtual link at the demand origin and prohibit any incoming flow there, respectively. At the destination of each demand, exactly one link ends (Constraints (5.9)) and none leaves the node (Equations (5.10)). Furthermore, the number of incoming links must match the number of outgoing links at each transit node according to Constraints (5.11).
- Constraints (5.12) guarantee statistically independent failures of standard and virtual links belonging to the same end-to-end connection. The sequence of links must not traverse any edge or node more than once.
  - On the one hand, this means that a node may be the source node of at most one outgoing link and/or the target node of at most one incoming link. The first term on the right-hand side of Constraints (5.12) summarizes the number of incoming and outgoing standard and virtual links at each node n_3. Applying the factor 0.5 in combination with the upper bound one on the left-hand side restricts the maximum number of ingress and egress links at each node to two. In conjunction with the flow continuity provided by Equations (5.11) there are either one incoming link and one outgoing link at a transit node or no links at all.
  - On the other hand, we have to examine the virtual links in detail because they consist of disjoint routes that pass through intermediate nodes. The second term on the right-hand side of the equations thus adds the virtual links traversing the considered node n_3. We note that source and target node of a link are not considered as transit nodes.
  - All in all, the constraints allow at most one of both configurations. A node is either the source node and/or target node of a link or it is traversed by a virtual link. The third option is that a node is not involved in the routing at all. Consequently, each node and link can be represented adequately by a serial or parallel element in the logical reliability diagram.

- Based on the reliability block diagram depicted in Figure 5.6, the end-to-end unavailability of the routing configuration is calculated in Constraints (5.13). It is given by the sum of the individual link and node unavailabilities. The quantity of link end nodes along the routing flow is equivalent to the number of links plus one. Transit nodes within a virtual link are already considered by the virtual link's unavailability. The resulting unavailability must not exceed the maximum allowable connection unavailability.

5.5 Case Studies

This section presents the results of our case studies for the three reference networks. The considered topologies have been computed by the topological network design described in Chapter 3. Three disjoint paths were routed to facilitate triple virtual links and the number of network edges was limited to create reasonably meshed topologies with an average nodal degree of 3.5.

German Network

Before examining the virtual link routing in the 30-edge German network topology (see Figure 5.7) we want to analyze the basic end-to-end availability potential of unprotected, 1:1, and 2:1 path configurations. For now, we consider an unavailability per link kilometer u^{ED} of $4 \cdot 10^{-6}$ and assume that the unavailability u^{NO} for each network node equals $4 \cdot 10^{-5}$.

The mean length of a single path in the German network is 418 km when carrying out a shortest distance routing for all node pairs. The corresponding average number of hops in this case amounts to 2.4. For the overall link unavailability, we get $418 \cdot 4 \cdot 10^{-6}$, which is approximately $1.67 \cdot 10^{-3}$. When assuming a two-hop path, the total unavailability of all path nodes is $3 \cdot 4 \cdot 10^{-5}$ equaling $1.2 \cdot 10^{-4}$, i.e. one order of magnitude smaller than the total link unavailability. In general, this relation holds true for any reasonable routing between any node pair. For smaller node unavailabilities, this effect becomes even stronger. In total we get a single path end-to-end unavailability of $1.79 \cdot 10^{-3}$ that allows to guarantee an availability of two nines.

For 1:1 path protection with respect to any single transit node failure, the average route length of the working path is 423 km and 595 km for the protection path. These values are obtained by selecting the shortest of both disjoint paths as primary connection and the other one as backup connection. The transmission distance causes an unavailability of $1.69 \cdot 10^{-3}$ for the working path and $2.38 \cdot 10^{-3}$ for the protection path. The mean hop length of both paths is 2.4 and 3.4, respectively. When assuming a two-hop and a four-hop route there is one intermediate node in the former path and three nodes in the latter path. These serial elements with respect to the paths' reliability block diagram result in unavailability terms of $4 \cdot 10^{-5}$ and $1.2 \cdot 10^{-4}$, respectively. As a result, the additive

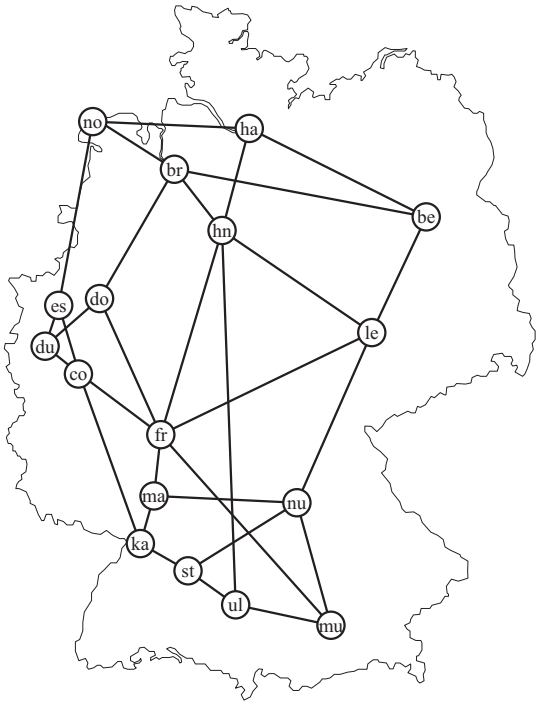

Figure 5.7: Topology of the German reference network scenario with 30 edges.

degradation effect of the transit nodes is comparatively small. The multiplication of both path segment unavailabilities leads to a preliminary unavailability of $4.3 \cdot 10^{-6}$. However, the end nodes yield an unavailability of $8 \cdot 10^{-5}$ that clearly dominates the overall unavailability. A 1:1 path configuration thus provides sufficient performance for availability warranties of four nines if the node unavailability is below $5 \cdot 10^{-5}$.

Although the influence of links and transit nodes of a node-disjoint path pair is small, the corresponding unavailability penalty leaves only a small gap to achieve five nines end-to-end availability for small node unavailabilities. Since the end node unavailabilities inevitably add to the connection unavailability, it may be necessary to include one more redundant path. The topology facilitates three node-disjoint paths between all node pairs. The average length of the shortest route is 426 km which may be used for the working path. For the second shortest and the longest route we get 600 km and 914 km, respectively. The mean hop quantity is 2.5 for the working route, 3.4 for the shortest protection route, and 4.2 for the remaining one. A configuration of two three-hop routes and one four-hop route yields a triple path segment unavailability of approximately $1.7 \cdot 10^{-8}$. Now, the overall connection unavailability is determined by the sum of origin and destination node unavailability even for very small node unavailabilities.

The main conclusion of this analysis is that the unavailability of the links dominates the total node unavailability for single path connections, whereas the unavailability of the end nodes dictates the outcome for 1:1 and 2:1 path protection. In contrast to allocating alternative transmission routes to compensate a failure on the links or transit nodes of the primary path, the influence of the connection's end nodes cannot be diminished

easily. For strict unavailability requirements, this term forms the major unavailability penalty and may demand special redundant node structures in order to achieve a total availability of five nines.

Figure 5.8 depicts the average connection capacity in terms of total link kilometers over the maximum allowable end-to-end unavailability. There are curves for different node unavailabilities ranging from $2 \cdot 10^{-6}$ to $6 \cdot 10^{-5}$. The unavailability per link kilometer of $4 \cdot 10^{-6}$ remains constant. For decreasing target unavailabilities when moving to the left-hand side on the x-axis, i.e. higher connection availabilities, the link capacity increases because redundant resources are necessary to allow for alternative transmission paths. Each diagram point indicates that a valid routing configuration satisfying the required end-to-end availability can be computed for all traffic demands in the network.

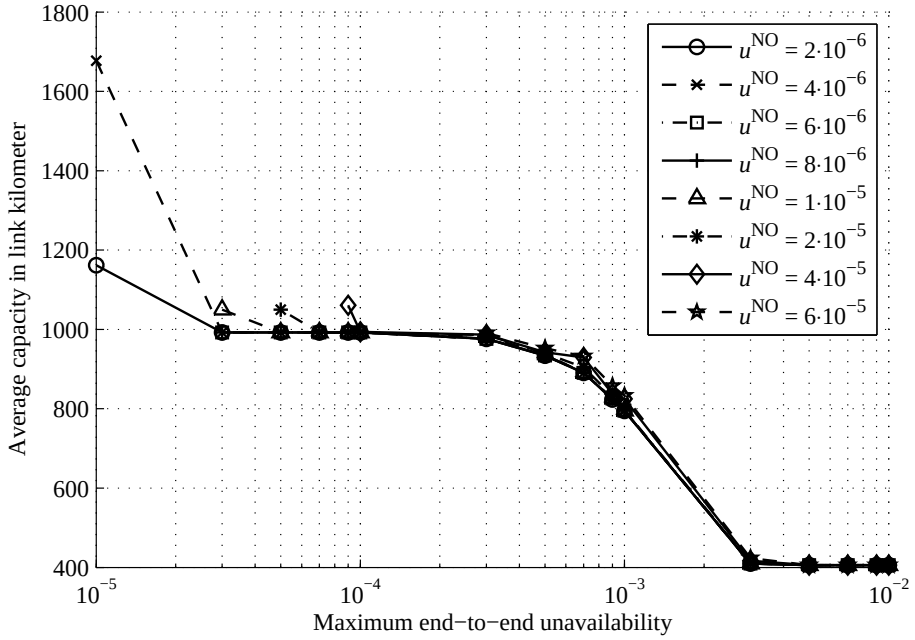

Figure 5.8: Average connection capacity subject to maximum unavailability to be met in the German reference network for various node unavailabilities u^{NO} and link kilometer unavailability $u^{ED} = 4 \cdot 10^{-6}$.

In order to guarantee two nines connection availability, a single path is adequate irrespective of the node unavailability as shown before. We note that the average capacity of 406 link kilometers in the diagram slightly differs from the mean shortest single path length of 418 km in the network. This is due to the fact that we now consider the specific traffic matrix with non-uniform demand quantities between the nodes in our case study whereas the latter value is an average path distance over all node pairs. For slightly higher connection unavailabilities up to $5 \cdot 10^{-3}$, the capacity requirements are identical and there is only a marginal increase for $3 \cdot 10^{-3}$. Beyond this point, the resource consumption abruptly duplicates if three nines end-to-end availability are stipulated. Single path connections are no longer adequate by default because every path element

represents a single point of failure. Instead, redundant segments must be added which help to compensate outages. We will evaluate the selected routing configurations in detail in the next figure. When intensifying the availability requirements from three nines to four nines, the capacity rises from about 800 to 993 link kilometers. In case of a node unavailability of $6 \cdot 10^{-5}$, it is not possible to provide four nines connection availability since the total end node unavailability already exceeds the threshold. We notice that the resource consumptions for all other node unavailabilities differ by at most 5% for a maximum end-to-end unavailability between $1 \cdot 10^{-2}$ and $1 \cdot 10^{-4}$. This is an important finding when considering the trade-off between the design of more expensive nodes with higher availability versus cheaper ones that are more failure-prone. Beyond four nines connection availability, we observe increasing link capacities if the sum of the end node unavailabilities is close to the desired target unavailability. Five nines target unavailability can only be achieved for the two smallest node unavailabilities $2 \cdot 10^{-6}$ and $4 \cdot 10^{-6}$. However, this configuration involves high extra capacity of 17% in the former case and 69% in the latter case.

The resulting routing configurations for link kilometer unavailability $4 \cdot 10^{-6}$ and node unavailability $4 \cdot 10^{-6}$ are illustrated in Figure 5.9. Out of all possible combinations we observe four different link compositions: single paths (sequence of normal links), dual paths (end-to-end dual links), triple paths (end-to-end triple links), and combinations of normal and dual links. The required connection unavailability is again depicted on the x-axis.

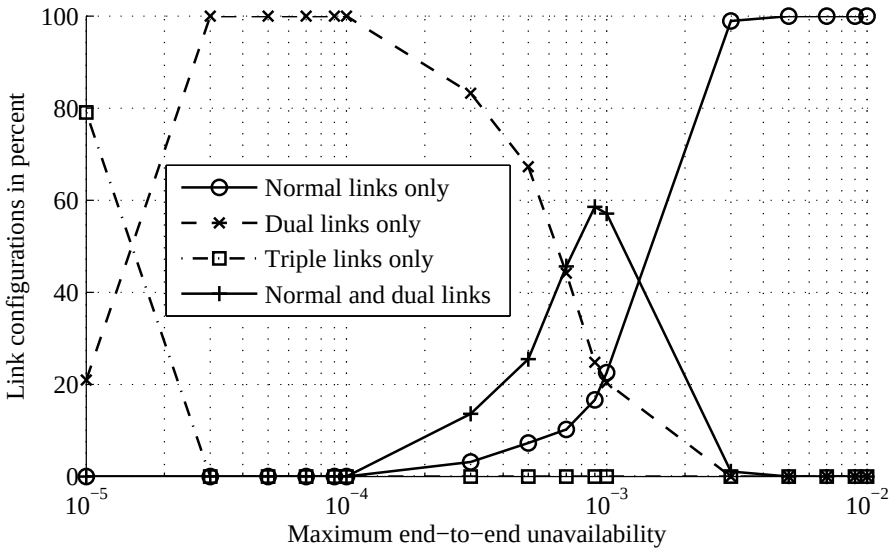

Figure 5.9: Routing configurations over maximum unavailability to be met in the German reference network for an unavailability of $4 \cdot 10^{-6}$ per node and link kilometer.

As shown before, unprotected paths can offer two nines end-to-end unavailability between all nodes. They represent the most capacity-efficient solution of routing demands and are exclusively selected for desired connection unavailabilities greater than $5 \cdot 10^{-3}$.

In order to guarantee an availability of three nines, only 23% of all connections can be routed via a single path. All paths longer than 248 km cannot fulfill the availability condition because the total link plus total node unavailability (at least $8 \cdot 10^{-6}$) is too large. The majority of connections (57%) consist of a combination of regular links and a dual link. The average edge length in the network is 202 km. We analyze a series of one dual link and one normal link. The total unavailability of all three serial nodes in the reliability block diagram is given by $1.2 \cdot 10^{-5}$. In contrast, the average single link unavailability $8.1 \cdot 10^{-4}$ clearly exceeds the critical nodes' unavailability. When forming a sequence of a dual and a normal link to establish connections between any node pair, the dual link is shorter than the mean end-to-end dual path length in the network. Thus, the unavailability of a dual link segment without considering the end nodes is smaller than the unavailability of a dual path segment which amounts to $4.3 \cdot 10^{-6}$ as calculated before. Compared to the former two unavailability terms, this term can be neglected. In order to achieve an availability gain compared to a single path solution, one normal link or two normal links with short physical distance are promising. This configuration can achieve an overall connection availability of three nines, which might be sufficient for a number of network services. It can often be realized using less link capacity as opposed to pure 1:1 path protection. As a consequence, 57% of all connections are formed accordingly for three nines end-to-end unavailability. The remaining configurations are divided into 23% single path and 20% dual link constellations. Unprotected paths are the most capacity-efficient solution for end nodes which can be connected via one or two short links. On the other hand, if the shortest route between two nodes is too long and the network topology does not offer an efficient combination of a single and a dual link, an exclusive dual link configuration comes into play.

We note that the "dual links only" classification is not limited to end-to-end node-disjoint 1:1 path protection, solely. Instead, a sequence of two dual links can provide sufficient service availability and may require less capacity than two disjoint paths between the end nodes. As an example, we want to point out the routing between nodes "es" and "ka". The network topology provides a short dual link "es-co"/"es-du-co" between nodes "es" and "co" and the short dual link "co-ka"/"co-fr-ma-ka" from "co" to "ma". The shortest alternative node-disjoint 1:1 path protection solution consists of path "es-co-ka" and path "es-du-do-fr-ma-ka". The former solution is preferable because it fulfills the availability requirements and is more capacity-efficient. Such configurations of two dual links are interesting as long as the additive unavailability of the common transit node is tolerable. As a prerequisite, three times the node unavailability (for both connection end nodes and the intermediate node) must be less than the connection unavailability. The considered sequence of two dual links represents the optimal routing strategy for maximum end-to-end unavailabilities between $1 \cdot 10^{-4}$ and $3 \cdot 10^{-5}$. For a slightly higher connection unavailability $3 \cdot 10^{-4}$, a single link plus dual link constellation is selected. Although "dual link only" configurations often consist of one end-to-end dual link, the ILP based virtual link design can identify situations where a combination of two dual links, i.e. 1:1 path protection routing over a common transit node, is preferable.

If the maximum connection unavailability must be further decreased below 10^{-3}, the number of configurations with a single path declines. The same holds for the dual link plus normal link approach after its maximum at $9 \cdot 10^{-4}$. Dual paths are applied more frequently to be able to compensate any single edge or transit node failure. Eventually, four nines service availability require 1:1 path protection for all connections. Going back to the previous diagram we figure out that this corresponds to an average capacity of 993 km. Three nines availability warranty on the other hand only require 795 km link resources when applying the virtual link concept. A network operator who sticks to classical 1:1 path protection to route connections that should offer an availability of three nines consequently performs a 25% capacity overprovisioning compared to the flexible virtual link design.

Once the total unavailability of the end nodes is close to the unavailability target, end-to-end triple links emerge. For the considered node unavailability $4 \cdot 10^{-6}$, 79% of all routing configurations require three disjoint end-to-end paths to offer five nines of connection availability. Because of the dominating influence of the serial components in the reliability circuit, a triple link can only show to advantage in terms of an end-to-end configuration. This is due to the fact that the total unavailability of three nodes (end nodes plus intermediate node) in the reliability circuit would already exceed the target unavailability. For the same reason, classical link protection configurations characterized by serial nodes in the reliability block diagram for each working path link do not occur during the availability-based design process unless the working path consists of a single link only (which is equivalent to path protection). Besides, the path protection concept permits a more efficient utilization of link resources because the protection path does not have to traverse every transit node of the working path as is the case for link protection.

Figure 5.10 illustrates the influence of various unavailabilities per link kilometer u^{ED} on the resource requirements of the routing configuration. It portrays the link capacity over the maximum end-to-end unavailability when assuming a node unavailability u^{NO} of $4 \cdot 10^{-6}$. For a desired connection availability of two nines, the capacity consumption is identical for all network edge unavailabilities. However, if the target unavailability is in the range of 10^{-3}, there are significant resource discrepancies. This tendency can be attributed to the configuration transition from a single path to two disjoint paths. The majority of connections consist of a sequence of one or two standard links and one dual link for link kilometer unavailability $4 \cdot 10^{-6}$ as shown previously. Thus, the variation of the link availability causes a relevant shift toward more unprotected paths or 1:1 path protection. A duplication of the link unavailability per fiber kilometer from $2 \cdot 10^{-6}$ to $4 \cdot 10^{-6}$ yields an average capacity growth of 51%, for example. The link unavailability mainly depends on the frequency of fiber cuts and inline amplifier outages and their repair times. Installing acoustic alarm systems in the ground that detect construction works near cable conduits can be an approach to reduce the number of fiber cuts. The investments for such measures may easily pay off when considering the enormous savings on network capacity. Four nines end-to-end availability require dual links for virtually all connections and any considered link unavailability. This

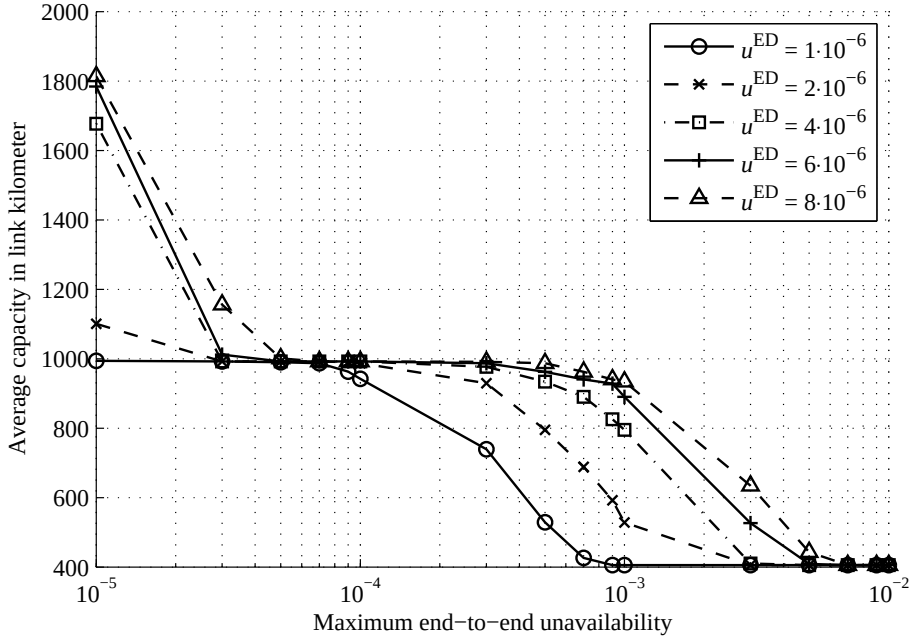

Figure 5.10: Average connection capacity subject to maximum unavailability to be met in the German reference network for various link kilometer unavailabilities u^{ED} and node unavailability $u^{NO} = 4 \cdot 10^{-6}$.

is because the capacity equals or is close to 993 link kilometers which represents the resource requirements of pure 1:1 path protection. As a result, special measures to improve the link unavailability are not promising from an economical point of view in this availability range. Even for the highest link kilometer unavailability $8 \cdot 10^{-6}$, the virtual link design can guarantee five nines connection availability. However, the capacity demand strongly depends on the actual link unavailability. An increase by factor two from $2 \cdot 10^{-6}$ to $4 \cdot 10^{-6}$ implicates a link capacity penalty of an extra 52%.

European Network

This section presents the results for the European network scenario. The underlying topology consisting of 19 edges is shown in Figure 5.11. Again, we want to analyze the virtual link routing configurations to assess their end-to-end availability and capacity requirements.

In the European network, the mean length of all shortest routes between any node pair equals 879 km, which is more than twice the path length in the German network (418 km). The destination node is reached after 1.9 hops on an average. When considering the node unavailability $4 \cdot 10^{-5}$ and link unavailability $4 \cdot 10^{-6}$ per kilometer, we calculate a total link unavailability of $3.52 \cdot 10^{-3}$ and an overall node unavailability of $1.2 \cdot 10^{-4}$ for a two-hop path. As a result, the single path unavailability $3.6 \cdot 10^{-3}$ is

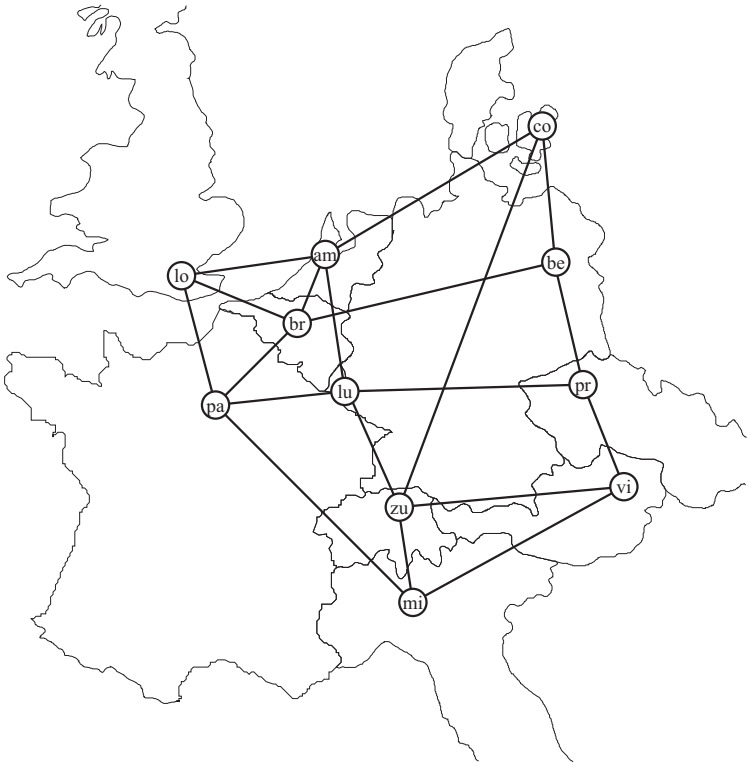

Figure 5.11: Topology of the European reference network scenario with 19 edges.

clearly dominated by the link unavailabilities. Nonetheless, unprotected connections can guarantee an end-to-end availability of two nines.

A pair of node-disjoint paths in this network consists of an 886 km path and a 1334 km path on an average. In terms of hop count this is equivalent to 1.9 and 2.8, respectively. We assume a two-hop/three-hop configuration and obtain a disjoint path segment unavailability of $1.9 \cdot 10^{-5}$ when excluding the end nodes. This unavailability term is significantly higher than for the German network ($4.3 \cdot 10^{-6}$) and in the same order of magnitude as the unavailability $8 \cdot 10^{-5}$ of both end nodes. The total connection unavailability thereby adds up to $9.9 \cdot 10^{-5}$ yielding an end-to-end availability of just four nines.

Three disjoint routes between two nodes have a mean length of 888 km, 1345 km, and 1925 km. The corresponding hop metrics are 1.9, 2.8, and 3.6, respectively. For the average triple path segment we calculate an unavailability of $1.5 \cdot 10^{-7}$. Despite longer transmission distances compared to the German network, the total unavailability $8.02 \cdot 10^{-5}$ of a 2:1 path protection configuration is characterized by the end node unavailabilities.

Figure 5.12 shows the mean network capacity to route all demands and satisfy a maximum connection unavailability. The influence of various node unavailabilities is visualized by different curves for the constant unavailability $4 \cdot 10^{-6}$ per link kilometer. Details about the virtual link configuration are presented in Figure 5.13. It depicts the

relative frequency of the resulting types of link constellations that are observed for node unavailability $4 \cdot 10^{-6}$.

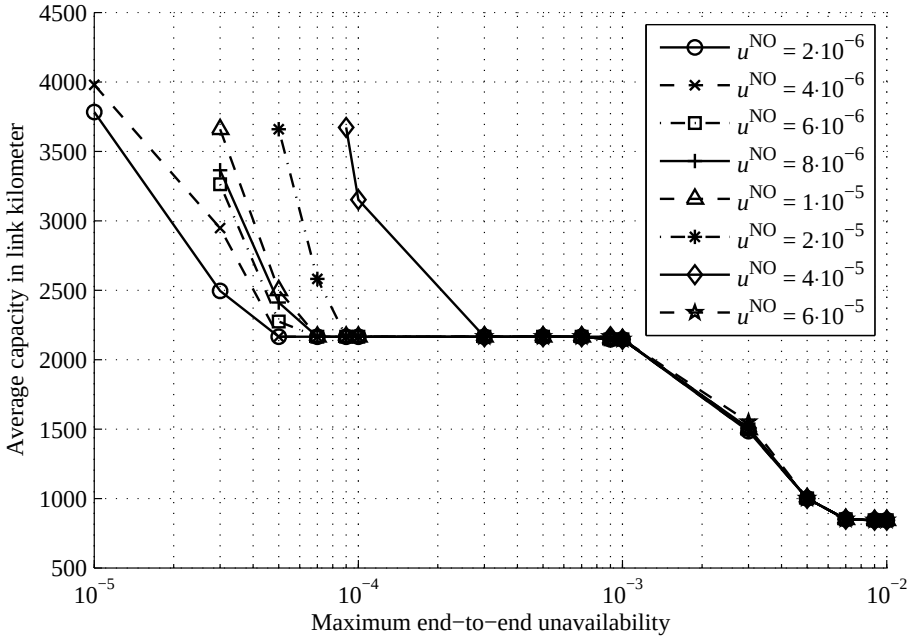

Figure 5.12: Average connection capacity subject to maximum unavailability to be met in the European reference network for various node unavailabilities u^{NO} and link kilometer unavailability $u^{ED} = 4 \cdot 10^{-6}$.

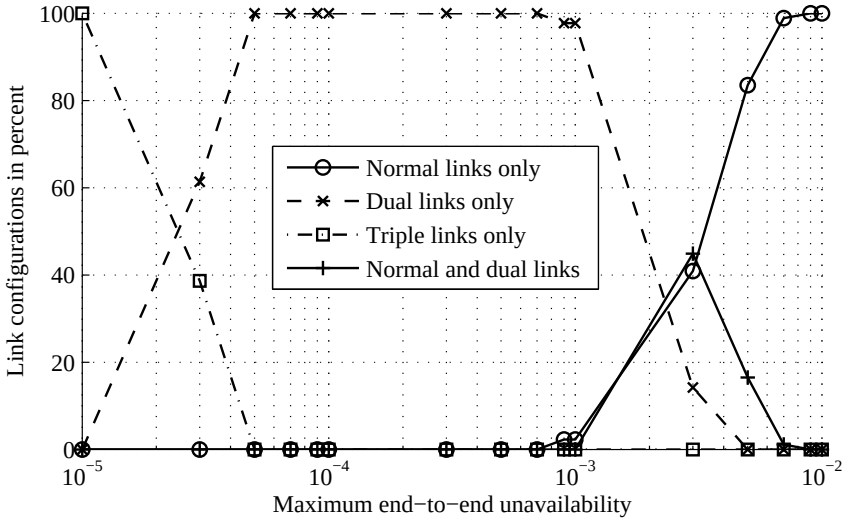

Figure 5.13: Routing configurations over maximum unavailability to be met in the European reference network for an unavailability of $4 \cdot 10^{-6}$ per node and link kilometer.

If the maximum allowable end-to-end unavailability is between $1 \cdot 10^{-2}$ and $3 \cdot 10^{-4}$, the routing configurations for all considered node unavailabilities are similar or identical

with respect to the selected routes and capacity requirements. According to Figure 5.13, single paths are already adequate to guarantee two nines connection availability. Three nines on the other hand necessitate the massive usage of dual links which increases link resources by 157%. For target availabilities between two and three nines, the optimal routing between two nodes may involve single links only, a sequence of single link and a dual link, or dual links only. The actual configuration depends on the distance between origin and destination node and the network topology. Different node unavailabilities hardly influence the routing because even the highest node unavailability is two orders of magnitude smaller than the considered range of connection unavailabilities. Only when the desired service unavailability approaches the double node unavailability, the downtime of the end nodes becomes the decisive factor. Since their outage cannot be compensated, the only way to improve the end-to-end availability is to reduce the unavailability of the interconnecting routing segment as much as possible. However, mandatory 2:1 path protection boosts the link resources enormously. For node unavailability $4 \cdot 10^{-6}$, we observe a capacity penalty of 36% compared to the "dual link only" solution if 39% of all demands are routed via end-to-end triple links. The worst case of 2:1 path protection for all traffic requests implicates even 84% extra capacity.

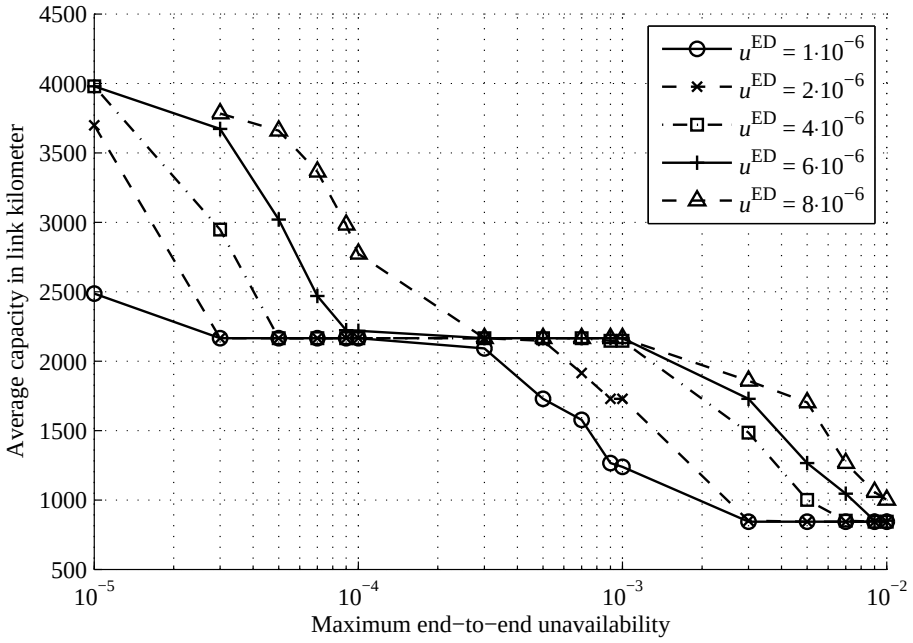

Figure 5.14: Average connection capacity subject to maximum unavailability to be met in the European reference network for various link kilometer unavailabilities u^{ED} and node unavailability $u^{NO} = 4 \cdot 10^{-6}$.

Figure 5.14 visualizes the average link capacity for various link kilometer unavailabilities over the maximum tolerable connection unavailability. For the target unavailability limit $3 \cdot 10^{-4}$ and two nines end-to-end availability, the required network capacity is similar for all considered link unavailabilities. In the former case, 1:1 path protection is used which offers an alternative end-to-end segment that can compensate higher single

path unavailabilities to some extent. The latter scenario mainly corresponds to single path configurations whose availability performance exceeds two nines for most link unavailabilities. Other service availabilities can cause noteworthy capacity differences subject to the link unavailability. For example, in order to offer availability guarantees of three nines, a network operator must allocate 24% extra capacity if the link kilometer unavailability is $4 \cdot 10^{-6}$ instead of $2 \cdot 10^{-6}$. Another duplication of the unavailability per link kilometer to $8 \cdot 10^{-6}$ on the other hand can be compensated by less than 1% ancillary resources.

US Network

In the US network depicted in Figure 5.15, the mean length of the 25 edges is 1156 km. All node pairs in the network can be connected by a 2574 km shortest path via 2.3 hops on an average. The total link unavailability based on the transmission distance amounts to $1.03 \cdot 10^{-2}$. Compared to this, $1.2 \cdot 10^{-4}$ unavailability of all nodes included in a two-hop path is negligible. Now, the mean unavailability $1.04 \cdot 10^{-2}$ of an unprotected path does not even provide an end-to-end availability of two nines.

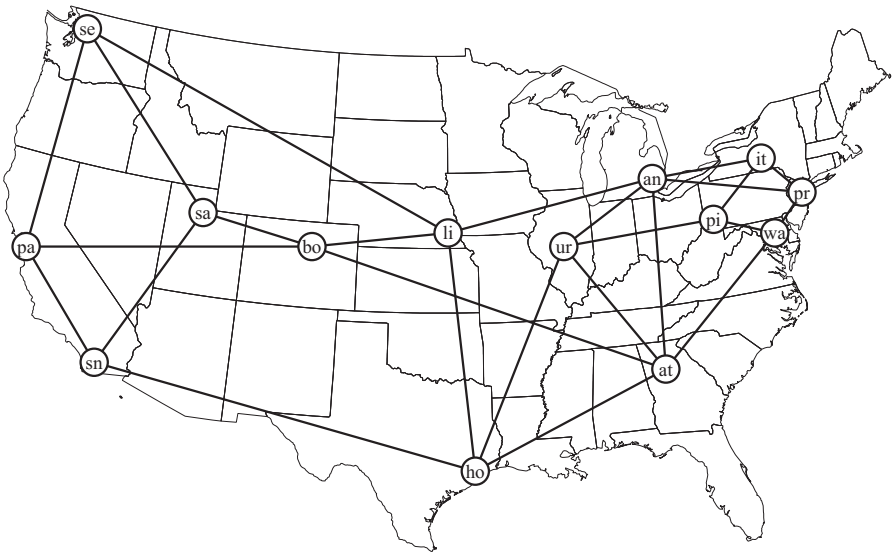

Figure 5.15: Topology of the US reference network scenario with 25 edges.

Two node-disjoint paths between all nodes consist of a 2.3 hop 2575 km route and a 3615 km route with 3.1 edges. The overall unavailability associated with the dual path segment considering a two-hop/three-hop configuration yields a value of $1.5 \cdot 10^{-4}$. This is still higher than the total end node unavailability $8 \cdot 10^{-5}$. Thus, 1:1 path protection reduces the mean unavailability to $2.3 \cdot 10^{-4}$.

The characteristics of a disjoint path triple are as follows. The shortest route has a length of 2695 km, 3692 km is the average transmission distance of the second shortest route, and the longest route covers a distance of 4867 km. The corresponding hop numbers

are 2.3, 3.1, and 3.8, respectively. After rounding the hop quantities we calculate a triple path segment unavailability of $3.1 \cdot 10^{-6}$. Together with the end nodes, the total 2:1 path protection unavailability amounts to $8.3 \cdot 10^{-5}$.

Figure 5.16 shows the average network capacity in terms of link kilometers for all virtual link routing connections. In contrast to the German and European reference network, the resources already increase slightly when reducing the maximum connection unavailability from $1 \cdot 10^{-2}$ to $9 \cdot 10^{-3}$. The corresponding routing configurations for node unavailability $4 \cdot 10^{-6}$ are depicted in Figure 5.17.

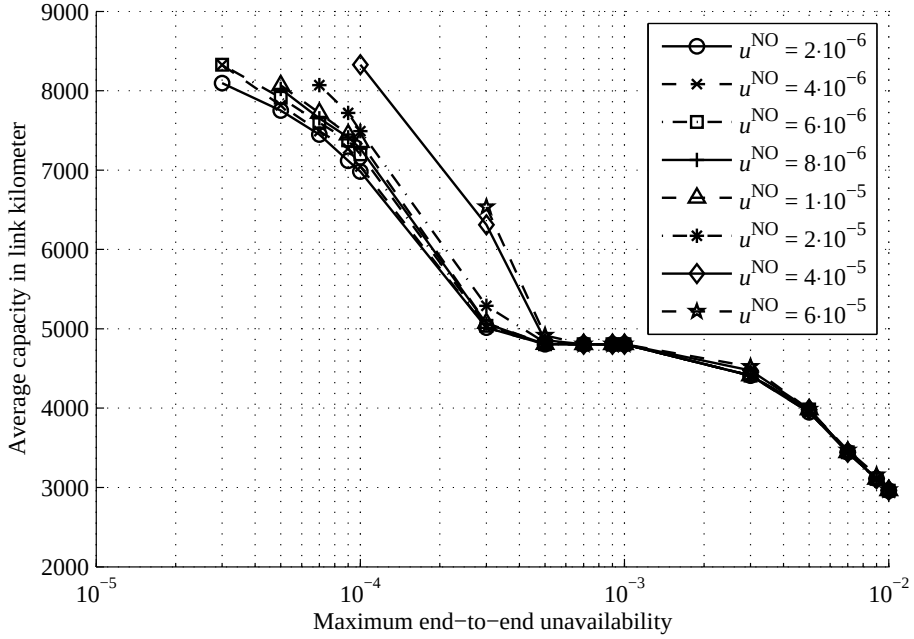

Figure 5.16: Average connection capacity subject to maximum unavailability to be met in the US reference network for various node unavailabilities u^{NO} and link kilometer unavailability $u^{ED} = 4 \cdot 10^{-6}$.

We discover that a relevant portion of 30% normal and dual link sequences and only 1% exclusive dual link configurations are necessary in addition to 69% unprotected paths to achieve two nines end-to-end availability for all demands. This conclusion is confirmed by the previous calculation of the average single path unavailability of $1.04 \cdot 10^{-2}$ which slightly exceeds the two nines availability limit.

For higher target availabilities, dual links more and more replace single paths and normal plus dual link patterns. In order to support three nines connection availability, 100% dual link routing is necessary for all considered node unavailabilities. Diagram 5.17 shows that the exclusive usage of dual links for node unavailability $4 \cdot 10^{-6}$ persists up to target unavailability $3 \cdot 10^{-4}$. Nevertheless, we observe a resource growth when jumping from connection unavailability $5 \cdot 10^{-4}$ to $3 \cdot 10^{-4}$ according to Figure 5.16. This effect arises from the trade-off between different dual link configurations. An example for such a configuration is the direct dual link "an-li-bo-pa"/"an-ur-ho-sn-pa" versus the

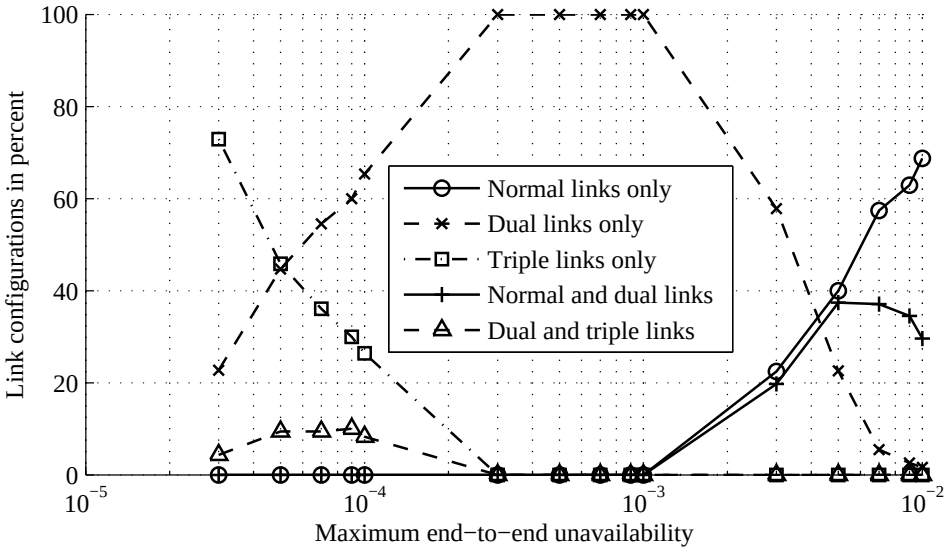

Figure 5.17: Routing configurations over maximum unavailability to be met in the US reference network for an unavailability of $4 \cdot 10^{-6}$ per node and link kilometer.

dual link combination "an-li-bo"/"an-at-bo" and "bo-pa"/"bo-sa-sn-pa" between the end nodes "an" and "pa". Although the former arrangement has only two single points of failure, namely the end nodes, as opposed to three single points of failure for the dual link sequence due to the extra intermediate node, the total connection availability of the latter solution is significantly higher ($3.6 \cdot 10^{-4}$ versus $2.1 \cdot 10^{-4}$). 1:1 path protection based on node-disjoint routes may be favorable due to fewer resources in this case, but each path is prone to outages due to the very long transmission distances in the US network. If there is a failure on one path, any outage on the remaining path interrupts the connection as long as the first defect has not been repaired. For a sequence of two dual links, the 1:1 segments are much shorter and failures can be compensated as long as one path of every virtual link is functional. The extra unavailability of the transit node is tolerable. Thus, the common assumption that a pair of node-disjoint paths performs better than a pair of edge-disjoint paths crossing at an intermediate node does not necessarily hold true when being able to choose the route segments at the transit node. This finding is another motivation to include knowledge about the resulting availability in the routing process.

Four nines end-to-end availability require a considerable amount of end-to-end triple links instead of dual link routing even for small node unavailabilities. Furthermore, the virtual link design produces a new routing mode by combining a short dual link with a triple link. Low node unavailabilities such as $4 \cdot 10^{-6}$ still permit to include an intermediate node as single point of failure. Thus, a capacity-efficient sequence of a short dual link and a triple link can fulfill the desired end-to-end availability.

Figure 5.18 depicts the network resources to realize unavailability-aware connections for varying link unavailabilities represented by distinct curves. Due to long transmission

distances in the US network, different link kilometer unavailabilities have a strong impact on the allocated capacity even for two nines end-to-end availability. Moreover, the convergence of all curves to a common network resource level when applying 1:1 node-disjoint path protection in the range of three nines target availability is not that distinctive. Measures to reduce the link unavailability are especially promising if two or four nines of service availability are to be offered because of highly varying routing resources.

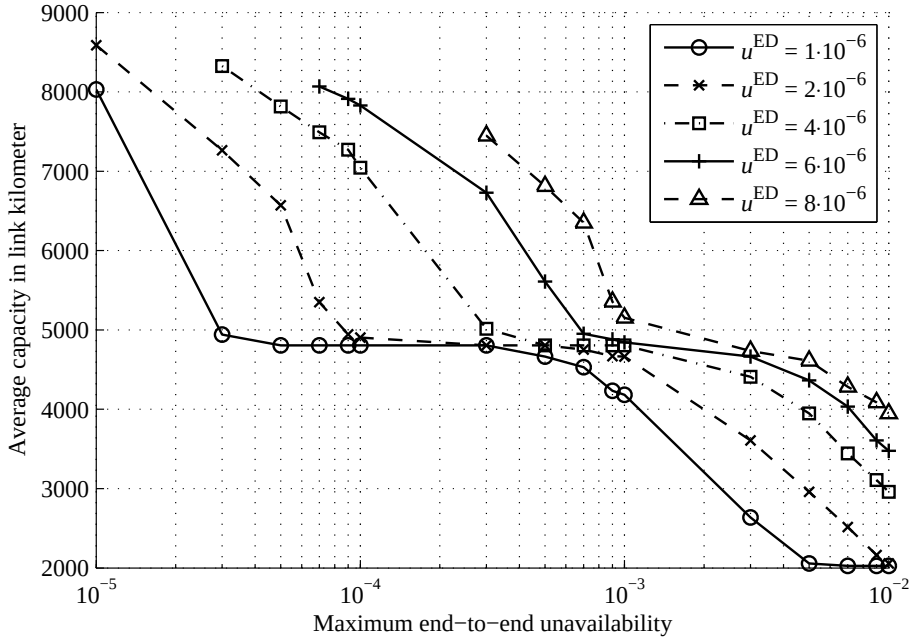

Figure 5.18: Average connection capacity subject to maximum unavailability to be met in the US reference network for various link kilometer unavailabilities u^{ED} and node unavailability $u^{NO} = 4 \cdot 10^{-6}$.

5.6 Summary

In this chapter, a novel availability-aware routing concept has been presented. It is based on virtual links that represent redundant path segments between two not necessarily adjacent nodes. The virtual link routing strategy allows to flexibly combine normal links and virtual links to form a sequence of interconnected links and establish a connection. We have formulated an integer linear programming (ILP) model that facilitates a minimization of network resources and guarantees minimum end-to-end availabilities for all connections at the same time. Numerous case studies for a German, a European, and a US network have been carried out to analyze the trade-off between high service availabilities and cost-efficient network resource allocation. Moreover, the influence of varying node and link unavailabilities has been investigated. Our results show that the capacity requirements strongly depend on the desired connection

availability and the unavailabilities of the network elements. In some cases, the service availability can be improved with no or little extra capacity. On the other hand, there are scenarios where a reduction of the node or link unavailabilities via a more reliable design should be considered to dramatically reduce investments in network resources.

6 Conclusion

6.1 Summary

This work has investigated optimal planning strategies for optical core networks based on wavelength division multiplexing (WDM). We analyzed the network planning process including all major challenges. Due to high computational complexity, the overall design problem was subdivided into smaller task groups. We developed three optimization models that can be solved independently of each other and yield optimal or near-optimal results for realistic network scenarios. Numerous case studies were carried out for a German, European, and US reference network.

In the first model, we determine suitable network topologies by considering the trade-off between infrastructure and routing costs. Based on given node sites, we pre-calculate a subset of eligible network edges that have the highest potential of improving shortest path routing in reasonably meshed topologies. An integer linear program minimizes the routing costs in terms of total wavelength link capacity in kilometers, i.e. the length of all routed lightpaths. The number of network edges that can be allocated for the topology is restricted to different values in order to analyze the impact of the average node degree on the routing costs. Our results reveal that there is a significant cost penalty when excessively restricting the topology. Moreover, network failures can only be compensated if there exist alternative routes along which affected traffic can be sent. Thus, we determine network configurations that can recover from any single or even dual failure by path protection. The computed topologies are used as input for the following studies.

Our second analysis investigates the routing, resilience, and dimensioning problem for opaque and translucent optical networks by means of a detailed cost model. Opaque networks apply electrical switching at the nodes and therefore must convert all incoming optical connections to electrical form and transform outgoing signals conversely. Transparent networks on the other hand cross-connect wavelengths in the optical domain via optical switches. However, purely transparent networks have a restricted maximum transmission distance because the signal impairments induced at the links and nodes along the path accumulate. Thus, we consider translucent networks which provide sparse electrical signal regeneration to refresh the signal-to-noise ratio. Two preliminary steps are performed before solving the mathematical program: translucent paths are designed by allocating transponders plus intermediate regenerators and a set of shortest disjoint routes is computed to restrict the routing options. The wavelength

assignment for the lightpaths including a potential allocation of extra wavelength converters is examined in a subsequent step. Case studies confirm that capital expenditures can be reduced greatly when applying a translucent network design instead of an opaque one due to savings on transceiver equipment. Although most fibers do not have any free wavelength channels left, it is possible to eliminate wavelength blocking in virtually all network configurations.

Specific availability requirements stipulated in service level agreements commit network providers to limit the amount of time during which network services are disturbed from the customers' point of view. In the third model, we develop an availability-adaptive routing strategy that can flexibly conform to arbitrary end-to-end availabilities. Redundant and unprotected path segments are concatenated to compensate failures that would exceed the maximum service outage time per year. Our investigations show that conventional failure-oriented routing configurations like 1:1 path protection provide highly varying availability performance depending on the link and node unavailabilities and the network topology. This often means over- or underprovisioning of network resources with respect to the desired service availability. The virtual link concept can overcome these limitations and minimizes the resource consumption in terms of total link kilometers for each wavelength connection.

6.2 Outlook

The optimization models developed in this work can serve as a basis for further research. Two ideas are briefly highlighted in the following.

The provisioning of connections in optical core networks is expected to become more dynamic due to changing traffic demand patterns. This means that it is not sufficient to compute an optimal network configuration only once. Instead, the status must be continuously monitored to be able to react accordingly. In order to efficiently use the network capacity, a reconfiguration of existing lightpaths might be necessary to remove bottlenecks in the network and accommodate for new demands. Thus, a close coupling of long-term network planning and online operation is desirable. Moreover, there is a continuous network evolution due to technological improvements and the complexity of running an optical network is high. In order to minimize the total cost of ownership, it is beneficial to consider the capital and operational expenditures simultaneously to get the full picture. Currently, there is ongoing work in this area emphasized by the availability of versatile control and management plane architectures. Due to tremendously increasing network traffic, technological advance, and the network operators' pressure to reduce the cost per tranmitted bit, there is ample room for further research on the design of optical core networks.

A Reference Networks

This appendix presents the characteristics of the communication networks that are used as reference scenarios in the thesis. Node locations and traffic demands of the German/ US and the European network are taken from [HBB+04] and [BDH+99], respectively. The candidate topologies comprise all edges that were identified as most attractive options by the preselection strategy in Section 3.2.

German Network

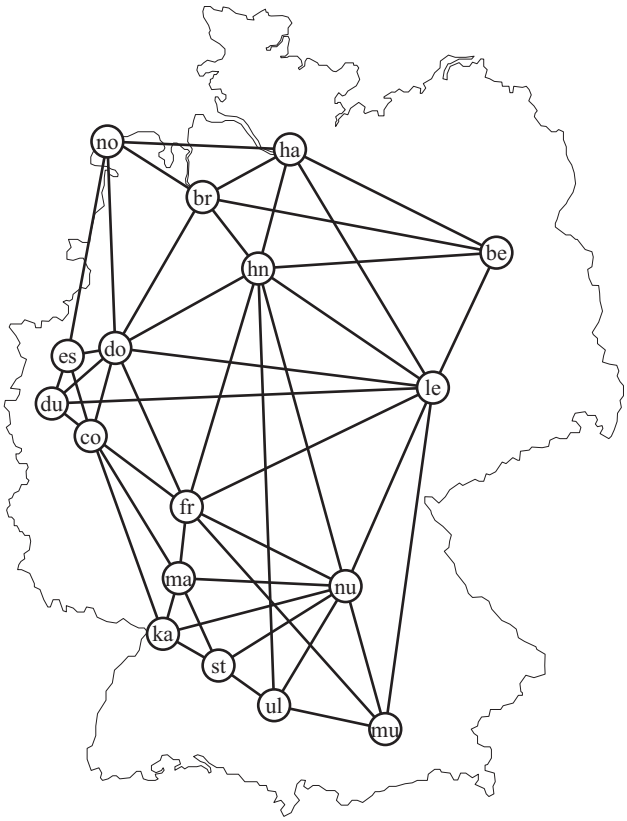

Figure A.1: Candidate topology of the German reference network.

Table A.1: Nodes in the German reference network.

Label	Town	Latitude	Longitude
be	Berlin	52.5167	13.4167
br	Bremen	53.0667	8.8167
co	Cologne	50.9500	6.9667
do	Dortmund	51.5167	7.4667
du	Düsseldorf	51.2333	6.7833
es	Essen	51.4500	7.0167
fr	Frankfurt am Main	50.1167	8.6833
ha	Hamburg	53.5500	9.9833
hn	Hanover	52.3667	9.7167
ka	Karlsruhe	49.0167	8.4000
le	Leipzig	51.3333	12.3833
ma	Mannheim	49.4833	8.4667
mu	Munich	48.1333	11.5667
no	Norden	53.5833	7.1833
nu	Nuremberg	49.4500	11.0833
st	Stuttgart	48.7767	9.1775
ul	Ulm	48.4000	9.9833

Table A.2: Candidate edges in the German reference network.

Label	Towns	Length [km]
be–br	Berlin – Bremen	378
be–ha	Berlin – Hamburg	308
be–hn	Berlin – Hanover	302
be–le	Berlin – Leipzig	179
br–be	Bremen – Berlin	378
br–do	Bremen – Dortmund	234
br–ha	Bremen – Hamburg	113
br–hn	Bremen – Hanover	118
br–no	Bremen – Norden	147
co–do	Cologne – Dortmund	86
co–du	Cologne – Düsseldorf	41
co–es	Cologne – Essen	67
co–fr	Cologne – Frankfurt am Main	183
co–ka	Cologne – Karlsruhe	286
co–ma	Cologne – Mannheim	234
do–br	Dortmund – Bremen	234
do–co	Dortmund – Cologne	86
do–du	Dortmund – Düsseldorf	68

(continues)

Table A.2: Candidate edges in the German reference network *(continued)*.

Label	Towns	Length [km]
do–es	Dortmund – Essen	38
do–fr	Dortmund – Frankfurt am Main	213
do–hn	Dortmund – Hanover	217
do–le	Dortmund – Leipzig	410
do–no	Dortmund – Norden	277
du–co	Düsseldorf – Cologne	41
du–do	Düsseldorf – Dortmund	68
du–es	Düsseldorf – Essen	35
du–le	Düsseldorf – Leipzig	467
es–co	Essen – Cologne	67
es–do	Essen – Dortmund	38
es–du	Essen – Düsseldorf	35
es–no	Essen – Norden	285
fr–co	Frankfurt am Main – Cologne	183
fr–do	Frankfurt am Main – Dortmund	213
fr–hn	Frankfurt am Main – Hanover	312
fr–le	Frankfurt am Main – Leipzig	352
fr–ma	Frankfurt am Main – Mannheim	87
fr–mu	Frankfurt am Main – Munich	365
fr–nu	Frankfurt am Main – Nuremberg	225
ha–be	Hamburg – Berlin	308
ha–br	Hamburg – Bremen	113
ha–hn	Hamburg – Hanover	159
ha–le	Hamburg – Leipzig	354
ha–no	Hamburg – Norden	222
hn–be	Hanover – Berlin	302
hn–br	Hanover – Bremen	118
hn–do	Hanover – Dortmund	217
hn–fr	Hanover – Frankfurt am Main	312
hn–ha	Hanover – Hamburg	159
hn–le	Hanover – Leipzig	259
hn–nu	Hanover – Nuremberg	406
hn–ul	Hanover – Ulm	530
ka–co	Karlsruhe – Cologne	286
ka–ma	Karlsruhe – Mannheim	63
ka–nu	Karlsruhe – Nuremberg	241
ka–st	Karlsruhe – Stuttgart	75
le–be	Leipzig – Berlin	179
le–do	Leipzig – Dortmund	410
le–du	Leipzig – Düsseldorf	467

(continues)

Table A.2: Candidate edges in the German reference network *(continued)*.

Label	Towns	Length [km]
le–fr	Leipzig – Frankfurt am Main	352
le–ha	Leipzig – Hamburg	354
le–hn	Leipzig – Hanover	259
le–mu	Leipzig – Munich	433
le–nu	Leipzig – Nuremberg	275
ma–co	Mannheim – Cologne	234
ma–fr	Mannheim – Frankfurt am Main	87
ma–ka	Mannheim – Karlsruhe	63
ma–nu	Mannheim – Nuremberg	227
ma–st	Mannheim – Stuttgart	113
mu–fr	Munich – Frankfurt am Main	365
mu–le	Munich – Leipzig	433
mu–nu	Munich – Nuremberg	181
mu–ul	Munich – Ulm	145
no–br	Norden – Bremen	147
no–do	Norden – Dortmund	277
no–es	Norden – Essen	285
no–ha	Norden – Hamburg	222
nu–fr	Nuremberg – Frankfurt am Main	225
nu–hn	Nuremberg – Hanover	406
nu–ka	Nuremberg – Karlsruhe	241
nu–le	Nuremberg – Leipzig	275
nu–ma	Nuremberg – Mannheim	227
nu–mu	Nuremberg – Munich	181
nu–st	Nuremberg – Stuttgart	189
nu–ul	Nuremberg – Ulm	170
st–ka	Stuttgart – Karlsruhe	75
st–ma	Stuttgart – Mannheim	113
st–nu	Stuttgart – Nuremberg	189
st–ul	Stuttgart – Ulm	87
ul–hn	Ulm – Hanover	530
ul–mu	Ulm – Munich	145
ul–nu	Ulm – Nuremberg	170
ul–st	Ulm – Stuttgart	87

European Network

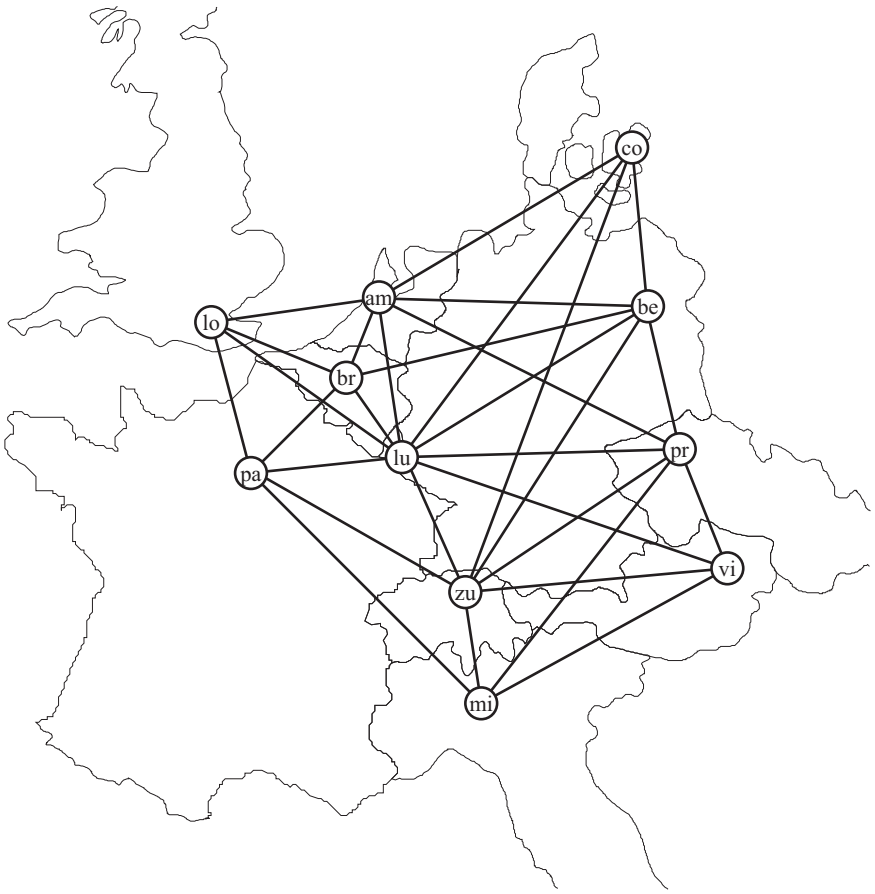

Figure A.2: Candidate topology of the European reference network.

Table A.3: Nodes in the European reference network.

Label	Town	Latitude	Longitude
am	Amsterdam	52.3731	4.8922
be	Berlin	52.5167	13.4167
br	Brussels	50.8436	4.3575
co	Copenhagen	55.6750	12.5687
lo	London	51.5000	−0.1167
lu	Luxembourg	49.6000	6.1167
mi	Milan	45.4636	9.1884
pa	Paris	48.8667	2.3331
pr	Prague	50.0833	14.4167
vi	Vienna	48.2086	16.3719
zu	Zurich	47.3667	8.5500

Table A.4: Candidate edges in the European reference network.

Label	Towns	Length [km]
am–be	Amsterdam – Berlin	693
am–br	Amsterdam – Brussels	209
am–co	Amsterdam – Copenhagen	745
am–lo	Amsterdam – London	428
am–lu	Amsterdam – Luxembourg	384
am–pr	Amsterdam – Prague	852
be–am	Berlin – Amsterdam	693
be–br	Berlin – Brussels	781
be–co	Berlin – Copenhagen	427
be–lu	Berlin – Luxembourg	725
be–pr	Berlin – Prague	335
be–zu	Berlin – Zurich	804
br–am	Brussels – Amsterdam	209
br–be	Brussels – Berlin	781
br–lo	Brussels – London	384
br–lu	Brussels – Luxembourg	224
br–pa	Brussels – Paris	316
co–am	Copenhagen – Amsterdam	745
co–be	Copenhagen – Berlin	427
co–lu	Copenhagen – Luxembourg	963
co–zu	Copenhagen – Zurich	1157
lo–am	London – Amsterdam	428
lo–br	London – Brussels	384
lo–lu	London – Luxembourg	586
lo–pa	London – Paris	409
lu–am	Luxembourg – Amsterdam	384
lu–be	Luxembourg – Berlin	725
lu–br	Luxembourg – Brussels	224
lu–co	Luxembourg – Copenhagen	963
lu–lo	Luxembourg – London	586
lu–pa	Luxembourg – Paris	344
lu–pr	Luxembourg – Prague	717
lu–vi	Luxembourg – Vienna	918
lu–zu	Luxembourg – Zurich	368
mi–pa	Milan – Paris	770
mi–pr	Milan – Prague	774
mi–vi	Milan – Vienna	751
mi–zu	Milan – Zurich	261
pa–br	Paris – Brussels	316
pa–lo	Paris – London	409

(continues)

Table A.4: Candidate edges in the European reference network *(continued)*.

Label	Towns	Length [km]
pa–lu	Paris – Luxembourg	344
pa–mi	Paris – Milan	770
pa–zu	Paris – Zurich	589
pr–am	Prague – Amsterdam	852
pr–be	Prague – Berlin	335
pr–lu	Prague – Luxembourg	717
pr–mi	Prague – Milan	774
pr–vi	Prague – Vienna	303
pr–zu	Prague – Zurich	631
vi–lu	Vienna – Luxembourg	918
vi–mi	Vienna – Milan	751
vi–pr	Vienna – Prague	303
vi–zu	Vienna – Zurich	710
zu–be	Zurich – Berlin	804
zu–co	Zurich – Copenhagen	1157
zu–lu	Zurich – Luxembourg	368
zu–mi	Zurich – Milan	261
zu–pa	Zurich – Paris	589
zu–pr	Zurich – Prague	631
zu–vi	Zurich – Vienna	710

US Network

Figure A.3: Candidate topology of the US reference network.

Table A.5: Nodes in the US American reference network.

Label	Town	Latitude	Longitude
an	Ann Arbor (Michigan)	42.2754	−83.7308
at	Atlanta (Georgia)	33.7600	−84.3900
bo	Boulder (Colorado)	40.0176	−105.2797
ho	Houston (Texas)	29.7500	−95.3500
it	Ithaca (New York)	42.4436	−76.5001
li	Lincoln (Nebraska)	40.8099	−96.6753
pa	Palo Alto (California)	37.4445	−122.1602
pi	Pittsburgh (Pennsylvania)	40.4400	−80.0000
pr	Princeton (New Jersey)	40.3522	−74.6571
sa	Salt Lake City (Utah)	40.7547	−111.8926
se	Seattle (Washington)	47.6100	−122.3300
sn	San Diego (California)	32.7800	−117.1500
ur	Urbana (Illinois)	40.1097	−88.2042
wa	Washington (D.C.)	38.8900	−77.0300

Table A.6: Candidate edges in the US American reference network.

Label	Towns	Length [km]
an–at	Ann Arbor – Atlanta	1138
an–it	Ann Arbor – Ithaca	713
an–li	Ann Arbor – Lincoln	1306
an–pi	Ann Arbor – Pittsburgh	447
an–pr	Ann Arbor – Princeton	944
an–ur	Ann Arbor – Urbana	534
at–an	Atlanta – Ann Arbor	1138
at–bo	Atlanta – Boulder	2374
at–ho	Atlanta – Houston	1353
at–li	Atlanta – Lincoln	1606
at–pi	Atlanta – Pittsburgh	1006
at–ur	Atlanta – Urbana	940
at–wa	Atlanta – Washington	1046
bo–at	Boulder – Atlanta	2374
bo–ho	Boulder – Houston	1746
bo–li	Boulder – Lincoln	880
bo–pa	Boulder – Palo Alto	1787
bo–sa	Boulder – Salt Lake City	679
bo–se	Boulder – Seattle	1923
bo–sn	Boulder – San Diego	1597
ho–at	Houston – Atlanta	1353
ho–bo	Houston – Boulder	1746
ho–li	Houston – Lincoln	1483
ho–pi	Houston – Pittsburgh	2195
ho–sa	Houston – Salt Lake City	2318
ho–sn	Houston – San Diego	2514
ho–ur	Houston – Urbana	1587
it–an	Ithaca – Ann Arbor	713
it–pi	Ithaca – Pittsburgh	440
it–pr	Ithaca – Princeton	335
it–wa	Ithaca – Washington	477
li–an	Lincoln – Ann Arbor	1306
li–at	Lincoln – Atlanta	1606
li–bo	Lincoln – Boulder	880
li–ho	Lincoln – Houston	1483
li–se	Lincoln – Seattle	2601
li–ur	Lincoln – Urbana	865
pa–bo	Palo Alto – Boulder	1787
pa–sa	Palo Alto – Salt Lake City	1150
pa–se	Palo Alto – Seattle	1357

(continues)

Table A.6: Candidate edges in the US American reference network *(continued)*.

Label	Towns	Length [km]
pa–sn	Palo Alto – San Diego	828
pi–an	Pittsburgh – Ann Arbor	447
pi–at	Pittsburgh – Atlanta	1006
pi–ho	Pittsburgh – Houston	2195
pi–it	Pittsburgh – Ithaca	440
pi–pr	Pittsburgh – Princeton	543
pi–ur	Pittsburgh – Urbana	836
pi–wa	Pittsburgh – Washington	369
pr–an	Princeton – Ann Arbor	944
pr–it	Princeton – Ithaca	335
pr–pi	Princeton – Pittsburgh	543
pr–wa	Princeton – Washington	312
sa–bo	Salt Lake City – Boulder	679
sa–ho	Salt Lake City – Houston	2318
sa–pa	Salt Lake City – Palo Alto	1150
sa–se	Salt Lake City – Seattle	1352
sa–sn	Salt Lake City – San Diego	1203
se–bo	Seattle – Boulder	1923
se–li	Seattle – Lincoln	2601
se–pa	Seattle – Palo Alto	1357
se–sa	Seattle – Salt Lake City	1352
se–sn	Seattle – San Diego	2047
sn–bo	San Diego – Boulder	1597
sn–ho	San Diego – Houston	2514
sn–pa	San Diego – Palo Alto	828
sn–sa	San Diego – Salt Lake City	1203
sn–se	San Diego – Seattle	2047
ur–an	Urbana – Ann Arbor	534
ur–at	Urbana – Atlanta	940
ur–ho	Urbana – Houston	1587
ur–li	Urbana – Lincoln	865
ur–pi	Urbana – Pittsburgh	836
wa–at	Washington – Atlanta	1046
wa–it	Washington – Ithaca	477
wa–pi	Washington – Pittsburgh	369
wa–pr	Washington – Princeton	312

B Acronyms

ASON Automatically Switched Optical Network

BA booster amplifier

BPA booster/pre-amplifier

CC cable conduit

CAPEX capital expenditures

DCF dispersion compensating fiber

DGE dynamic gain equalizer

EES edge eligibility score

EO electrical-to-optical

ELH extended long haul

ES electrical switch

ESF electrical switch fabric

FC fiber cable

FIT failure in time

FS fiber span

GMPLS generalized multiprotocol label switching

IA inline amplifier

ILP integer linear programming

IP Internet Protocol

IPA inline/pre-amplifier

ITU International Telecommunication Union

LP linear programming

LH long haul

LLC long reach line card

MTD maximum transmission distance

MEMS micro-electro-mechanical system
MTBF mean time between failures
MTTF mean time to failure
MTTR mean time to repair
OS optical switch
OSI Open Systems Interconnection
OSF optical switch fabric
OMD optical multiplexer/demultiplexer
OD optical demultiplexer
OM optical multiplexer
OE optical-to-electrical
OEO optical-to-electrical-to-optical
OPEX operational expenditures
PA pre-amplifier
PVWP partial virtual wavelength path
QoS quality of service
RG regenerator
SDH Synchronous Digital Hierarchy
SONET Synchronous Optical Network
SLA service level agreement
SLC short reach line card
TBF time between failures
TDM time division multiplexing
TP transponder
TPA transparent node pre-amplifier
TTF time to failure
TTR time to repair
ULH ultra long haul
VWP virtual wavelength path
WAN wide area network

WC wavelength converter

WDM wavelength division multiplexing

WP wavelength path

C Notation

This annex includes the most important expressions and symbols used in the thesis.

Table C.1: Mathematical expressions.

Expression	Description
$\forall \ldots$	For all …
$\text{expr}_1 : \text{expr}_2$	Expression expr_1 such that expression expr_2 holds true
$\lvert\mathcal{X}\rvert$	Cardinality of set $\mathcal{X}$, i.e. the number of elements in $\mathcal{X}$
$\mathcal{X} \subset \mathcal{Y}$	Set $\mathcal{X}$ is a subset of set $\mathcal{Y}$, i.e. all elements of $\mathcal{X}$ are also elements of $\mathcal{Y}$
$\mathcal{X} \setminus \mathcal{Y}$	Set of elements which are included in $\mathcal{X}$ but not in $\mathcal{Y}$
$\{x_1, x_2\} \subset \mathcal{X} : x_1 \neq x_2$	Set of unordered pairs of elements x_1 and x_2 of set $\mathcal{X}$
$\lfloor x \rfloor$	Largest integer less than or equal to value x
$\lceil x \rceil$	Smallest integer greater than or equal to value x
$\vee$	Logical disjunction operator (OR)
$\wedge$	Logical conjunction operator (AND)
$\min(\ldots)$	Minimum value of all arguments
$\max(\ldots)$	Maximum value of all arguments

Table C.2: Explanatory symbols.

Symbol	Description
BD	Bidirected
CO	Connection
DI	Directed
DR, $\lVert$	Disjoint routes
ED	Edge
NO	Node
RO	Route
VL	Virtual link

Table C.3: Element symbols.

Symbol	Description
e	Network edge
n	Network node
r	Route

Table C.4: Set symbols.

Symbol	Description
$\emptyset$	Empty set
$\mathcal{B}$	Bitrates
$\mathcal{E}, \mathcal{E}^{\mathrm{BD}}$	Bidirected network edges
$\mathcal{E}^{\mathrm{DI}}$	Directed network edges
$\mathcal{E}_r^{\mathrm{RO}}$	Bidirected edges of route r
$\mathcal{I}$	Identifiers
$\mathcal{N}$	Network nodes
$\mathcal{N}_r^{\mathrm{RO}}$	Nodes of route r, i.e. origin, destination, and all traversed nodes
$\mathcal{R}_{z^{\mathrm{DR}}}$	Routing configurations consisting of z^{DR} mutually disjoint routes between any node pair
$\mathcal{R}_{z^{\mathrm{DR}},n_1,n_2}$	Routing configurations consisting of z^{DR} mutually disjoint routes with origin node n_1 and destination node n_2
$\mathbb{R}$	Real values
$\mathcal{T}$	Long range transmission technologies
$\mathcal{V}$	Virtual Edges
$\mathcal{W}$	Wavelengths
$\mathbb{Z}$	Integer numbers

Table C.5: Parameter symbols.

Symbol	Range	Description
a	$[0,1]$	Availability
c	$\mathbb{R}_0^+$	Costs
d	$\mathbb{Z}_0^+$	Number of demands
f	$\mathbb{Z}_0^+$	Number of fibers
l	$\mathbb{R}_0^+$	Length
m	$\mathbb{R}_0^+$	Metric
q	$\mathbb{R}_0^+$	Quantifier to convert the costs of 10 Gbit/s long range transmission equipment to corresponding 2.5 Gbit/s equipment
u	$[0,1]$	Unavailability
$\alpha_{e,n}$	$\{0,1\}$	Edge e is incident on node n (=1) or not (=0)

(continues)

Table C.5: Parameter symbols *(continued)*.

Symbol	Range	Description
$\delta_{r,e}$	$\{0,1\}$	Route r uses edge e (=1) or not (=0)
$\epsilon_{r,n}$	$\{0,1\}$	Route r uses node n (=1) or not (=0)
$\theta_{n,e}$	$\{0,1\}$	Node n is source of edge e (=1) or not (=0)
$\iota_{n,e}$	$\{0,1\}$	Node n is target of edge e (=1) or not (=0)
$\kappa_{r,n}$	$\{0,1\}$	Node n is origin of route r (=1) or not (=0)
$\lambda_{r,n}$	$\{0,1\}$	Node n is destination of route r (=1) or not (=0)
$\chi_{r,n,t}$	$\{0,1\}$	Transmission technology t at node n is required to support a path on route r (=1) or not (=0)
ψ_{r_1,r_2}	$\{0,1\}$	Route r_1 is a subroute of route r_2 (=1) or not (=0)
$\phi_{r^{\mathrm{WP}},r}$	$\{0,1\}$	Route r^{WP} is a wavelength path subroute of route r (=1) or not (=0)
z^{DR}	$\mathbb{Z}^+$	Number of redundant disjoint paths to compensate a failure of the primary path

Table C.6: Variable symbols.

Symbol	Range	Description
C_n^{NO}	$\mathbb{R}_0^+$	Costs of node n
C_e^{ED}	$\mathbb{R}_0^+$	Costs of edge e
E_e	$\{0,1\}$	Edge e is allocated
F_e	$\mathbb{Z}_0^+$	Number of fibers of edge e
$L_{e,b}$	$\mathbb{Z}_0^+$	Number of links on edge e with bitrate b
$L_{n_1,n_2,e}$	$\mathbb{Z}_0^+$	Number of links for connection between nodes n_1 and n_2 on edge e
$L_{n_1,n_2,r,i,e,w}$	$\mathbb{Z}_0^+$	Number of links for connection between nodes n_1 and n_2 on route r with identifier i on edge e at wavelength w
$P_{n_1,n_2,r^{\parallel}}$	$\mathbb{Z}_0^+$	Number of paths for connection between nodes n_1 and n_2 on route r
$P_{n_1,n_2,r^{\parallel},b}$	$\mathbb{Z}_0^+$	Number of paths for connection between nodes n_1 and n_2 on route r with bitrate b
P_r	$\mathbb{Z}_0^+$	Number of paths along route r
R_r	$\mathbb{Z}_0^+$	Number of routes along route r
$V_{n_1,n_2,r^{\parallel}}$	$\mathbb{Z}_0^+$	Number of virtual links between nodes n_1 and n_2 on disjoint routes $r^{\parallel}$
$W_{n_1,n_2,r^{\mathrm{WP}},i,n}$	$\mathbb{Z}_0^+$	Number of wavelength converters for wavelength path between nodes n_1 and n_2 on route r^{WP} with identifier i on node n

List of Figures

List of Tables

Bibliography

Publications of the Author

[GS07] W. D. Grover and M. Scheffel. Resolving a Question about Span Restoration: Do Loopbacks Involve a Capacity Penalty? In *International Workshop on the Design of Reliable Communication Networks (DRCN)*, 2007.

[KS07] A. Koster and M. Scheffel. A Routing and Network Dimensioning Strategy to Reduce Wavelength Continuity Conflicts in All-Optical Networks. In *International Network Optimization Conference (INOC)*, 2007.

[MSSW05] D. Mello, D. Schupke, M. Scheffel, and H. Waldman. Availability Maps for Connections in WDM Optical Networks. In *International Workshop on the Design of Reliable Communication Networks (DRCN)*, 2005.

[Sch04] M. Scheffel. Establishing All-Optical Transparency Domains in WDM Networks. In *Open European Summer School and IFIP WG 6.3 Workshop on the Advances in Fixed and Mobile Networks (EUNICE)*, 2004.

[Sch05a] M. Scheffel. Optimal Topology Planning of Optical Networks with Respect to Overall Design Costs. *Optical Switching and Networking*, 2(4):239–248, 2005.

[Sch05b] M. Scheffel. Regenerator Allocation Strategies for Optical Transparency Domains Considering Transmission Limitations. In *IEEE International Conference on Communications (ICC)*, 2005.

[Sch05c] M. Scheffel. Topology Design of Transport Networks Considering Path Protection Against Single and Dual Failures. In *Conference on Optical Network Design and Modeling (ONDM)*, 2005.

[Sch06a] M. Scheffel. Adaptation of Failure Scenario Based Resilience Schemes Toward Availability Guarantees. *Journal of Optical Networking*, 5(7):521–531, 2006.

[Sch06b] M. Scheffel. An Availability-Oriented Network Resilience Scheme Using Virtual Link Concatenation. In *International Conference on Telecommunications (ICT)*, 2006.

[Sch06c] M. Scheffel. Robust and Survivable Network Design for Entirely Uncertain Traffic Demand Patterns. In *International Conference on Software, Telecommunications and Computer Networks (SoftCOM)*, 2006.

[Sch06d] M. Scheffel. Routing and Wavelength Assignment and Transmission Capacity Allocation for All-Optical Networks Based on Wavelength Groups. In *INFORMS Telecommunications Conference*, 2006.

[SGSP06] M. Scheffel, C. Gruber, T. Schwabe, and R. Prinz. Optimal Multi-Topology Routing for IP Resilience. *AEÜ - International Journal of Electronics and Communications*, 60(1):35–39, 2006.

[SKS07] M. Scheffel, M. Kiese, and T. Stidsen. A Clustering Approach for Scalable Network Design. In *International Network Optimization Conference (INOC)*, 2007.

[SPG+06] M. Scheffel, R. Prinz, C. Gruber, A. Autenrieth, and D. Schupke. Optimal Routing and Grooming for Multilayer Networks with Transponders and Muxponders. In *IEEE Global Communications Conference (GLOBECOM)*, 2006.

[SSG03a] D. Schupke, M. Scheffel, and W. D. Grover. Configuration of *p*-Cycles in WDM Networks with Partial Wavelength Conversion. *Photonic Network Communications*, 6(3):238–252, 2003.

[SSG03b] D. Schupke, M. Scheffel, and W. D. Grover. An Efficient Strategy for Wavelength Conversion in WDM *p*-Cycle Networks. In *International Workshop on the Design of Reliable Communication Networks (DRCN)*, 2003.

Other Publications

[AKM+09] S. Azodolmolky, M. Klinkowski, E. Marin, D. Careglio, J. S. Pareta, and I. Tomkos. A Survey on Physical Layer Impairments Aware Routing and Wavelength Assignment Algorithms in Optical Networks. *Computer Networks*, 53(7):926–944, 2009.

[AM08] E. M. Al Sukhni and H. T. Mouftah. A Novel Distributed Availability-Aware Provisioning Framework for Differentiated Protection Services in Optical Mesh Networks. In *Canadian Conference on Electrical and Computer Engineering (CCECE)*, 2008.

[AMP+03] D. Arci, G. Maier, A. Pattavina, D. Petecchi, and M. Tomatore. Availability Models for Protection Techniques in WDM Networks. In *International Workshop on the Design of Reliable Communication Networks (DRCN)*, 2003.

[BDH+99] P. Batchelor, B. Daino, P. Heinzmann, C. Weinert, J. Späth, B. Van Caenegem, D. Hjelme, R. Inkret, H. Jäger, M. Joindot, A. Kuchar, E. Le Coquil, P. Leuthold, G. de Marchis, F. Matera, B. Mikac, H.-P. Nolting, F. Tillerot, and N. Wauters. *Ultra High Capacity Optical Transmission Networks: Final Report of Action COST 239*. Faculty of Electrical Engineering and Computing, University of Zagreb, 1999.

[Bha99] R. Bhandari. *Survivable Networks: Algorithms for Diverse Routing*. Kluwer Academic Publishers, 1999.

[BSBS08] J. Berthold, A. A. Saleh, L. Blair, and J. M. Simmons. Optical Networking: Past, Present, and Future. *Journal of Lightwave Technology*, 26(9):1104–1118, 2008.

[BT97] D. Bertsimas and J. Tsitsiklis. *Introduction to Linear Optimization*. Athena Scientific, 1997.

[CBFMF10] D. A. R. Chaves, C. J. A. Bastos-Filho, and J. F. Martins-Filho. Multiobjective Physical Topology Design of All-Optical Networks Considering QoS and Capex. In *Optical Fiber Communication Conference (OFC)*, 2010.

[CG02] M. Clouqueur and W. D. Grover. Availability Analysis of Span-Restorable Mesh Networks. *IEEE Journal on Selected Areas in Communications*, 20(4):810–821, 2002.

[CG05] M. Clouqueur and W. D. Grover. Mesh-Restorable Networks with Enhanced Dual-Failure Restorability Properties. *Photonic Network Communications*, 9(1):7–18, 2005.

[CLE04] H. C. Cankaya, A. Lardies, and G. W. Ester. Availability Aware Cost Modeling of Mesh Architectures for Long-Haul Networks. In *IEEE International Symposium on Computers and Communications (ISCC)*, 2004.

[CMH+07] P. Cholda, A. Mykkeltveit, B. E. Helvik, O. J. Wittner, and A. Jajszczyk. A Survey of Resilience Differentiation Frameworks in Communication Networks. *IEEE Communications Surveys & Tutorials*, 9(4):32–55, 2007.

[DCG03] J. Doucette, M. Clouqueur, and W. D. Grover. On the Availability and Capacity Requirements of Shared Backup Path-Protected Mesh Networks. *Optical Networks Magazine*, 4(6):29–44, 2003.

[Def08] Definitions of Terms Related to Quality of Service (ITU-T Recommendation E.800), 2008.

[DGA+99] P. Demeester, M. Gryseels, A. Autenrieth, C. Brianza, L. Castagna, G. Signorelli, R. Clernente, M. Ravera, A. Jajszczyk, D. Janukowicz, K. Van Doorselaere, and Y. Harada. Resilience in Multilayer Networks. *IEEE Communications Magazine*, 37(8):70–76, 1999.

[DGMK+10] M. De Groote, K. Manousakis, P. Kokkinos, D. Colle, M. Pickavet, K. Christodoulopoulos, E. M. Varvarigos, and P. Demeester. Cost Comparison of Different Translucent Optical Network Architectures. In *Conference of Telecommunication, Media and Internet Techno-Economics (CTTE)*, 2010.

[Dij59] E. W. Dijkstra. A Note on Two Problems in Connexion with Graphs. *Numerische Mathematik*, 1(1):269—271, 1959.

[EKW09] J. Eberspächer, M. Kiese, and R. Wessäly. Optimierung von Kommunikationsnetzen. In M. Grötschel, K. Lucas, and V. Mehrmann, editors, *Produktionsfaktor Mathematik*. Springer, 2009.

[FHTG10] M. Fiedler, T. Hossfeld, and P. Tran-Gia. A Generic Quantitative Relationship between Quality of Experience and Quality of Service. *IEEE Network Magazine of Global Internetworking*, 24(2):36–41, 2010.

[GBB+06] A. Gladisch, R.-P. Braun, D. Breuer, A. Ehrhardt, H.-M. Foisel, M. Jaeger, R. Leppla, M. Schneiders, S. Vorbeck, W. Weiershausen, and F.-J. Westphal. Evolution of Terrestrial Optical System and Core Network Architecture. *Proceedings of the IEEE*, 94(1):869–891, 2006.

[GC05] W. D. Grover and M. Clouqueur. Span-Restorable Mesh Networks with Multiple Quality of Protection (QoP) Service Classes. *Photonic Network Communications*, 9(1):19–34, 2005.

[GD01a] W. D. Grover and J. Doucette. A Novel Heuristic for Topology Planning and Evolution of Optical Mesh Networks. In *Global Telecommunications Conference (GLOBECOM)*, 2001.

[GD01b] W. D. Grover and J. Doucette. Topological Design of Survivable Mesh-Based Transport Networks. *Annals of Operations Research*, 106(1-4):79–125, 2001.

[GG06] A. Grue and W. D. Grover. Characterization of Pre-Cross-Connected Trails for Optical Mesh Network Protection. *Journal of Optical Networking*, 5(6):493–508, 2006.

[GK77] M. Gerla and L. Kleinrock. On the Topological Design of Distributed Computer Networks. *IEEE Transactions on Communications*, 25(1):48–60, 1977.

[GKG+10] J. M. Gutierrez, K. Katrinis, K. Georgakilas, A. Tzanakaki, and O. B. Madsen. Increasing the Cost-Constrained Availability of WDM Networks with Degree-3 Structured Topologies. In *International Conference on Transparent Optical Networks (ICTON)*, 2010.

[GLW+06] M. Gunkel, R. Leppla, M. Wade, A. Lord, D. Schupke, G. Lehmann, C. Fürst, S. Bodamer, B. Bollenz, H. Haunstein, H. Nakajima, and J. Martensson. A Cost Model for the WDM Layer. In *International Conference on Photonics in Switching (PS)*, 2006.

[Gro03] W. D. Grover. *Mesh-Based Survivable Networks: Options and Strategies for Optical, MPLS, SONET and ATM Networking*. Prentice Hall PTR, 2003.

[Gru09] C. G. Gruber. CAPEX and OPEX in Aggregation and Core Networks. In *Optical Fiber Communication Conference (OFC)*, 2009.

[HBB+04] R. Hülsermann, S. Bodamer, M. Barry, A. Betker, M. Jäger, J. Späth, C. Gauger, and M. Köhn. A Set of Typical Transport Network Scenarios for Network Modelling. In *Beiträge zur 5. ITG-Fachtagung Photonische Netze*, 2004.

[HMS07] J. Hershberger, M. Maxel, and S. Suri. Finding the k Shortest Simple Paths: A New Algorithm and its Implementation. *ACM Transactions on Algorithms*, 3(4):45:1–45:19, 2007.

[HWHM04] Y. Huang, W. Wen, J. P. Heritage, and B. Mukherjee. A Generalized Protection Framework Using a New Link-State Availability Model for Reliable Optical Networks. *Journal of Lightwave Technology*, 22(11):2536–2547, 2004.

[JJU02] L. Jereb, T. Jakab, and F. Unghvary. Availability Analysis of Multi-Layer Optical Networks. *Optical Networks Magazine*, 3(2):84–95, 2002.

[KM10] B. Kantarci and H. T. Mouftah. SLA-Aware Protection Switching in Optical WDM Networks. In *Biennial Symposium on Communications (QBSC)*, 2010.

[KMES09] M. Kiese, V. Marcheva, J. Eberspächer, and D. Schupke. Diverse Routing Based on Shared Risk Link Groups. In *International Workshop on the Design of Reliable Communication Networks (DRCN)*, 2009.

[KMO09] B. Kantarci, H. T. Mouftah, and S. F. Oktug. Adaptive Schemes for Differentiated Availability-Aware Connection Provisioning in Optical Transport Networks. *Journal of Lightwave Technology*, 27(20):4595–4602, 2009.

[Kos06] A. M. Koster. Cost-Efficient Transparent Optical Networks with High Connection Availabilities. In *International Conference on Transparent Optical Networks (ICTON)*, 2006.

[LG04] D. Leung and W. D. Grover. Restorable Mesh Network Design Under Demand Uncertainty: Toward "Future Proof" Transport Investments. In *Optical Fiber Communication Conference (OFC)*, 2004.

[LG05] D. Leung and W. D. Grover. Capacity Planning of Survivable Mesh-based Transport Networks Under Demand Uncertainty. *Photonic Network Communications*, 10(2):123–140, 2005.

[LT08] H. Liua and F. A. Tobagi. Physical Topology Design for All-Optical Networks. *Optical Switching and Networking*, 5(4):219–231, 2008.

[LTMP09] D. Lucerna, M. Tornatore, B. Mukherjee, and A. Pattavina. Availability Target Redefinition for Dynamic Connections in WDM Networks with Shared Path Protection. In *International Workshop on the Design of Reliable Communication Networks (DRCN)*, 2009.

[MCL+03] S. D. Maesschalck, D. Colle, I. Lievens, M. Pickavet, P. Demeester, C. Mauz, M. Jäger, R. Inkret, B. Mikac, and J. Derkacz. Pan-European Optical Transport Networks: An Availability-Based Comparison. *Photonic Network Communications*, 5(3):203–225, 2003.

[MH06] A. Morea and I. B. Heard. Availability of Translucent Networks Based on WSS Nodes, Comparison with Opaque Networks. In *International Conference on Transparent Optical Networks (ICTON)*, 2006.

[MKH09] X. Ma, S. Kim, and K. Harfoush. Towards Realistic Physical Topology Models for Internet Backbone Networks. In *International Symposium on High Capacity Optical Networks and Enabling Technologies (HONET)*, 2009.

[MSE08] C. Meusburger, D. A. Schupke, and J. Eberspächer. Multiperiod Planning for Optical Networks – Approaches Based on Cost Optimization and Limited Budget. In *IEEE International Conference on Communications (ICC)*, 2008.

[MVZP06] L. Mason, A. Vinokurov, N. Zhao, and D. Plant. Topological Design and Dimensioning of Agile All-Photonic Networks. *Computer Networks*, 50(2):268–287, 2006.

[PHS+07] C. T. Politi, H. Haunstein, D. A. Schupke, S. Duhovnikov, G. Lehmann, A. Stavdas, M. Gunkel, J. Martensson, and A. Lord. Integrated Design and Operation of a Transparent Optical Network: A Systematic Approach

to Include Physical Layer Awareness and Cost Function. *IEEE Communications Magazine*, 45(1):40–47, 2007.

[PMD09] C. Pluntke, M. Menth, and M. Duelli. CAPEX-Aware Design of Survivable DWDM Mesh Networks. In *IEEE International Conference on Communications (ICC)*, 2009.

[PMdRP10] C. Pavan, R. M. Morais, J. R. F. da Rocha, and A. N. Pinto. Generating Realistic Optical Transport Network Topologies. *Journal of Optical Communications and Networking*, 2(1):80–90, 2010.

[PTFW06] Z. Pandi, M. Tacca, A. Fumagalli, and L. Wosinska. Dynamic Provisioning of Availability-Constrained Optical Circuits in the Presence of Optical Node Failures. *Journal of Lightwave Technology*, 24(9):3268–3279, 2006.

[Rob98] T. G. Robertazzi. *Planning Telecommunication Networks*. Wiley-IEEE Press, 1998.

[RSS09] R. Ramaswami, K. Sivarajan, and G. Sasaki. *Optical Networks: A Practical Perspective*. Morgan Kaufmann, 2009.

[Rub78] F. Rubin. Enumerating All Simple Paths in a Graph. *IEEE Transactions on Circuits and Systems*, 25(8):641–642, 1978.

[Sch05] D. A. Schupke. Guaranteeing Service Availability in Optical Network Design. In *Asia-Pacific Optical Communications Conference (APOC)*, 2005.

[SCV+08] J. Segovia, E. Calle, P. Vila, J. Marzo, and J. Tapolcai. Topology-Focused Availability Analysis of Basic Protection Schemes in Optical Transport Networks. *Journal of Optical Networking*, 7(4):351–364, 2008.

[Sem08] G. Semaan. Designing Networks with the Optimal Availability. In *Optical Fiber Communication Conference (OFC)*, 2008.

[SG04] G. Shen and W. D. Grover. Segment-Based Approaches to Survivable Translucent Network Design Under Various Ultra-Long-Haul System Reach Capabilities. *Journal of Optical Networking*, 3(1):1–24, 2004.

[SGCB02] G. Shen, W. D. Grover, T. H. Cheng, and S. K. Bose. Sparse Placement of Electronic Switching Nodes for Low-Blocking in Translucent Optical Networks. *Journal of Optical Networking*, 1(12):424–441, 2002.

[SM08] L. Song and B. Mukherjee. On the Study of Multiple Backups and Primary-Backup Link Sharing for Dynamic Service Provisioning in Survivable WDM Mesh Networks. *IEEE Journal on Selected Areas in Communications*, 26(6):84–91, 2008.

[ST07] G. Shen and R. S. Tucker. Translucent Optical Networks: The Way Forward. *IEEE Communications Magazine*, 45(2):48–54, 2007.

[Sta09] R. F. Stapelberg. *Handbook of Reliability, Availability, Maintainability and Safety in Engineering Design*. Springer, 2009.

[TML+09] M. Tornatore, B. Mukherjee, R. Lucadello, S. Cavallaro, D. Lucerna, and A. Pattavina. Grooming and Protection with Availability Guarantees in Multilayer Optical Networks. In *Conference on Optical Network Design and Modeling (ONDM)*, 2009.

[TMP05] M. Tornatore, G. Maier, and A. Pattavina. Availability Design of Optical Transport Networks. *IEEE Journal on Selected Areas in Communications*, 23(8):1520–1532, 2005.

[TMP06] M. Tornatore, G. Maier, and A. Pattavina. Capacity Versus Availability Trade-Offs for Availability-Based Routing. *Journal of Optical Networking*, 5(11):858–869, 2006.

[TN94] M. To and P. Neusy. Unavailability Analysis of Long-Haul Networks. *IEEE Journal on Selected Areas in Communications*, 12(1):100–109, 1994.

[TTGA08] K. Tutschku, P. Tran-Gia, and F.-U. Andersen. Trends in Network and Service Operation for the Emerging Future Internet. *AEÜ - International Journal of Electronics and Communications*, 62(9):705–714, 2008.

[VCD+05] S. Verbrugge, D. Colle, P. Demeester, R. Huelsermann, and M. Jaeger. General Availability Model for Multilayer Transport Networks. In *International Workshop on the Design of Reliable Communication Networks (DRCN)*, 2005.

[VCP+06] S. Verbrugge, D. Colle, M. Pickavet, P. Demeester, S. Pasqualini, A. Iselt, A. Kirstädter, R. Hülsermann, F.-J. Westphal, and M. Jäger. Methodology and Input Availability Parameters for Calculating OpEx and CaPex Costs for Realistic Network Scenarios. *Journal of Optical Networking*, 5(6):509–520, 2006.

[Wax88] B. M. Waxman. Routing of Multipoint Connections. *IEEE Journal on Selected Areas in Communications*, 6(9):1617–1622, 1988.

[WH04] L. Wosinska and M. Held. Optimization of Optical Networks: Price and Value of Reliability. In *International Conference on Transparent Optical Networks (ICTON)*, 2004.

[WM10] H. Waldman and D. A. A. Mello. SLA-Aware Survivability. *Journal of Networks*, 5(2):251–255, 2010.

[WS07] L. Wosinska and T. K. Svensson. Analysis of Connection Availability in an All-Optical Mesh Network. *Fiber and Integrated Optics*, 26(2):99–110, 2007.

[ZJM00] H. Zang, J. Jue, and B. Mukherjee. A Review of Routing and Wavelength Assignment Approaches for Wavelength-Routed Optical WDM Networks. *Optical Networks Magazine*, 1(1):47–60, 2000.

[ZKZM03] J. Zhang, KeyaoZhu, H. Zang, and B. Mukherjee. A New Provisioning Framework to Provide Availability-Guaranteed Service in WDM Mesh Networks. In *IEEE International Conference on Communications (ICC)*, 2003.